Phylogenetic Diversity, Morphological Disparity and Niche Adaptation in Seabirds

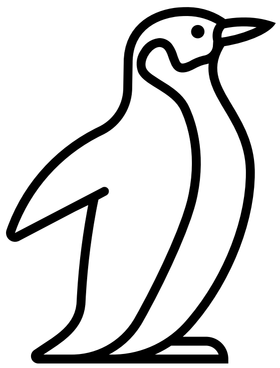

Author: Joshua Tyler

Lead Supervisor: Professor Matthew Wills

Co-Supervisor: Dr. Nicholas Priest

Co-Supervisor: Dr. Jane Younger

A thesis submitted in fulfilment of the requirements for the degree of Doctor of Philosophy

Milner Centre for Evolution
Department of Life Sciences

University of Bath

You know my methods, Watson. There was not one of them which I did not apply to the inquiry. And it ended by my discovering traces, but very different ones from those which I had expected.

The Memoirs of Sherlock Holmes

There is nothing more deceptive than an obvious fact.

The Boscombe Valley Mystery

Education never ends, Watson. It is a series of lessons, with the greatest for the last.

His Last Bow

Arthur Conan Doyle

DECLARATION OF AUTHORSHIP

Copyright notice

Attention is drawn to the fact that copyright of this thesis rests with the author and copyright of any previously published materials included (Chapters 2, 3 & 4) may rest with third parties. A copy of this thesis has been supplied on condition that anyone who consults it understands that they must not copy it or use material from it except as licensed, permitted by law or with the consent of the author or other copyright owners, as applicable.

Signed: *Joshua Tyler*

Declaration of any previous submission of the work

The material presented here for examination for the award of a higher degree by research has not been incorporated into a submission for another degree.

Signed: *Joshua Tyler*

Declaration of Authorship

I am the author of this thesis, and the work described therein was carried out by myself personally, with the exception of co-authored manuscripts in Chapters 2-4 where the contribution of the work carried out by other researchers is detailed at the start of each manuscript.

Signed: *Joshua Tyler*

ACKNOWLEDGEMENTS

There have been many times where I felt I would not finish this PhD. Without the unwavering support and belief of my supervisors, funders, family, and friends, it certainly wouldn't have been possible. I thank them for helping me reach this great achievement and know that I am eternally thankful.

I would like to thank Prof Matt Wills for always being a voice of reassurance and belief, Dr Nick Priest for always challenging me to be the best scientist I can be, and Dr Jane Younger who has been a constant mentor and guide through this journey and without whom the incredible science here would not have been possible.

I would like to also thank the Evolution Education Trust and the University of Bath for funding my PhD Studentship. Being given the opportunity to follow my passion and engage with the research community has been a tremendous gift and one that I will always be grateful for.

Most of all, I thank my wife, who has been my pillar of strength throughout it all. Beyond her incredible kindness and ability to make the impossible feel achievable, it's been her unfaltering confidence in me that will stay with me forever.

P.S. Whilst his main contribution was constantly distracting me by running around and demanding food, I also thank my cat, Hubble, for always listening and showing me that it's the simple things that matter most.

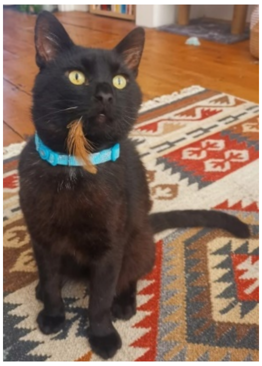

SUMMARY

Operating on higher temporal and taxonomic scales, macroevolution seeks to understand the biodiversity of the world through the lens of great change. Phylogenetic diversity, morphological disparity and niche adaptation are core tenets of macroevolution, and their interactions are of great interest. In the 21st Century, analytical methodologies and high-dimensional datasets have become the leading macroevolutionary approaches and allow researchers to return to fundamental hypotheses posited in the years since Darwin. Seabirds are a highly diverse and speciose group that occupy ranges that span from the equator to the poles. By leveraging the latest methodologies and techniques, I return to the core tenets of macroevolution to shed new light on old problems using seabirds. Gentoo penguins have a circumpolar distribution and have been reported to have significant morphological and genetic variation across this range. Here I show that four distinct populations of gentoo penguins (Iles Kerguelen, Falkland Islands, South Georgia, South Shetlands/Western Antarctic Peninsula) are genetically and morphologically distinct from one another and update the taxonomy to reflect these divergences. The results further highlight the importance of reassessing species boundaries as methodological advances are made, particularly for taxa of conservation concern. Alongside several wing adaptations, albatrosses and other *Procellariiformes* have augmented rhamphothecas constructed of several jointed keratinous plates rather than a single structure. Using 3D reconstructions of upper bills, I investigated the range of morphologies present within twelve species of albatross and the relative predictive strength of intrinsic (size & species assignment) and extrinsic (diet) factors. Species are separated both in shape and size reducing niche overlap and simple dietary classifications can distinguish bill shapes. Size is relatively unimportant when allometry models are considered with species assignment accounting for ten times more variation in bill shape. The results show that both intrinsic and extrinsic factors should be considered when understanding morphological evolution. Diving as a foraging behaviour is displayed across waterbirds but the history of the trait has rarely been investigated in a phylogenetic context. I find that diving has evolved numerous times but the transition to diving is irreversible. The transition to diving is accompanied by a shift in disparity as diving forms evolve towards a heavier body mass, while concurrently occupying new diversification regimes that exhibit increased extinction rates. Our findings highlight the vulnerability of highly specialised lineages during the ongoing sixth mass extinction.

Jointly, these analyses show that there is considerable interaction between the different elements comprising macroevolution and that these linkages are complex, even when viewed through simple questions. Only by considering all aspects of macroevolution and utilising the latest techniques can we start to comprehend the patterns and trends in biodiversity.

TABLE OF CONTENTS

1 INTRODUCTION

The study of biodiversity sits at the heart of evolutionary biology. Fundamentally, biodiversity is the framework within which we measure the variety of life on our planet and species represent the building blocks. Operating on larger temporal and taxonomic scales, macroevolution seeks to understand the biodiversity of the world through the lens of great change (D. Jablonski, 2017a, 2017b). Within macroevolution, there are three core biological questions: 1) how many different species there are, 2) how they are different from one another and 3) how they interact with each other and the environment. These questions relate directly to the fields of phylogenetic diversity, morphological disparity, and niche adaptation, each of which is a core tenet of macroevolution. This thesis will explore these themes and their interactions using the latest analytical techniques with an application to seabird evolution. This study of macroevolution in seabirds aims to provide a richer and more detailed understanding of the biodiversity, adaptation, and survival strategies of these important marine species.

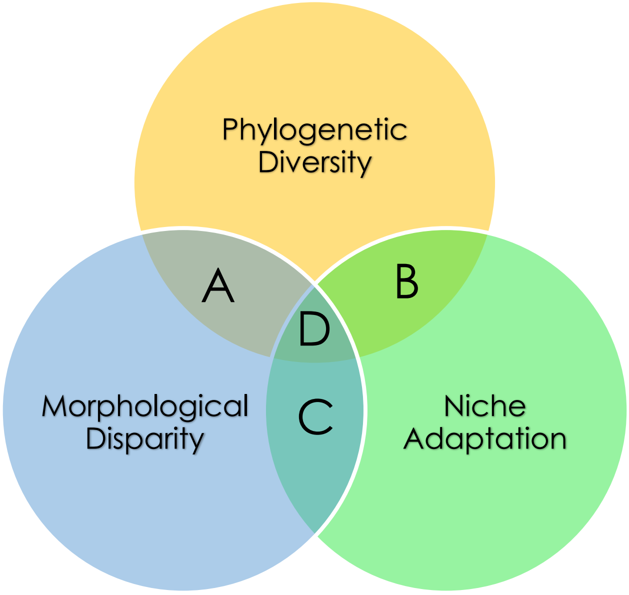

Figure 1.1: Macroevolutionary Tenets and their relationships. Coupled regions identified by A, B, C & D.

1.1 Macroevolutionary Tenets

1.1.1 Phylogenetic Diversity

What is a species and why does the definition and number seem to change through time? Under the Linnean system of classification, species are the principal taxonomic unit when discussing phylogenetic diversity (von Linnaeus, 1735). Species concepts therefore represent how we delimit species and when a group of organisms can be recognised as a species. It is the varied application of different species concept that has resulted in the total number of species being in constant flux (Stankowski & Ravinet, 2021). Classically, the Biological Species Concept (BSC) has been employed across ornithology, defining species based on reproductive isolation (Ripley & Mayr, 1943). In practical terms, testing reproductive isolation in the real world is difficult; if taxa are not occupying the same geographic areas, then we cannot know if they are truly reproductively isolated in the biological sense. In recent years there has been a noticeable shift towards the use of the Phylogenetic Species Concept (PSC), defining a species as the smallest diagnosable cluster of individuals sharing ancestry and descent (Cracraft, 1983). There are, however, a plethora of other concepts that each carry their own merits and issues (De Queiroz, 2007).

One of the main drivers for understanding phylogenetic diversity from a taxon counting standpoint is conservation. Many international conservation organisations operate at the species level, therefore any distinct populations or subspecies will not be assessed or actively protected despite potentially harbouring hidden biodiversity (BirdLife International, 2018; IUCN, 2021). The total number of species changes not only when a new species is discovered but also when scientists revise species lists through taxonomic lumping and splitting. Lumping refers to the combination of several species into a single species, often aligning with the themes of the BSC and reproductive arguments, whilst splitting involves the designation of several recognised species from a single species, invoking diagnosable cluster arguments of the PSC. These processes constantly shift the overall number of species, leading to potential over- or under-estimates of phylogenetic diversity.

1.1.2 Morphological Disparity

Morphological disparity is a result of the "quantification of morphological variation at a set taxonomic level" (Hopkins & Gerber, 2021). This could be within a population, between species or even across entire clades like birds, tetrapods, or vertebrates. Quantification of morphological disparity is based on variation in homologous features between individuals. Morphometric analyses fall broadly into two categories: those based on discrete characters (e.g., presence/absence, fixed forms, etc) and those based on continuous measures (e.g., length of bone, area of wing, coordinates of landmarks etc). These datasets can be used to construct a functional space or morphospace, depending on the traits used, from which shape relationships can be visualised, with distances in the spaces inferred as morphological disparity (Foote, 1997; Goswami et al., 2019; Guillerme, Cooper, et al., 2020; Guillerme, Puttick, et al., 2020; Hopkins & Gerber, 2021).

Morphospaces can be used in conjunction with other data types (e.g., ecological data, phylogenetic trees etc) to answer key questions in relation to shape, i.e., how has disparity evolved over time, how does disparity relate to ecology, are phylogenetic diversity and morphological disparity coupled? Several studies have attempted to answer these questions in relation to the avian tree. Applications of 3D geometric morphometrics to huge swathes of the bird phylogeny have helped to understand the range of avian bill and skull morphologies. Large scale phylogenetic analyses have also been performed to predict ancestral morphological states and to estimate rates of morphological evolution (Cooney et al., 2017; Felice & Goswami, 2018).

By utilising linear morphometrics, it is possible to include far more species within analyses and the importance of different morphological features can be quantified across birds as a whole (Pigot et al., 2020), in particular in relation to overarching convergence between bird families.

1.1.3 Niche Adaptation

Niches are fundamentally a description of the position a species occupies within an ecological system, both in terms of the abiotic environment and biological species interactions. For over a century, ecologists and evolutionary biologists have been grappling with how to define niches: from Grinnellian discussions on habitat, Eltonian ponderings on foraging strategies and Hutchinsonian mathematical abstractions through the definitions of adaptive zones of Van Valen, to more recent approaches combining mathematical and applied approaches (Elton, 2001; Grinnell, 1917; Holt, 2009; Hutchinson, 1957; Soberón, 2007; Valen, 1971).

Niche adaptation for the purposes of this thesis primarily describes form-function relationships and the correlations and covariations of shape, habitat, diet, geographic overlap, and phylogenetic relatedness. Studies have repeatedly sought to find the relationship between shape and diet or foraging strategy and found that the strength of that relationship depends on the phylogenetic scale used and the particular skeletal elements analysed (Bright et al., 2016; Felice et al., 2019; Pigot et al., 2020). These studies and approaches combine the various definitions of niche to further elucidate the macroevolutionary patterns present.

1.1.4 Understanding the coupled nature of Diversity, Disparity and Niche

Figure 1.1 presents one simplified perspective on the nature of Macroevolution. Whilst the three tenets described previously can be thought of in isolation, they can be thought of in conjunction, leading to investigations into the strength of their correlation and the biological implications of their relationship.

1.1.4.1 Diversity & Disparity (Region A)

Do new species need new forms? Do more species-rich clades occupy wider arrays of morphological forms? Are more distantly related species proportionally disparate? These questions test the coupled nature of diversity and disparity.

When we model the evolution of morphological traits on phylogenies, a null hypothesis often chosen is that of Brownian Motion, implying that the expected difference in phenotype is proportional to the divergence time of the species (Hansen, 1997; Hansen & Martins, 1996). In fact, the majority of evolutionary models, bar those that are phylogenetically independent, are inherently making assumptions about the relationship between diversity and disparity, collectively known as Phylogenetic Comparative Methods (PCMs) (Adams & Collyer, 2018; Cornwell & Nakagawa, 2017; Garamszegi, 2014; Uyeda et al., 2018). These methodologies connect hypotheses of species relationships with investigations into the distributions and ranges of morphological traits. Studies have consistently shown that the morphological disparity of clades is influenced by their respective diversities (Clavel & Morlon, 2017; Cooney et al., 2017; Marx & Fordyce, 2015; Schweizer et al., 2014; Wang & Clarke, 2014).

From a conservation perspective, understanding whether efforts should be focussed on preserving phylogenetic diversity and/or morphological disparity, is a particularly vibrant area of discussion (Faith, 1992; Hughes et al., 2022; Lean & Maclaurin, 2016; Minelli, 2019). Basing conservation on phylogenetic diversity ensures that the greatest range of evolutionary history and potential for adaptation is maintained whilst focussing on morphological disparity can often simultaneously preserve ecosystem functions which may avoid system collapses (Cadotte et al., 2011, 2012; Devictor et al., 2010; Srivastava et al., 2012; M. Winter et al., 2013). The conservation theme is explored throughout the thesis but particularly in Chapters 2 & 4.

1.1.4.2 Diversity & Niche (Region B)

There are several modes of speciation, ranging from sympatric (geographically overlapping) to allopatric (geographically separated) and scenarios in between (Fitzpatrick et al., 2009). In sympatry, niche partitioning between species is invoked to reduce competitive interactions (Clarke et al., 2017; Coyne, 2007; Jonathan Davies et al., 2007; Kleynhans et al., 2011; Petalas et al., 2021). Niche adaptation is often the driving force in sympatric speciation and therefore phylogenetic diversity is a measurable outcome of the process. How similar do we expect sister taxa to be in their niches and does it depend on their range overlap? Do more speciose clades partition niches on a finer scale? Are environments with a greater range of available niches necessarily filled with a greater number of species? To appreciate the distribution of species across the tree of life, we need a corresponding understanding of the environments within which they exist, which fundamentally defines their niche.

1.1.4.3 Disparity & Niche (Region C)

One area where Disparity & Niche overlap considerably is form-function relationships. Darwin originally wrote about beneficial traits that would allow organisms to be successful in their environments and therefore increase survival (Darwin, 1859). Since then, evolutionary biologists have focussed on understanding how morphological traits can predict function, and vice-versa. Numerous studies of vertebrates have investigated correlations between diet and feeding apparatus (Bright et al., 2016; Gómez & Lois-Milevicich, 2021; Marugán-Lobón et al., 2022; Pigot et al., 2020), limb morphologies and locomotor & foraging strategies (Baumgart et al., 2021; Dickson & Pierce, 2019; Lowi-Merri et al., 2021; Nations et al., 2019, 2021; Rothier et al., 2023; Sheard et al., 2020; Steell et al., 2023) and other combinations of traits and the species environments (Burress & Muñoz, 2022; Burton et al., 2023; de Brito et al., 2022; Dickson et al., 2017; Navalón et al., 2022).

The strength of form-function relationships and their variation across the tree of life speaks to an interesting conundrum within evolutionary biology: to what extent are these relationships predictable and how are they connected to deterministic or contingent processes? Studies on convergent evolution have found connections between disparity and niche, with repeatedly evolved shapes & structures performing the same function (Gómez & Lois-Milevicich, 2021; Goswami et al., 2011; McCurry et al., 2017; Pigot et al., 2020; Zelditch et al., 2017). Despite this apparent predictability functionally (e.g., the flight function in bats, birds and insects using wings), the actual anatomical structures used are biologically different (Anderson & Ruxton, 2020; Gleiss et al., 2011; Losos, 2011). The focus within this thesis is on the evolution of seabirds which, while morphologically alike, provides an excellent opportunity to study the repeated convergence on an array of foraging strategies and diets.

1.1.4.4 Diversity, Disparity & Niche (Region D)

The central region of Figure 1.1 represents the overtly linked nature of macroevolution. One example question that straddles all three areas could be: do new species need new forms to occupy new niches? Several studies have aimed to understand this triple dynamic by looking at each of the overlapping regions in an integrative manner (Cooney et al., 2017; Pigot et al., 2020; Watanabe et al., 2019). They each find that the level to which these tenets are correlated is scale dependent, highlighting a theme that is repeated throughout the analysis chapters here. Hypotheses & questions can be represented as points in the Venn diagram of Macroevolution. This thesis takes an approach that explores the regions of Venn diagram by asking a variety of questions and attempts to map the theoretical landscape of the tenets and ascertain whether they can be navigated independently or if they are truly linked.

1.2 R as a tool for Macroevolutionary Studies

R is an open-source programming language used for statistical analysis pipelines and visualisation (R Core Team, 2022). It has enormous utility within evolutionary biology and supports a vast collection of packages for analysing common datasets (e.g., phylogenies, trait measures, geospatial data etc)(Gearty et al., 2022). By using these cutting-edge techniques and packages, it provides the ability to manipulate huge new datasets and streamline analytical pipelines to answer novel questions. Within this thesis, R is used for nearly all the analysis, from data cleaning through statistical testing and modelling to visualisations and graphs. One key reason behind this is the perpetuation of open science and data sharing, on which the analyses herein are grounded. Within the supplementary material, all the analysis code is available freely, alongside all the datasets required to recreate all the results and graphs.

1.3 Taxonomic Focus – Seabirds

Seabirds are bird species that are adapted to marine environments. In this thesis, I focus on the seabirds within the waterbird (Aequorlitornithes) clade (Prum et al., 2015; Sangster & Mayr, 2021), therefore excluding the members of the family Anatidae, which includes some marine ducks (Howell & Zufelt, 2019; Parkes & Austin, 1962). This distinction was made to allow PCMs to be more readily implemented, given the phylogenetic distance between the various clades under the seabird designation (Ericson et al., 2006; Hackett et al., 2008; Kear, 2005; Prum et al., 2015).

There are many reasons why seabirds make for an exciting focus. Primarily, they show huge variety in species density between clades (Figure 1.2), important ranges of morphologies between species including wing morphologies, bills and hind-limb forms, and broad diets given differing foraging niches and global marine ranges (Baumgart et al., 2021; Sausner et al., 2016; Van Oordt et al., 2018; Wang & Clarke, 2014). These characteristics are epitomised by Penguins (Spheniscidae) and Albatross (Diomedeidae), both of which exhibit extreme morphological and behavioural adaptations to the marine environment (Ksepka et al., 2006; Piro, 2022; Wang & Clarke, 2014; Warham, 1977; Watanuki et al., 2006). By choosing groups that span the macroevolutionary spectrum in terms of their diversity, disparity & niche, and have a rich research history, I have been able to ask novel questions which led to surprising results.

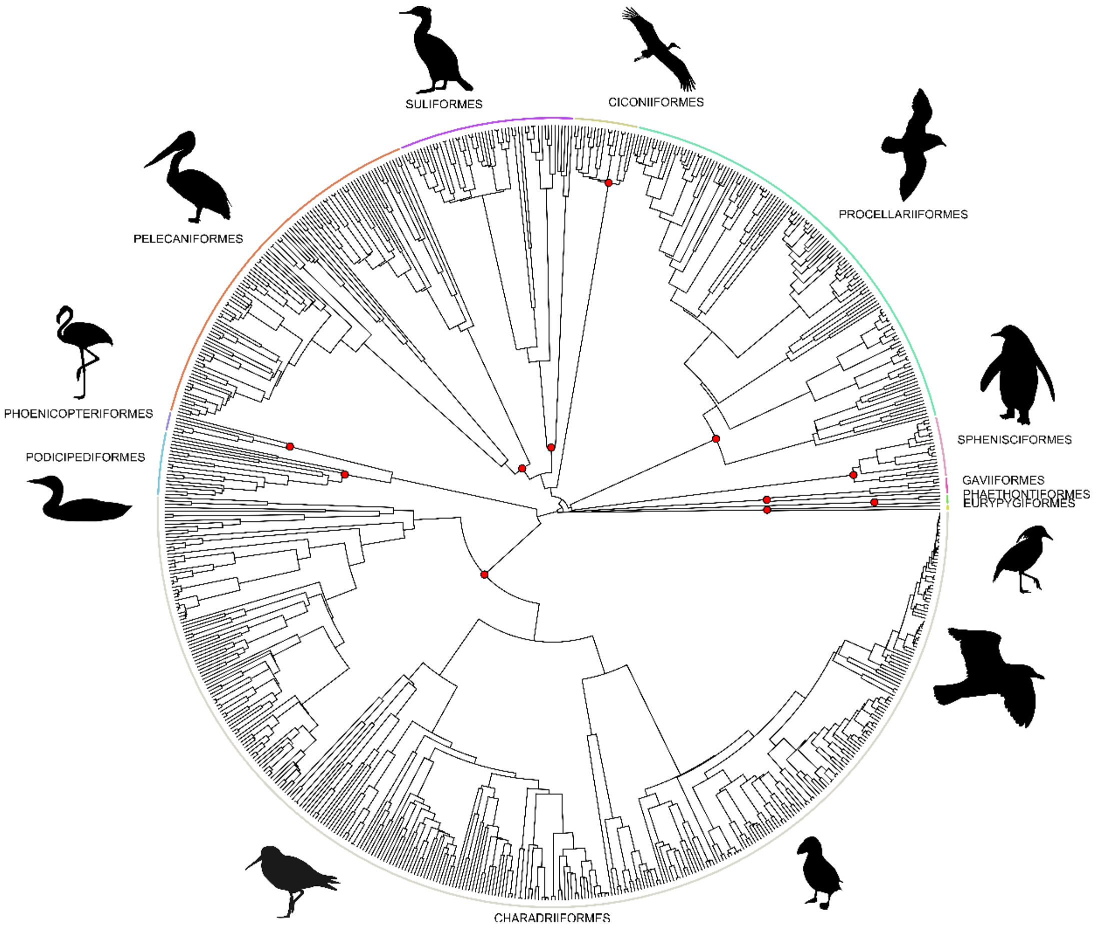

Figure 1.2: Phylogenetic relationships between seabirds. Avian Orders shown around edge. Red dots indicate MRCA for each of the 11 orders. Based on composite tree constructed from (Hackett et al., 2008; Jetz et al., 2012; Prum et al., 2015)

Seabird conservation, particularly of those with polar distributions (e.g., albatross, petrels & penguins), is of utmost importance given the currently estimated extinction risks (Dias et al., 2019; Hickcox et al., 2019; IUCN, 2021). Of the 727 waterbird species considered across the analyses of this thesis, over 20% (156 species) are listed by the IUCN as Vulnerable, Endangered or Critically Endangered (IUCN, 2021). Given the rapidly changing climate impacting seabird habitats globally, understanding their speciation processes, morphological adaptability and niche selection will be vital to predict their future adaptation and likelihood of survival (Bestley et al., 2020; Clucas et al., 2014; Friesen, 2015; McMahon et al., 2019; Sauve et al., 2019).

1.4 Objectives and Outline

The objective of this thesis is to explore the interconnected nature of macroevolutionary ideas through the lens of seabirds and modern computational techniques. Moreover, it seeks to provide deeper insights into the evolutionary history of seabirds that led to their current biodiversity and how future changes my manifest. Specifically, I have considered each of the three areas outlined in the introduction (phylogenetic diversity, morphological disparity, and niche adaptation) and explore their interactions.

Chapter 2 models phylogenetic diversity in the context of hidden and cryptic species within Gentoo penguins. By using evidence from morphology and ecology, I aimed to estimate the association of disparity & niche with diversity.

Chapter 3 uses Albatross to understand the relationships between form and function, a facet of morphological disparity. Here, I employed 3D geometric morphometric techniques to capture shape variation. I then examined how different species & diets affect the evolution of the bill structure across the clade.

Chapter 4 has a broader taxonomic remit including all 727 species of waterbird and uses mathematical modelling tools to reconstruct the evolution of the diving niche across the entire clade. The ancestral state predictions are then used to assess the influence of diversity (in this case speciation & diversification rate) and disparity (body mass as a key trait) on this specialist niche adaptation.

Chapter 5 closes the thesis with a discussion on the tangled nature of macroevolutionary tenets and a broader assessment on limitations and future work.

2 MORPHOMETRIC AND GENETIC EVIDENCE FOR FOUR SPECIES OF GENTOO PENGUIN

2.1 Opening Remarks

In the Introduction chapter, I explored the topic of phylogenetic diversity and how species are the building blocks of biodiversity. Beyond the philosophical and academic implications of the definition of a species, there are also more practical considerations. Conservation initiatives aiming to protect biodiversity often consider species as a whole rather than the particulars of individual populations (IUCN, 2021). Biological variation can be overlooked by initiatives and that biodiversity could then be lost if hidden species have not been recognised by science. A recent example was seen in giraffes, where the traditionally single species (*Giraffa camelopardalis*) was found to be four distinct groups with species level diversity (Fennessy et al., 2013, 2016; S. Winter et al., 2018).

Penguins are a long explored and iconic group, both scientifically and to the wider public audience. In particular, the gentoo penguin has been repeatedly studied and while datasets about Southern Ocean populations have continued to grow, there had been no integrative studies bringing all the disparate data together to assess whether there was indeed hidden and cryptic diversity. By using an integrative taxonomic framework combining morphometrics, genetics and ecological data, I provide credible evidence of species level diversity within Gentoo penguins and that four species should be recognised.

2.2 Authorship and Permissions

This declaration concerns the article entitled:			
Morphometric and genetic evidence for four species of gentoo penguin			
Publication status (tick one)			
Draft manuscript ☐ **Submitted** ☐ **In review** ☐ **Accepted** ☐ **Published** ☒			
Publication details (reference)	Tyler J, Bonfitto MT, Clucas GV, Reddy S, Younger JL. Morphometric and genetic evidence for four species of gentoo penguin. Ecol Evol. 2020;10:13836–13846. https://doi.org/10.1002/ece3.6973		
Copyright status (tick the appropriate statement)			
The material has been published with a CC-BY license ☒	The publisher has granted permission to replicate the material included here ☐		
Candidate's contribution to the paper (provide details, and indicate as a percentage)	**Josh Tyler**: Conceptualization (supporting), Data curation (equal); formal analysis (equal); investigation (equal); visualization (equal); writing–original draft (lead). **Matthew T. Bonfitto**: Data curation (supporting); formal analysis (supporting). **Gemma Clucas**: Conceptualization (supporting); data curation (equal); formal analysis (equal); investigation (equal). **Sushma Reddy**: Conceptualization (supporting); data curation (equal); investigation (supporting). **Jane Younger**: Conceptualization (lead); data curation (equal); formal analysis (equal); investigation (equal); project administration (lead); supervision (lead); writing–original draft (supporting). Overall: J Tyler 75%, MT Bonfitto 5%, GV Clucas 5%, S Reddy 5%, JL Younger 10%		
Statement from Candidate	This paper reports on original research I conducted during the period of my Higher Degree by Research candidature.		
Signed (Typed signature)	Joshua Tyler	**Date**	29 August 2023

2.3 Manuscript: Morphometric and genetic evidence for four species of gentoo penguin

2.3.1 Abstract

Gentoo penguins (*Pygoscelis papua*) are found across the Southern Ocean with a circumpolar distribution and notable genetic and morphological variation across their geographic range. Whether this geographic variation represents species-level diversity has yet to be investigated in an integrative taxonomic framework. Here we show that four distinct populations of gentoo penguins (Iles Kerguelen, Falkland Islands, South Georgia, South Shetlands/Western Antarctic Peninsula) are genetically and morphologically distinct from one another. We present here a revised taxonomic treatment including formal nomenclatural changes. We suggest the designation of four species of gentoo penguin: *P. papua* in the Falkland Islands, *P. ellsworthi* in the South Shetland Islands/Western Antarctic Peninsula, *P. taeniata* in Iles Kerguelen, and a new gentoo species *P. poncetii*, described herein, in South Georgia. These findings of cryptic diversity add to many other such findings across the avian tree of life in recent years. Our results further highlight the importance of reassessing species boundaries as methodological advances are made, particularly for taxa of conservation concern. We recommend reassessment by the IUCN of each species, particularly *P. taeniata* and *P. poncetii*, which both show evidence of decline.

2.3.2 Introduction

A recent investigation into global species diversity of birds proposed that the number of species may be underestimated by as much as a factor of two when unrecognised species are accounted for (Barrowclough et al., 2016). This discrepancy exists in part due to the historical application of the Biological Species Concept (BSC) in ornithology. The BSC defines a species as a "group of actually or potentially interbreeding natural populations, which are reproductively isolated from other such groups" (Ripley & Mayr, 1943). Whilst generally applicable, the BSC is complicated in ornithology by the ability of birds to hybridise with deeply divergent relatives (Prager & Wilson, 1975). It is also often impossible to test for reproductive isolation in wildlife taxa that do not have overlapping ranges. As a result, the widespread application of the BSC led to an underestimation of avian species diversity. The Phylogenetic Species Concept (PSC), conceived by Cracraft (1983) and applied in Barrowclough et al (2016), defines a species as "the smallest diagnosable cluster of individual organisms within which there is a parental pattern of ancestry and descent" or more simply as "a group of organisms that have a unique and shared evolutionary history (i.e., monophyletic)". This definition allows for species delimitation without the need to invoke reproductive isolation. Another factor leading to the recognition of greater avian species diversity is the advancement of species delimitation tools, including genomic sequencing and multivariate morphometrics. Unrecognised (or hidden) species are distinguishable using physical characters but were not previously recognised as full species due to either limitations in analytical methods or historical interpretations of the species concept. Cryptic species, on the other hand, refers to taxa that cannot be readily identified using physical characters, but can be discerned using genetic and/or ecological evidence (Hosner et al., 2018). Cryptic and hidden diversity in birds has been uncovered across the world in recent years by using the PSC in conjunction with integrative taxonomic approaches combining genomics and morphometrics, particularly in biodiversity hotspots such as the old-world tropics and neotropics (Hosner et al., 2018; Pulido-Santacruz et al., 2018; Singh et al., 2020; Younger et al., 2018, 2019). To manage conservation priorities in light of ongoing environmental change, it is vital to understand the true number of species that exist and their range-limits, rather than relying on historic estimates.

Given their large geographic range and already noted genetic and morphological differences (Clucas et al., 2018; Stonehouse, 1970), gentoo penguins could be strong candidates for harbouring hidden species-level biodiversity. First described by Forster (1781), the gentoo penguin (*Pygoscelis papua*) is the largest of the three Pygoscelis species and identifiable by its charismatic, red-toned bill, black head, and two contrasting white patches on the face. Gentoos have a circumpolar distribution spanning the Antarctic Convergence between 65°16' S and 46°00'S, ranging from the Antarctic Peninsula to the Crozet Islands (Figure 2.1) (Forster, 1781; H. J. Lynch et al., 2012; Woehler, 1994). Given this geographic spread and the considerable heterogeneity in environmental conditions among extant populations, it is important to understand not only global trends in gentoo penguin numbers, but also how each of the individual populations are faring in the rapidly changing Antarctic climate. Individual populations may also provide evidence for how gentoo penguins adapt to specific environmental conditions which could be missed when generalising over the polytypic species.

The global population size of gentoo penguins has increased 6-fold over the past 40 years, despite a changing ecological landscape due to climate change (McMahon et al., 2019). Newly established colonies on the southern extent of the gentoo range seem to be growing due to the increasing breeding habitat brought about by receding sea ice (Juáres et al., 2020; H. J. Lynch et al., 2012). Established populations, however, show varying patterns of success, with populations at Port Lockroy, Kerguelen Island and Macquarie Island seeing 1.4%, 2.3% and 1.8% per annum decreases respectively based on multi-decadal studies (Bingham, 1998; Dunn et al., 2016, 2019; Juáres et al., 2020; Lescroël & Bost, 2006; Pascoe et al., 2020).

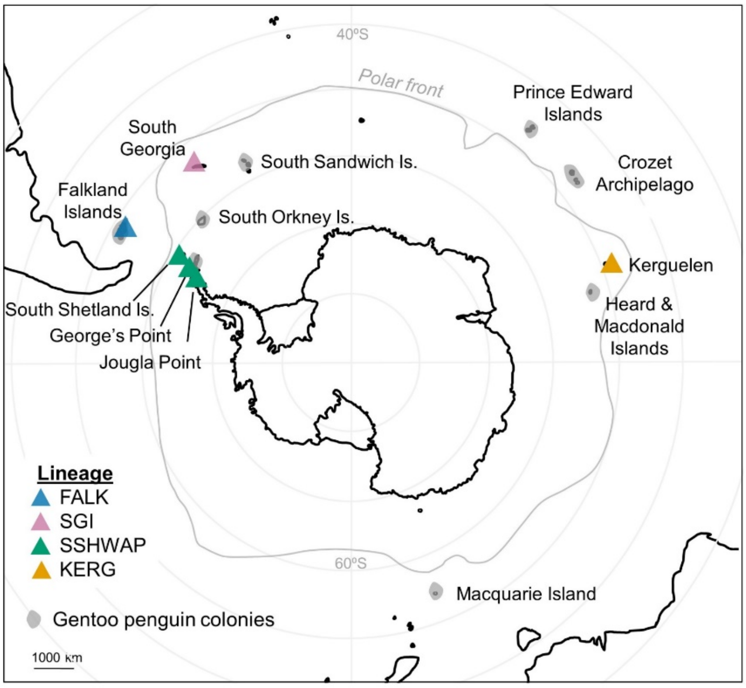

Figure 2.1: Geographic range of gentoo penguins. Grey zones show existing gentoo penguin colonies whilst coloured triangles show populations included in this study. FALK, Falklands; SGI, South Georgia Island; SSHWAP, South Shetland Islands & Western Antarctic Peninsula; KERG, Kerguelen.

Several subspecies of gentoo penguin have been proposed over the past century, however, subspecies limits have differed depending on the author. These have been based on measurable phenotypic variation as there are no noted plumage differences among proposed taxa. The nominate subspecies, *Pygoscelis papua papua*, was part of the original species description by Forster (1781). Mathews (1927) described *P. p. taeniata*, which included populations on Marion, Crozet, Heard, Kerguelen & the Falkland Islands. These subspecies were redefined by Peters (1935) who designated the populations of Macquarie, Heard, Kerguelen and Marion Islands as *taeniata* whilst gentoos from the Falklands, South Orkney, South Shetland, South Georgia and the Western Antarctic Peninsula were assigned to papua. The next update to the taxonomy was by Murphy (1947), who designated the subspecies *P. p. ellsworthi* for the populations on the

South Shetland Islands and Western Antarctic Peninsula. Stonehouse (1970) then investigated the subspecies boundaries, focusing on morphological variation. Stonehouse focused on the classic hypothesis that revolved around the influence of the Antarctic Polar Front and the extent of pack ice on geographic variation in gentoos, and thus split *P. papua* into a northern (*P. p. papua*) and southern subspecies (*P. p. ellsworthi*), found north and south of 60°S respectively, whilst discounting Mathews' or Peters' claim for an eastern subspecies *P. papua taeniata* (Mathews, 1927; Murphy, 1947; Peters, 1935; Stonehouse, 1970). The analysis used a univariate approach based on six measures (culmen length, foot length, flipper length, flipper area, dorsal plumage, ventral plumage) and confirmed a north/south gentoo split in line with the Antarctic Polar Front hypothesis, with the South Georgia Island population belonging to the northern subspecies. Individuals measured from Kerguelen and Macquarie Islands were found to be statistically indistinguishable in this study and were different only slightly from those from South Georgia and the Falkland Islands, and therefore were also included in the nominate northern subspecies *P. p. papua* (Stonehouse, 1970). A recent study found support for a new clade in the sub-Antarctic Indian Ocean based on morphological analyses but was not formally assigned to a new sub-species (de Dinechin et al., 2012) whilst investigations into geographic variation in gentoo vocalisations found no patterns connected with regions or subspecies (M. A. Lynch & Lynch, 2017).

Recent genetic analyses from across the penguin family have uncovered significant genetic divergence among populations across the Southern Ocean (Clucas et al., 2018; Frugone et al., 2019; Levy et al., 2016; Pertierra et al., 2020; Vianna et al., 2017). These studies, in combination with documented regional heterogeneity in population responses to climate change, highlight the importance of interrogating traditional ideas of subspecies limits within gentoo penguins (Levy et al., 2016; Vianna et al., 2017). Both Clucas et al., 2018 & Pertierra et al., 2020 suggested that cryptic species of gentoo penguins exist based on genetic methodology. Using an integrative taxonomic framework combining contemporary multivariate morphological analyses with previous genomics results, we aim to test whether the four genetic lineages of gentoo penguins described in Clucas et al., (2018)(Kerguelen, Falklands, South Georgia, South Shetlands/Western Antarctic Peninsula) are morphologically distinct, and therefore warrant recognition as distinct species under the Phylogenetic Species Concept. We then take the next step of formally describing distinct species so they will be included in assessment frameworks such as the IUCN Red List and conservation plans.

2.3.3 Materials and Methods

2.3.3.1 Taxon sampling

Our geographic sampling within gentoo penguins (Figure 2.1) includes representatives from Kerguelen, the Falkland Islands, South Georgia, South Shetland Islands, and the West Antarctic Peninsula. This sampling spans the two currently recognised subspecies, namely the northern gentoo (the nominate subspecies, *Pygoscelis papua papua* (Forster, 1781)) distributed north of 60°S; and the southern gentoo (*Pygoscelis papua ellsworthi*), distributed on the Antarctic Peninsula and maritime Antarctic islands south of 60°S (Clements et al., 2019; Murphy, 1947; Stonehouse, 1970). Additionally, we include the putative Indian Ocean subspecies (de Dinechin et al., 2012),which is still classified as *P. p. papua* (Clements et al., 2019), and the South Georgia population, also classified as *P. p. papua*, but which multiple genetic studies show to be more closely related to *P. p. ellsworthi* (Clucas et al., 2014, 2018; Levy et al., 2016). Previous work has shown that gentoo penguin colonies on the South Shetlands and West Antarctic Peninsula are not reciprocally monophyletic in phylogenetic analyses (Clucas et al., 2018; Vianna et al., 2017), therefore, here we group these populations into one unit for the purposes of this species delimitation study. There are therefore four putative species to be assessed: South Shetlands and the West Antarctic Peninsula (SSHWAP); Kerguelen (KERG); South Georgia (SGI), and the Falklands (FALK).

For genetic analyses, we used a published dataset (Clucas et al., 2018) of RAD-Seq generated single nucleotide polymorphisms (SNPs). The dataset consists of 10,108 neutral SNPs for 69 gentoo penguins, with a median SNP coverage of 27X and a mean minor allele frequency (MAF) of 0.091 (SD 0.11). For morphometric comparisons, we measured all study skins of adult gentoo penguins from Kerguelen, the Falkland Islands, South Georgia, South Shetlands and West Antarctic Peninsula available in the Natural History Museum (Tring, UK) and American Museum of Natural History (New York, USA) collections, totalling 39 individuals (Supplementary Table A). Birds with evidence of juvenile plumage were excluded.

2.3.3.2 Genetic variation

We used Genodive (Meirmans & Van Tienderen, 2004) to calculate the Weir and Cockerham unbiased weighted F_{ST} estimator (Weir & Cockerham, 1984) between all pairs of populations, with significance calculated using 10,000 permutations of the data. Expected heterozygosity (H_S) was also calculated for each population using Genodive. Principal components analysis (PCA) was used to visualise genetic variation among all individuals, using the adegenet package (Jombart, 2008; Jombart & Ahmed, 2011) in R. Allele frequencies were scaled and centred, and missing values replaced with the mean allele frequency using the scaleGen function. PCA was computed with the dudi.pca function from the ade4 v1.7-11 package.

We previously carried out maximum likelihood (ML) phylogenetic analysis and Bayes factor species delimitation for the gentoo penguin SNP dataset (Clucas et al., 2018). In brief, we used RAxML v8.2.7 (Stamatakis, 2014) to infer an ML phylogeny with a SNP ascertainment bias correction applied to the likelihood calculations. 20 independent ML tree inferences were carried out using the GTRGAMMA model and then the best scoring topology identified and annotated with bootstrap supports from 1,000 replicates. Coalescent-based, Bayes factor species delimitation was carried out using the BFD* method (Leaché et al., 2014) as implemented within the SNAPP package (Bryant et al., 2012) of BEAST 2.4.3 (Bouckaert et al., 2014). The BFD* method estimates marginal likelihoods for competing species delimitation models using path sampling. We used four representative individuals for each lineage (KERG, FALK, SGI, SSHWAP) and tested four models: 1) the current taxonomy (P. p. papua vs. P. p. ellsworthi); 2) the three-taxa model suggested by mitochondrial DNA studies (Clucas et al., 2018; Vianna et al., 2017), wherein SGI and SSHWAP are grouped together; 3) the four-taxa model (FALK, KERG, SSHWAP, SGI); 4) a two-taxa model with all colonies grouped except for Kerguelen, which is the most divergent according to our other analyses. For expanded details of these analyses, please refer to (Clucas et al., 2018).

2.3.3.3 Morphological variation

To determine if genetic lineages are morphologically distinct, one of us (JY) took nine linear measurements from each museum study skin, representing key morphological traits of both the crania and post-crania (Baldwin et al., 1931): culmen length (CL; taken along the medial line), bill width at the base (BWB), bill height at gonys angle (BH), bill width at gonys angle (BWG), flipper width (FW; shortest distance from anterior surface of flipper above the radiale to the posterior side of the flipper), radius length (RL), manus length (ML; indent at radiale/radius/ulna to distal wing tip), tarsus length (TML; anterior surface), and middle toe length (MTL; digit I11 excluding nail). Measurements were taken with Mitutoyo Digital Callipers to an accuracy of 0.01 mm. All measurements were repeated three times, checked for outliers (by confirming that all measurements were within one standard deviation), and then averaged. The summary statistics of these measurements for each of the four clades are given in Supplementary Table A. All measures were log-transformed before the analyses. To identify traits that significantly differed between sexes, we carried out an analysis of variance (ANOVA) of sex within lineage for each trait (Supplementary Table B). Our testing found that only Flipper Width had a statistically significant difference between sexes ($p = 0.024$). This trait was therefore excluded from subsequent analyses to remove any potential bias introduced by uneven sampling of sexes.

Both univariate and multivariate analyses were used to investigate morphological differentiation between lineages. We carried out pairwise ANOVAs to determine whether any individual traits differed among lineages, and pairwise multivariate analysis of variance (MANOVA) on the combined trait dataset to assess overall morphological differentiation, using the F statistic for significance testing. These analyses were performed using base R (R Core Team, 2022). Principal components analysis (PCA) and linear discriminant analysis (LDA) were used as dimension-reduction methods to aid with visualisation and prediction, with lineage as a grouping variable using the fviz_pca_biplot function in factoextra and lda function in MASS in R (Kassambara & Mundt, 2020; Kemp, 2003; R Core Team, 2022). Confusion matrices and cross-validation tests were constructed and performed using predict function in the MASS package in R (Kemp, 2003)

2.3.4 Results

2.3.4.1 Genetic variation

All our genetic analyses show the four lineages (FALK, KERG, SGI, SSHWAP) to be significantly genetically distinct. Pairwise F_{ST} values among the four groups ranged from 0.130 to 0.341 and were all highly significant ($p < 0.001$, Table 2.1). Genetic diversity of the four lineages were all significantly different (Figure 2.2). Our PCA clearly differentiates the four lineages, with no evidence of overlap among the visible clusters (Figure 2.3). The ML phylogeny (Figure 2.4) resolved each lineage as 100% supported, with no well-supported (>70%) splits within any of the four lineages. Our coalescent-based species delimitation supported the four-taxa model over all other models. The comparison of marginal likelihoods gave a Bayes factor of 17,595 for the four-taxa model compared to the current taxonomy, and of 1,231 over the next most supported model (the three-taxa model) (Table 2.2). Note that a Bayes factor of 10 is considered decisive (Kass & Raftery, 1995). The currently accepted taxonomy had the lowest marginal likelihood estimate.

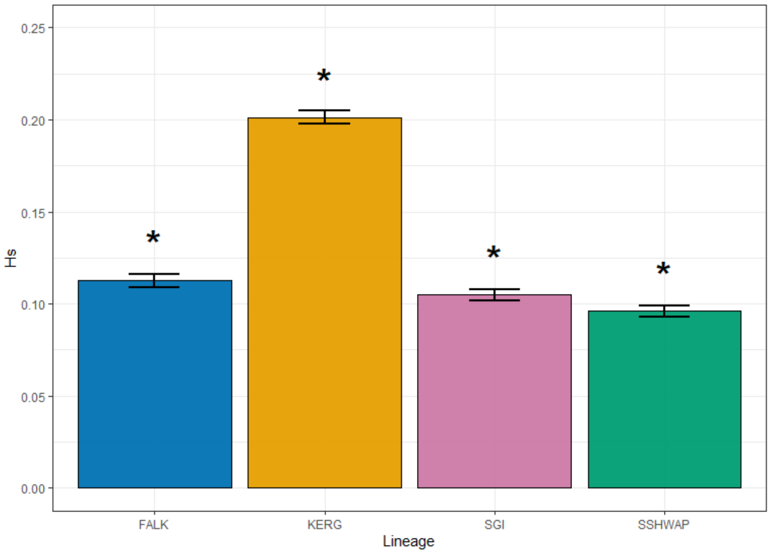

Figure 2.2: Heterozygosity. Genetic diversity (expected heterozygosity, Hs) of gentoo penguin lineage, with statistically significant differences indicated with asterisks.

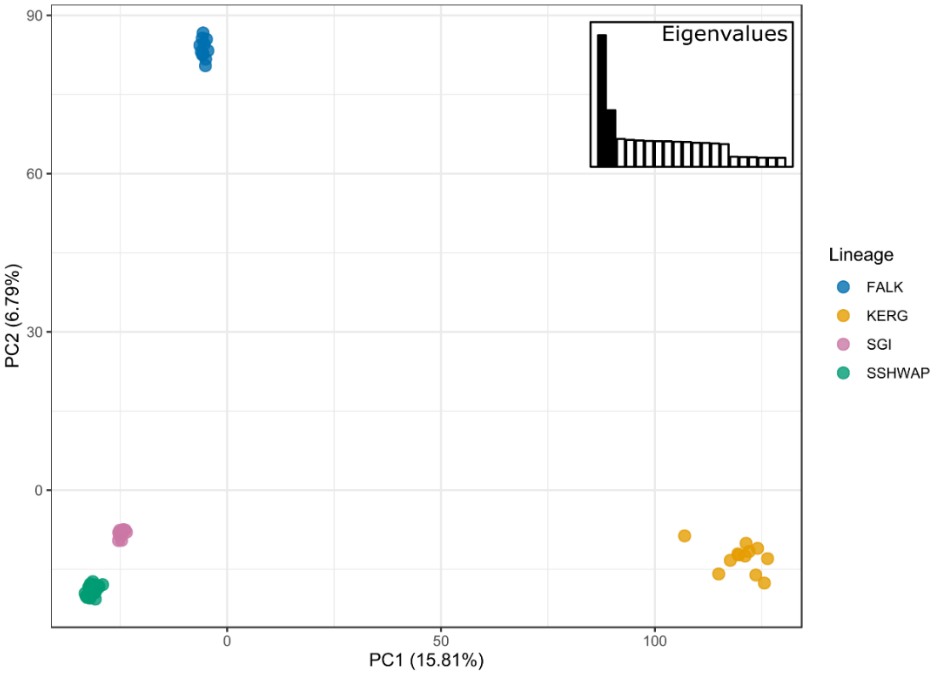

Figure 2.3: Principal Components Analysis based on genetic data. The amount of variance explained by each principal component (PC) is displayed on the inset bar graphs and on the axes, and the number of PCs retained is indicated in black.

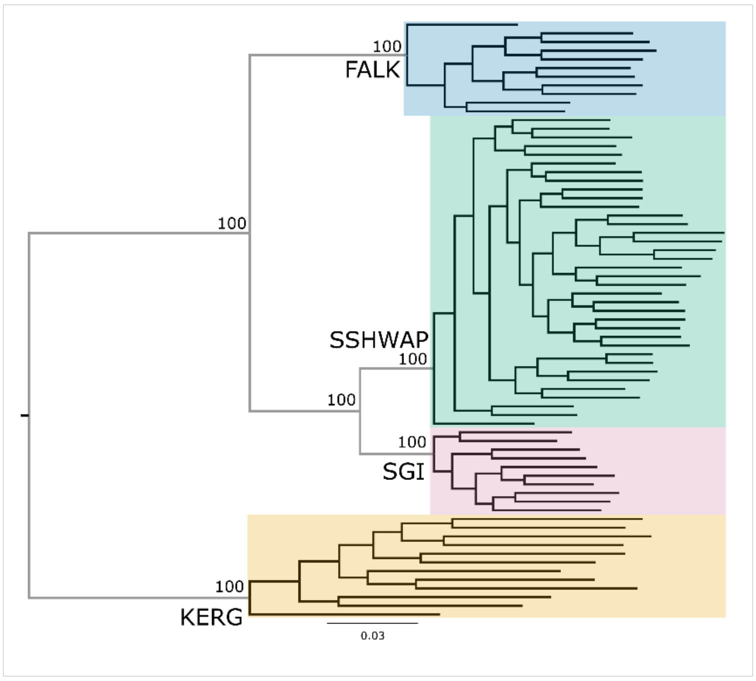

Figure 2.4: Best Scoring maximum likelihood phylogeny based on 10,108 neutral SNPs. Support values shown for branches that received >90% bootstrap support.

Table 2.1. Pairwise FST values between all gentoo penguin populations. FST values are below the diagonal with p values above. No correction for multiple tests was performed as the range of the p-values was too small.

	FALK	KERG	SGI	SSHWAP
FALK	***	<0.001	<0.001	<0.001
KERG	0.26	***	<0.001	<0.001
SGI	0.247	0.265	***	<0.001
SSHWAP	0.281	0.341	0.13	***

Table 2.2. Path sampling results for four species delimitation models. All Bayes factor (BF) calculations are made against the most strongly supported model. MLE = Marginal likelihood estimate.

Rank	Model	Number of taxa	MLE	BF
1	four nuclear clades	4	-83455.94	-
2	mitochondrial DNA hypothesis	3	-84071.77	1231.67
3	Kerguelen vs. all others	2	-87197.45	7483.02
4	current taxonomy	2	-92253.54	17595.2

2.3.4.2 Morphological variation

Our pairwise MANOVA tests determined that all genetically distinct populations are significantly morphologically distinct from each other overall ($p < 0.05$; Table 2.3). Our PC and LD analyses show some overlap in morphospace among the four lineages (Figures 2.5-2.6). In the PC analysis, PC1 explains 64.4% of the overall variation and is dominated by a size signal, with all traits increasing in size with increasingly negative PC1 scores. PC2 accounts for 13.3% of the variation and shows a split between cranial and post-cranial measures, with all limb measures excluding tarsus length increasing with negative PC2 scores and all bill measures increasing with increasingly positive scores. On visual inspection of the LDA, the lineages are predominantly separate, with a small number of specimens occupying positions closer to other lineages. This is supported by the confusion matrices which found an error rate of 10.2% for the whole dataset and 35.9% with cross-validation (Supplementary Table C).

Our pairwise ANOVA testing of traits showed that several individual traits enable discrimination of all four lineages (Table 2.4). The South Shetlands/West Antarctic Peninsula lineage is smaller than all other lineages and can be differentiated from South Georgia, the most closely related lineage in our genetic analyses, by its significantly smaller Culmen Length, Radius Length, Manus Length, Tarsus Length, and Middle Toe Length. The Falklands Islands birds are significantly larger than the other lineages for the majority of our measured traits. The Kerguelen and South Georgia lineages are intermediate in size and most similar to each other in our morphometric comparisons but can be differentiated by the significantly larger Manus Length and Middle Toe Length of the South Georgia lineage.

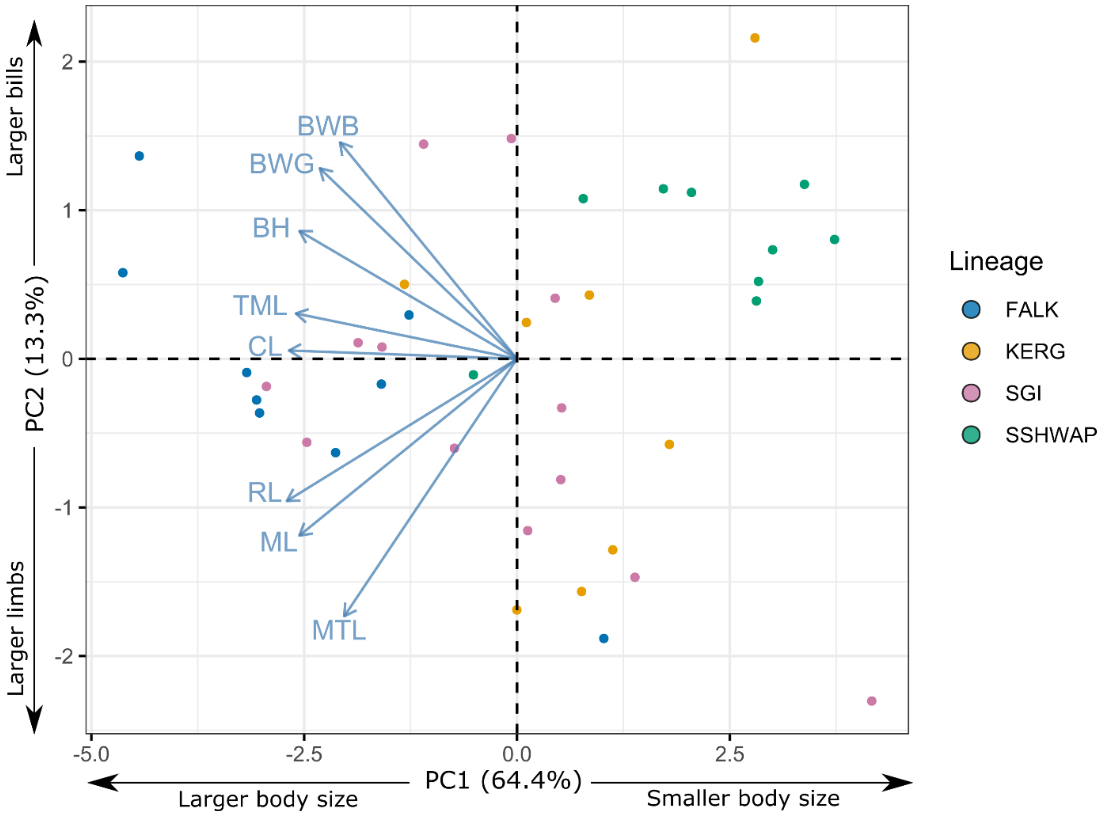

Figure 2.5: Principal Components Analysis of linear morphometrics. Acronyms: CL – culmen length; BWB – bill width at base; BH – bill height; BWG – bill width at gonys angle; RL – radius length; ML – manus length; TML – tarsus length; MTL – middle toe length.

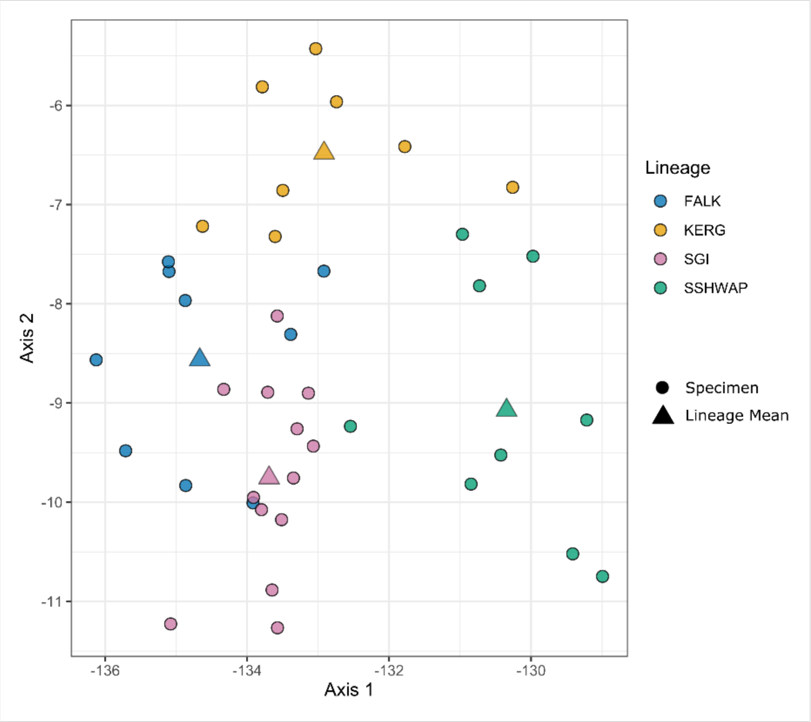

Figure 2.6: Linear Discriminant Analysis of linear morphometrics. Circles represent individual specimens with triangles showing the lineage mean.

Table 2.3. Pairwise MANOVA results between all gentoo penguin populations for linear traits. Approx. F values are below the diagonal with p values above. p values below .05 are indicated in bold. FALK – Falkland Islands, KERG – Kerguelen Island, SGI – South Georgia Island, SSHWAP – South Shetlands/Western Antarctic Peninsula.

	FALK	KERG	SGI	SSHWAP
FALK	***	**0.0446**	**0.0328**	**0.0017**
KERG	3.5921	***	**0.0008**	**0.0381**
SGI	3.1375	7.9891	***	**0.0003**
SSHWAP	9.0501	3.8098	9.0188	***

Table 2.4. ANOVA p-values between all gentoo penguin populations for individual traits. p values below 0.05 are indicated in bold. FALK – Falkland Islands, KERG – Kerguelen Island, SGI – South Georgia Island, SSHWAP – South Shetlands/Western Antarctic Peninsula. Culmen length (CL; taken along the medial line), bill width at the base (BWB), bill height at gonys angle (BH), bill width at gonys angle (BWG), flipper width (FW; shortest distance from anterior surface of flipper above the radiale to the posterior side of the flipper), radius length (RL), manus length (ML; indent at radiale/radius/ulna to distal wing tip), tarsus length (TML; anterior surface), and middle toe length (MTL; digit I11 excluding nail).

Lineage		Trait							
A	B	CL	BWB	BH	BWG	RL	ML	TML	MTL
FALK	KERG	0.0818	**0.0186**	**0.0046**	**0.0259**	**0.0063**	**0.0032**	**0.0011**	**0.0088**
FALK	SGI	0.0894	0.1339	**0.0208**	0.2493	**0.0003**	**0.0292**	**0.0242**	0.1997
FALK	SSHWAP	**0.0001**	0.0528	**0.0031**	**0.0384**	**0.0000**	**0.0000**	**0.0001**	**0.0006**
KERG	SGI	0.9107	0.1126	0.9795	0.1377	0.6134	**0.0232**	0.1164	**0.0286**
KERG	SSHWAP	**0.0005**	0.3824	0.3615	0.4174	**0.0056**	**0.0020**	0.5032	0.6737
SGI	SSHWAP	**0.0045**	0.4127	0.4413	0.2631	**0.0039**	**0.0000**	**0.0233**	**0.0024**

2.3.5 Discussion

Our integrative taxonomic approach has revealed four deeply divergent lineages within gentoo penguins. These lineages are associated with different regions in the Southern Ocean, formed reciprocally monophyletic clades and genetic clusters in all our analyses, and are morphologically distinct. The clusters found here differ slightly from those found in other recent studies. (Pertierra et al., 2020) studied individuals from three of the four lineages presented here alongside further island populations. Although they lacked samples from South Georgia and the South Sandwich Islands, they proposed a single Antarctic clade, grouping the Antarctic Peninsula, South Georgia, South Orkney Islands and South Sandwich Islands. This study finds that there is cryptic diversity within this clade, with the Antarctic Peninsula and South Georgia being both morphologically and genetically distinct from each other. Interestingly, when studying the usefulness of cranial versus postcranial traits in separating lineages, postcranial ANOVA tests produce far more significant results (19 out of 24, p<0.05) and are able to separate all pairwise lineages in comparison to the cranial trait tests (9 out of 24) which all failed to significantly separate the Kerguelen and South Georgia lineages. This strengthens the argument of not limiting analyses to only beak measures and instead including traits from the whole body. Given the evidence presented here, and the need to account for all species-level diversity in conservation planning, we recommend that the Pygoscelis genus be revised to include four species of gentoo penguin.

There are currently two recognised subspecies of gentoo penguin: *P. papua papua* and *P. papua ellsworthi*, representing the classic north/south split within gentoos (Stonehouse, 1970). Other subspecies of *P. papua* have been previously proposed, including P. *papua taeniata*, which has included various combinations of island populations since its inception in 1927 (Mathews, 1927; Peters, 1935). The Falkland Islands lineage will retain the name *P. papua*, given that *P. papua* was originally described from the Falkland Islands (Forster, 1781). The South Shetland Islands and Western Antarctic Peninsula lineage are currently considered as subspecies *P. p. ellsworthi*, therefore we propose that this lineage be elevated to a full species named *P. ellsworthi*. Based on previous genetic work, we conclude that the South Orkney Islands gentoos also belong to the *P. ellsworthi* lineage (Pertierra et al., 2020). The Kerguelen lineage was previously described as the subspecies *P. p. taeniata* (Mathews, 1927; Peters, 1935), which fell out of usage in the 1970s (Stonehouse, 1970), following which the Kerguelen gentoos have been classified as *P. p. papua*. We suggest the Kerguelen lineage now be designated as *P. taeniata* accordingly. We note that Mathews (1927) and Peters (1934) grouped Macquarie Island, Heard

Island, and Marion Island gentoos in *P. p. taeniata* with those from Kerguelen based on morphology. A genome-wide SNP study by Pertierra et al. (2020) showed that gentoos from Crozet and Marion Islands are effectively a single lineage, and Kerguelen Island gentoos are a distinct sister lineage. Analysis of Macquarie Islands gentoos is limited to mitochondrial DNA but shows this lineage to be sister to Crozet/Marion gentoos (Pertierra et al., 2020). At this stage we suggest that Crozet, Macquarie, and Marion Island gentoos are better considered as *P. taeniata* along with Kerguelen gentoos, rather than their current designation as *P. papua*, given the available evidence. However, this is subject to change pending detailed investigation with integrative taxonomic methods. Individuals from the South Orkneys, South Sandwich Islands, Price Edward Islands and Heard & Macdonald Islands should be assigned once further morphological and genome-wide studies are conducted given their geographical proximity to multiple lineages. The South Georgia lineage is currently classified as *P. p. papua* and, to our knowledge, there have been no previous subspecies or species suggested for South Georgian gentoos. We therefore describe this for the first time as

Pygoscelis poncetii sp. nov.

Common Name. South Georgia gentoo penguin

Zoobank Registry: urn:lsid:zoobank.org:pub:0DADF56F-ADD6-4A4C-A1DF-C18187700EF2

Holotype. American Natural History Museum (AMNH) 132462. Adult male collected by Robert C. Murphy at South Georgia, South Atlantic Ocean on 11th March 1913. The specimen was prepared as a museum flat skin and was used in the morphological analysis.

Paratypes. Specimens used in the morphological analyses. AMNH 132463, AMNH 132464, AMNH 132465: Adult males collected by Robert C. Murphy at South Georgia, South Atlantic Ocean on 11th March 1913. AMNH 269638: Adult female collected by Robert C. Murphy at Possession Bay, South Georgia, South Atlantic Ocean on 12th March 1913. AMNH 435821, AMNH 435822, AMNH 435823: Adults collected by Robert C. Murphy at Possession Bay, South Georgia, South Atlantic Ocean on 13th March 1913. AMNH 525826, AMNH 525827: Collected on South Georgia Island. Tring 1914_3_8_6, Tring 1914_3_8_7, Tring 1914_3_8_8: Adult males & female collected by P. Stammwitz at King Edward Point, South Georgia, South Atlantic Ocean in November 1913.

Etymology. *Pygoscelis poncetii* is named after Sally Poncet, whose body of work has significantly influenced the field of polar biology, particularly in relation to South Georgia.

Diagnosis. Morphologically, *P. poncetii* can be differentiated from all other species of gentoo by its manus length (mean length = 130.49 mm), being significantly smaller than *P. papua* (mean length = 135.08 mm, $p = 0.0292$) and significantly larger than both *P. ellsworthi* and *P. taeniata* (mean lengths = 115.38 mm and 125.27 mm, $p < 0.0001$ and $p = 0.0232$, respectively). Radius length differentiates *P. poncetii* (mean length = 52.68 mm) from the larger *P. papua* (mean length = 58.11 mm, $p = 0.0003$) and smaller *P. ellsworthi*
(mean length = 48.90 mm, $p = 0.0039$). Genetic comparative techniques (Pairwise F_{ST}, heterozygosity, clustering methods) found significant differences among all four species of gentoo penguin with the maximum likelihood phylogeny resolving each species as 100% supported. There are no discernible differences in plumage patterns among the four species.

Description of holotype. Black head with white band over the crown from eyebrow to eyebrow. Back dark blue grey with white on the ventral side between breasts and vent. Flippers dark blue grey edged with white. Black tipped orange bill. Orange/pink feet.

Measurements of the holotype. Culmen length: 59.85 mm, bill width at base: 18.27 mm, bill height at gonys angle: 17.07 mm, bill width at gonys angle: 9.88 mm, flipper width: 54.53 mm, radius length: 55.48 mm, manus length: 139.50 mm, tarsus length: 36.75 mm, middle toe length: 77.24 mm

Description of paratypes. No discernible variation in coloration was found in the proposed species, with all matching the description given for the holotype. Summarised as follows: Black head with white band over the crown from eyebrow to eyebrow. Back dark blue grey with white on the ventral side between breasts and vent. Flippers dark blue grey edged with white. Black tipped orange bill. Orange/pink feet.

Comparisons. The principal components analysis shows that size is the key delimiter among all species, with *P. ellsworthi* representing the smallest gentoo followed by *P. taeniata*, *P. poncetii* and *P. papua*. The separation of all species is supported by the significant pairwise MANOVAs across the full morphological dataset (Table 2.3). The individual pairwise ANOVAs of the univariate measures show that the new *P. poncetii* can be distinguished from all other species by its manus length (mean = 130.49 mm, range = 124.79-139.50 mm), with P. papua exhibiting a larger size (mean = 135.08 mm, range = 124.47-144.46 mm, $p = 0.0292$) whilst *P. ellsworthi* (mean = 115.38 mm, range = 110.07-126.72 mm) and *P. taeniata* (mean = 125.27 mm, range = 114.15-133.40 mm) are significantly smaller ($p < 0.0001$, and $p = 0.0232$ respectively). These morphological results show broad agreement with the univariate testing performed by (Stonehouse, 1970) but are now confirmed with modern multivariate methods.

In addition to morphology and genetics, there are notable ecological differences among the lineages. These include breeding habitat, which splits the flat beach and tussock grass nests of South Georgia and the Falkland Islands (Croxall & Prince, 1980; Reilly & Kerle, 1981) from the low-lying gravel beaches and dry moraines of the South Shetlands and West Antarctic Peninsula (B. Jablonski, 1984; Volkman & Trivelpiece, 1981). Lineages also differ in diet, particularly the proportions of crustaceans, fish, and squid consumed (Ratcliffe & Trathan, 2012). It has been observed that there is a trend of decreasing dietary variability and increasing krill consumption at higher latitudes (Bost & Jouventin, 1990). Importantly, several recent studies of gentoo penguin population sizes have reported very different trends, reinforcing the need to understand the risks to specific populations. Increases of 3.5% and 3.1% per annum have been recorded on the South Orkney Islands (*P. ellsworthi*) and South Shetland Islands (*P. ellsworthi*) respectively, whilst there has been a marked decrease of 1.4% and 2.3% per annum at Port Lockroy (a colony within *P. ellsworthi*) and across Kerguelen (*P. taeniata*), respectively, (Bingham, 1998; Dunn et al., 2016, 2019; Juáres et al., 2020; Lescroël & Bost, 2006).

Gentoo penguins are currently listed as “Least Concern” on the IUCN Red List, with their last assessment in 2018 (BirdLife International, 2018). In order to be listed as Vulnerable, a species must exhibit one or more risk criteria e.g., population size reduction greater than 30%, a limited geographic range, small population size, or evidence of likely extinction in the next 100 years (IUCN, 2021). Here we have shown that *P. papua* should be considered as at least four distinct species. While *P. papua* in the Falkland Islands and *P. ellsworthi* appear to be stable or increasing, (Baylis et al., 2012; Crofts & Stanworth, 2019; Dunn et al., 2016; Juáres et al., 2020), *P. taeniata* experienced a 30% reduction in numbers between 1987 and 2004 (Lescroël & Bost, 2006). *P. poncetii* may also be declining at South Georgia (Woehler et al., 2001). These two species should therefore be high priority for reassessment by the IUCN.

2.3.6 Concluding remarks

In this paper, we highlight hidden biodiversity within the species P. papua using genetic and morphometric methods, in keeping with recent assessments of hidden species diversity in birds. Our results clearly support the division of gentoo penguins into at least four species. We name a new species of gentoo, *P. poncetii*, and recommend elevation of three subspecies to species level (*P. taeniata*, *P. papua*, and *P. ellsworthi*). Our results show the importance of reassessing species boundaries as methodological advances are made. These findings have implications for the threat status of these species, and we urge that this diversity is considered in conservation planning for the Southern Ocean.

2.3.7 Data Accessibility Statement

Gentoo morphological data is provided in Supplementary Table A alongside accession numbers and location. Additional material is available from the Dryad Digital Repository: https://doi.org/10.5061/dryad.bs30388 for gentoo SNP data sets (Adapted from Clucas et al (2018) https://doi.org/10.1111/mec.14896).

2.4 Post-Commentary

If the argument for defining a species is that it represents an identifiable & evolutionarily unique set of organisms, the application of the phylogenetic species concept (Cracraft, 1983) seems to be the way forward, particularly in relation to the conservation implications of isolated populations for which reproductive isolation cannot be tested, as for Gentoo penguins. To discern hidden or cryptic species, an integrative approach should be taken, combining as many data sources as possible. There is a split between the theoretical and the practical when deciding on a species concept. Conservationists would argue that they are trying to protect the largest amount of biodiversity possible. As outlined in the manuscript, conservation initiatives are often focussed on protecting species level rather than population level diversity. Recognising cryptic species therefore enables accurate conservation assessments to be undertaken and strategies updated. Evolutionary Biologists may be less attuned to these problems and may be more interested in determining if a population is diagnostically distinct. Future collaborations between conservation organisations and evolutionary biologist should focus on organismal groups that show signs of cryptic speciation.

3 INTRINSIC & EXTRINSIC DRIVERS OF SHAPE VARIATION IN THE ALBATROSS COMPOUND BILL

3.1 Opening Remarks

Studies of morphological disparity at their heart are often answering two questions: 1) what is the phenotypic variation in the dataset as described by morphometrics? & 2) how do the measures of variation correlate with other data? In the context of the coupled nature of macroevolutionary tenets, the second question is of particular interest. Datasets containing information on phylogenetic diversity and niche adaptation are key in uncovering the drivers of morphological disparity. In evolutionary biology, these drivers or predictors of morphological disparity can be broadly split into two categories, intrinsic and extrinsic factors. Intrinsic factors are inherently organism specific like size and species relatedness (connecting to phylogenetic diversity) being predictors in shape analyses. Extrinsic drivers are measurable external datasets like climatic or dietary data relating to how the organism interacts with its surroundings, both relating to niche adaptation.

Studies on morphological disparity are having a renaissance through advancements in data collection and analysis pipelines. Not only can we now collect 3D data using high-throughput photogrammetry, surface scanning or medical scanning, there are new software approaches that allow automation in measuring and landmarking for geometric morphometrics (Baken et al., 2021; Bardua et al., 2019; Cooney et al., 2017; Felice et al., 2019; Goswami et al., 2019; Pigot et al., 2020). Museum collections allow for morphological studies that would be extremely difficult to achieve in the field. Seabirds, for example, have extremely large range sizes, and it would be near impossible to collect 3D data safely from living individuals. In this chapter, I use high-dimension morphological data, applying a 3D geometric morphometric framework to museum specimens, to answer key morphological questions about an iconic group of seabirds, Albatross.

3.2 Authorship and Permissions

This declaration concerns the article entitled:			
Intrinsic and extrinsic drivers of shape variation in the albatross compound bill			
Publication status (tick one)			
Draft manuscript ☐ **Submitted** ☐ **In review** ☐ **Accepted** ☐ **Published** ☒			
Publication details (reference)	Tyler Joshua, Hocking David P., and Younger Jane L. 2023. Intrinsic and extrinsic drivers of shape variation in the albatross compound bill. R. Soc. open sci.10230751230751 http://doi.org/10.1098/rsos.230751		
Copyright status (tick the appropriate statement)			
The material has been published with a CC-BY license ☒	The publisher has granted permission to replicate the material included here ☐		
Candidate's contribution to the paper (provide details, and also indicate as a percentage)	**J.T.**: conceptualization (lead), data collection (lead), formal analysis, investigation, methodology, writing—original draft, writing—review and editing; **D.H.**: conceptualization (supporting), data collection (supporting), writing—review and editing. **J.L.Y.**: supervision, writing—review and editing. Overall: J Tyler 85%, D Hocking 5%, JL Younger 10%		
Statement from Candidate	This paper reports on original research I conducted during the period of my Higher Degree by Research candidature.		
Signed (Typed signature)	Joshua Tyler	**Date**	29 August 2023

3.3 Manuscript: Intrinsic & extrinsic drivers of shape variation in the Albatross compound bill

3.3.1 Abstract

Albatross are the largest seabirds on earth and have a suite of adaptations for their pelagic lifestyle. Rather than having a bill made of a single piece of keratin, Procellariiformes have a compound rhamphotheca, made of several joined plates. Drivers of the shape of the albatross bill have not been explored. Here we use 3D scans of 61 upper bills from 12 species of albatross to understand whether intrinsic (species assignment & size) or extrinsic (diet) factors predict bill shape. Diet is a significant predictor of bill shape with coarse dietary categories providing higher R^2 values than dietary proportion data. We also find that of the intrinsic factors, species assignment accounts for ten times more variation than size (72% vs 6.8%) and that there is a common allometric vector of shape change between all species. When considering species averages in a phylogenetic framework, there are significant Blomberg's K results for both shape and size (K= 0.29 & 1.10) with the first axis of variation having a much higher K value (K=1.9), reflecting the split in shape at the root of the tree. The influence of size on bill shape is limited, with species assignment and diet predicting far more of the variation. The results show that both intrinsic and extrinsic factors are needed to understand morphological evolution.

3.3.2 Introduction

Albatross (*Diomedeidae*) are the largest flying birds on earth. They are pelagic specialists, with several adaptations across their morphology including extreme wingspans and complex bill structures (Billerman et al., 2023; Brooke, 2004; Howell & Zufelt, 2019). Their wingspans and high wing aspect ratio provide the ability for highly efficient soaring, allowing them to easily travel large distances from their colonies and avoid intense competition with other marine predators, whilst their charismatic tubenoses are used to filter seawater for drinking (Brooke, 2004; Howell and Zufelt, 2019; Billerman *et al.*, 2023). These adaptations allow albatross to spend years on the open ocean without making landfall (Brooke, 2004; Howell and Zufelt, 2019; Billerman *et al.*, 2023). Albatross, along with other members of the seabird order Procellariiformes, have a unique overarching bill structure. Rather than having a single piece of keratin forming the rhamphotheca as in the vast majority of bird species (Figure 3.1A), it is constructed out of several plates of keratin to form a compound bill (Figure 3.1B) (Hieronymus & Witmer, 2010; Lönnberg, 1904; Piro, 2022).

Despite their highly specialised pelagic niches, albatross do show inter-specific variation across the anatomy, including differences in their bill shape (Figure 3.2) (Howell and Zufelt, 2019; Billerman *et al.*, 2023). Body size is clearly an important factor in aerodynamics and therefore the evolution of the albatross body plan, but its influence on more specific anatomical structures, such as bill shape, has been often overlooked (Piro, 2022; Wang & Clarke, 2014; Warham, 1977). Allometry describes the relationship between changes in a measurable trait with changes in size and is an inherently intrinsic driver of variation. The presence of a strong allometric signal can be an indicator that the bill structure is experiencing evolutionary constraints limiting variation within species, whilst a lack of allometry could point towards more extrinsic drivers of shape (Yamasaki et al., 2018). We are interested in the relationship of size and bill shape both within species (ontogenetic allometry) and between species (evolutionary allometry) to understand the relative importance of intrinsic factors at different taxonomic levels (Klingenberg, 2016).

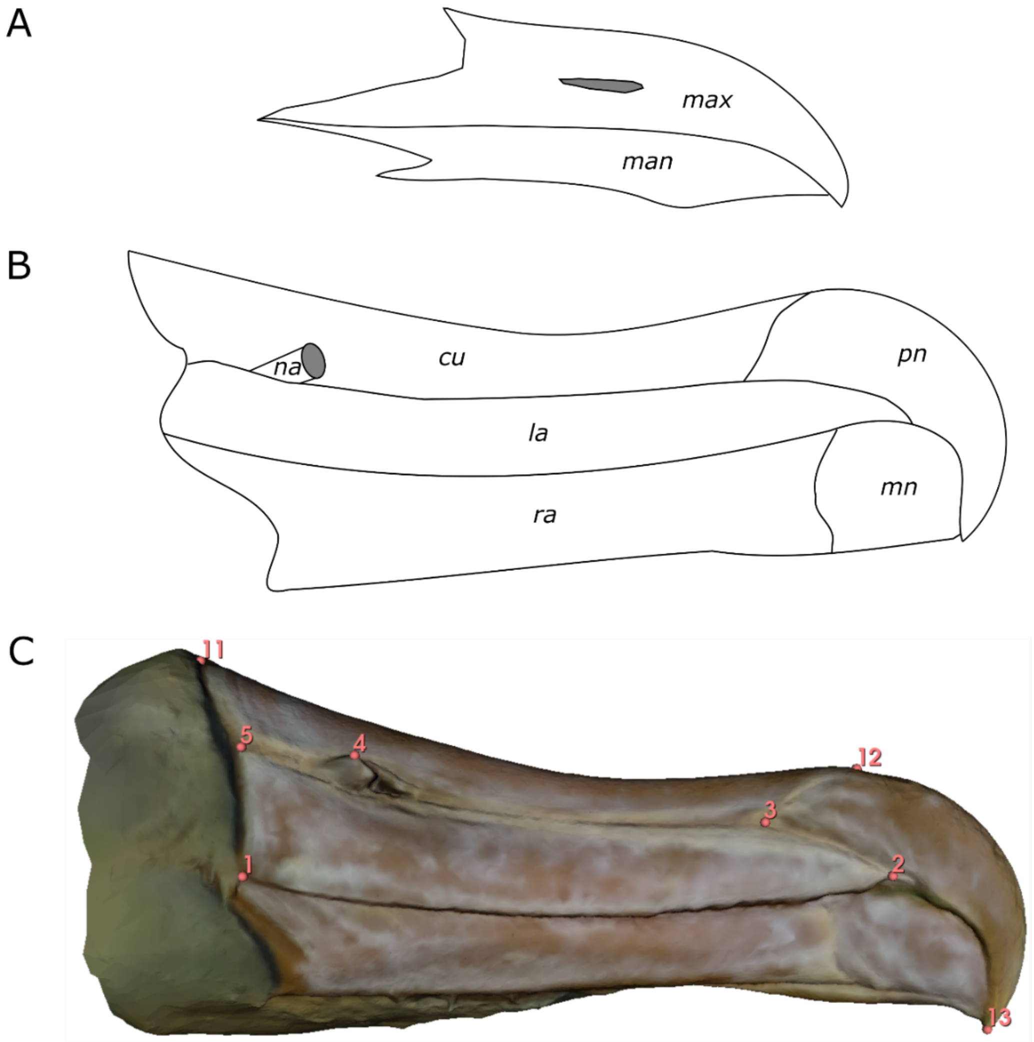

Figure 3.1: Compound Bill Morphology & Landmark Configuration. A) Bill morphology of European herring gull (*Larus argentatus*) B) Bill morphology of Wandering Albatross (*Diomedea exulans*) C) Landmarks 1-5 and 6-10 are paired (right-left) and landmarks 11-13 are found on the midline (see Table 3.1 for descriptions). Specimen B5348 (Campbell Albatross *Thalassarche impavida*). Abbreviations for A & B: max maxilla, man mandible, na naricorn, cu culminicorn, la latericorn, pn premaxillary nail, ra ramicorn, mn mandibular nail.

Figure 3.2: Albatross Study Species. Cladogram showing the twelve species included in the analyses alongside dorsal and lateral images of representative specimens. Green colouration due to image processing. Original specimen labels for TMAG B4827 & TMAG B5854 listed *Diomedea bulleri* and *Diomedea nigripes* respectively.

Table 3.1: Landmark descriptions. Landmarks 1-5 and 6-10 are paired (right-left) and landmarks 11-13 are found on the midline. See Figure 1C for visual.

#	Description
1	Posterior of latericorn along functional surface (right)
2	Anterior tip of latericorn (right)
3	Premaxillary nail, latericorn & culminicorn suture point on culminolabial groove (right)
4	Naricorn extreme (right)
5	Posterior of nasiolabial groove (right)
6	Posterior of latericorn along functional surface (left)
7	Anterior tip of latericorn (left)
8	Premaxillary nail, latericorn & culminicorn suture point on culminolabial groove (left)
9	Naricorn extreme (left)
10	Posterior of nasiolabial groove (left)
11	Posterior of culminicorn (Central)
12	Culminiolabial groove (Central)
13	Distal tip of premaxillary nail (Central)

The foraging ecology of many albatross species is closely monitored given their conservation risk (Billerman et al., 2023; Dias et al., 2019). During the breeding season, they operate as central place foragers but during the non-breeding season, this restriction is lifted and the foraging ranges for albatross species grow to almost oceanwide, with many species' ranges overlapping geographically (Hindell et al., 2020; Wakefield et al., 2009, 2014; Weimerskirch et al., 1988). Albatross diets cover a range of prey including cephalopods, fish, crustaceans, jellyfish, and other invertebrates, all found within the upper metres of the ocean surface, with some observations of opportunistic feeding on carrion (Cherel & Klages, 1998; McInnes et al., 2016, 2017). Variation in avian bill shape has been found to relate to divisions in foraging strategy in many taxa (Felice et al., 2019; Pigot et al., 2020; Tobias et al., 2022), therefore, understanding how albatross species are segregating in diet to avoid inter-specific competition may provide helpful insight into differences in phenotype, particularly in relation to bill shape. This raises the question of whether albatross bills and their associated keratinous plates are shaped through intrinsic constraints following allometric relationships or driven by extrinsic factors like diet and foraging ecology. Is the variation purely a function of body size differences or do they represent eco-morphological adaptations to minimise inter-specific competition?

Species identification and assignment in albatross is a complex challenge, especially for birds caught as fisheries bycatch far from their breeding colonies (Abbott et al., 2006). Over the last few decades, several studies have sought to clump and split species as advances in integrative taxonomic frameworks have evolved (Burg & Croxall, 2001, 2004; Nunn et al., 1996; Penhallurick, 2012; Penhallurick & Wink, 2004; Robertson, 1998). There are currently between 13 and 24 recognised species across four genera, with varying levels of sub-species assignment depending on the bird checklist (Billerman et al., 2023; Clements et al., 2019; Gill et al., 2021; Howard et al., 1991). Species identifications of wild albatross can be extremely difficult, with plumage colouration and size being key areas of evidence. In museum collections, this can be further complicated by preservation methods and historic species assignments. Shape and size variation in the bill could therefore be a useful tool for species identification, if species form discrete groups in the trait space.

In this study, we use 3D scans of albatross bills to assess patterns and drivers of shape variation. In particular, we address the following questions: (i) What are the key shape differences between albatross species, and can they be used for species delimitation? (ii) Do extrinsic and intrinsic factors like diet and size drive shape variation? (iii) What influence does phylogeny have in partitioning the morphospace of albatross bills?

3.3.3 Materials and Methods

3.3.3.1 Data collection & photogrammetry of museum specimens

Using specimens from the zoological collection at the Tasmanian Museum and Art Gallery, we sampled 61 individuals from 12 species of albatross covering all 4 genera, predominantly targeting Southern Ocean species (Figure 3.2). These included the Antipodean Albatross (*Diomedea antipodensis*, n=1), Southern Royal Albatross (*Diomedea epomophora*, n=3), Wandering Albatross (*Diomedea exulans*, n=10), Black-footed albatross (*Phoebastria nigripes*, n=1), Sooty Albatross (*Phoebetria fusca*, n=4), Light-mantled Albatross (*Phoebetria palpebrata*, n=4), Buller's Albatross (*Thalassarche bulleri*, n=2), Shy Albatross (*Thalassarche cauta*, n=6), Yellow-nosed Albatross (*Thalassarche chlororhynchos*, n=8), Grey-headed albatross (*Thalassarche chrysostoma*, n=8), Campbell Albatross (*Thalassarche impavida*, n=5) and Black-browed Albatross (*Thalassarche melanophris*, n=9). Whilst we have included most Southern Ocean taxa, we recognise that we have a much smaller sample of the North Pacific species, with only one of the four *Phoebastria* species included. The results are therefore focussed on Southern Ocean interpretations. For each individual, the upper bill was photographed as a representation of the functional surface of the bill. Each specimen was placed on a turntable within a lightbox, set one metre away from the camera (Canon SX70HS, resolution: 20.3 MP). A minimum of 62 images (4 concentric rings of 18 photos) were then taken by rotating the specimen 20° and photographing from four different heights (perpendicular to the specimen and 30°, 60° and 75° from the horizontal). Additional photographs were taken of the bill tip when the original 62 did not provide adequate coverage. This allowed the entire bill surface to be imaged with overlap between every photograph (i.e., every location on the bill appears in at least 2 photos to act as a tie-point in the photogrammetric reconstruction). A scaled 3D model was constructed within Agisoft Metashape, with each textured model being decimated to approximately 50,000 vertices for consistency (Agisoft, 2022). Models were then scaled to the nearest millimetre based on scales present in the images. The sample included a range of sizes for each species to reflect the change in size associated with ontogeny. All relevant permissions for handling the specimens were sought from the Tasmanian Museum and Art Gallery and granted.

3.3.3.2 Geometric morphometric analysis

Each scaled 3D model was imported into Slicer3D (Kikinis et al., 2014) and 13 type-I landmarks were applied (Figure 3.1C, Table 3.1). All subsequent analysis was conducted within R (R Core Team, 2022) using the "geomorph" & "RRPP" packages (Adams & Otárola-Castillo, 2013; Collyer & Adams, 2018, 2019). Once all specimens were landmarked, a generalised Procrustes alignment (GPA) was implemented using the "gpagen" function and the symmetric component of shape was retained for further analyses (symmetric shape=92% total variation; fluctuating asymmetry=8% total variation). Principal components analysis (PCA) was used to construct a bill morphospace for all specimens using the "gm.prcomp" function and all axes were retained for analysis. 3D warped meshes and wireframes were constructed to visualise the shape variation along PC axes using the *plotRefToTarget* function (Supplementary Material B).

3.3.3.3 Testing association between bill shape, ecology & size

To test for relationships between bill shape and ecology & size, we utilised the "procD.lm" function to perform Procrustes ANOVAs and MANOVAs. Diet data was collated from the EltonTraits database (Wilman et al., 2014) and includes a breakdown of proportion of invertebrates, proportion of fish and proportion of scavenging in the diet for each species. These proportions are then collated into one of three categories: Invertivore (66%+ invertebrates) or Vertebrate-Fish-Scavenging (66%+ fish & scavenging) or Omnivore (<66% in all categories). Only the Black-footed albatross is observed utilising scavenging in the data, with the remaining species consuming a mix of invertebrates or fish in inverse proportions. In the subsequent analyses, we therefore only use invertebrate proportion to reduce redundancy. Centroid size was extracted from the landmark data and was log-transformed for use in further analyses. We produced a size-shape PCA using the "plotAllometry" function with the "*size*.shape" method which combines the landmark data and centroid size data into a single matrix and performs a PCA, thereby reintroducing the size variable that was removed via the GPA. To test patterns in evolutionary and ontogenetic allometry, we fit 3 different linear models: 1) A Simple Allometric Model ($shape{\sim}Centroid\ Size$) where all taxa follow the same allometry vector, 2) A Common Allometric Model ($shape{\sim}Centroid\ Size + species$) where the vectors of shape change are parallel and the mean predictions are different (i.e. there is no interaction term with each species sharing the same gradient but having different intercepts), and 3) A Unique Allometric Model ($shape{\sim}Centroid\ Size + species + Centroid\ Size * species$) where the gradients and intercepts for each species are different (i.e. inclusion of an interaction parameter). We used the homogeneity of slopes (HOS) test, using the "*anova.lm.rrpp*" function, to compare the 3 different models with a significant result indicating that the allometric relationship is not the same for at least one species, either in terms of the species mean or the gradient of the regression line. In this case, we tested models sequentially in order of increasing complexity to test the inclusion of species means, excluding and then including the interaction term (i.e., Simple vs Common, then Common Vs Unique). The associated regressions, visualised in Figure 3.6, show if the individuals sat on the regression lines with no residuals. In this case, the y-axis is the first axis of a PCA on the expected fitted values of each individual (i.e., the model was a perfect fit). We also ran the simple allometry model for subsets of the data including for each species and for each genus.

3.3.3.4 Species averaging & phylogenetic analyses

To understand the influence of phylogeny, we averaged the landmark configurations of all specimens per species (excluding those that were identified as chicks) and then produced a new PCA onto which we mapped the phylogeny. The phylogenetic relationships were taken from the maximum clade credibility (MCC) tree of the Hackett backbone (Hackett et al., 2008) where the total bird tree was pruned to only the 12 species included in the analyses. To understand the phylogenetic signal, we used the "*physignal*" function to calculate Blomberg's K (Adams, 2014; Münkemüller et al., 2012) for both species shape and size. K=1 suggests that the signal strength is equal to that expected under Brownian Motion. Larger values mean that the taxa are more alike than expected under Brownian Motion with the opposite being true for K<1. For shape, the value of K was calculated for all axes of the phylogenetically aligned components analysis and also for each increasing dimension (K by p: i.e., 1, 1:2, 1:3) to understand how the addition of each dimension affects the signal.

3.3.4 Results

3.3.4.1 Shape variation in albatross bills

Variation across the albatross bill is split across several key axes of variation. The first principal component (47.59%) separates the *Thalassarche* genus from the *Diomedea, Phoebetria* & *Phoebastria* genera, with individuals from wandering & shy albatross representing the extreme positions. The axis is dominated by variation at the anterior and posterior of the bill, in particular the relative contribution of the latericorn and culminicorn to the overall caudal thickness. Individuals with more negative PC1 scores have thinner latericorns & thicker culminicorns caudally and a more upright premaxillary nail sutures versus individuals with positive scores having much thicker latericorns, thinner culminicorns and elongate premaxillary nail sutures. The variation caudally also has an impact on the relative position of the nares, being more dorsal & posterior at negative scores and more centred at positive scores. The second principal component (17.46%) describes the relative elongation of both the latericorn and culminicorn and more broadly a change in the aspect ratio. The plates are proportionally longer & thinner for individuals with positive PC2 scores and shorter & thicker for those with negative scores (Figure 3.3A, Figure 3.4, Supplementary Material B). In this case, there are no obvious taxonomic splits, instead the extremes are occupied by a range of species. PC3 & PC4 account for smaller amounts of the overall variation (11.00% & 8.19% respectively; Figure 3.3B, Supplementary Material B). PC3 relates to the relative curvature of various sutures whilst PC4 is dominated the relative proportion of the premaxillary nail. This fourth axis is dominated by a single individual outlier at the positive extreme which represents a *Diomedea exulans* chick. Most taxa are well differentiated in the PC1-PC2 morphospace (Figure 3.3A), but that separation is lost in the PC3-PC4 morphospace (Figure 3.3B). Bill size falls into 3 clusters, split at the genera level, with *Diomedea* being the largest, *Phoebetria* & *Phoebastria* being the smallest and *Thalassarche* occupying an intermediate range (Figure 3.3C).

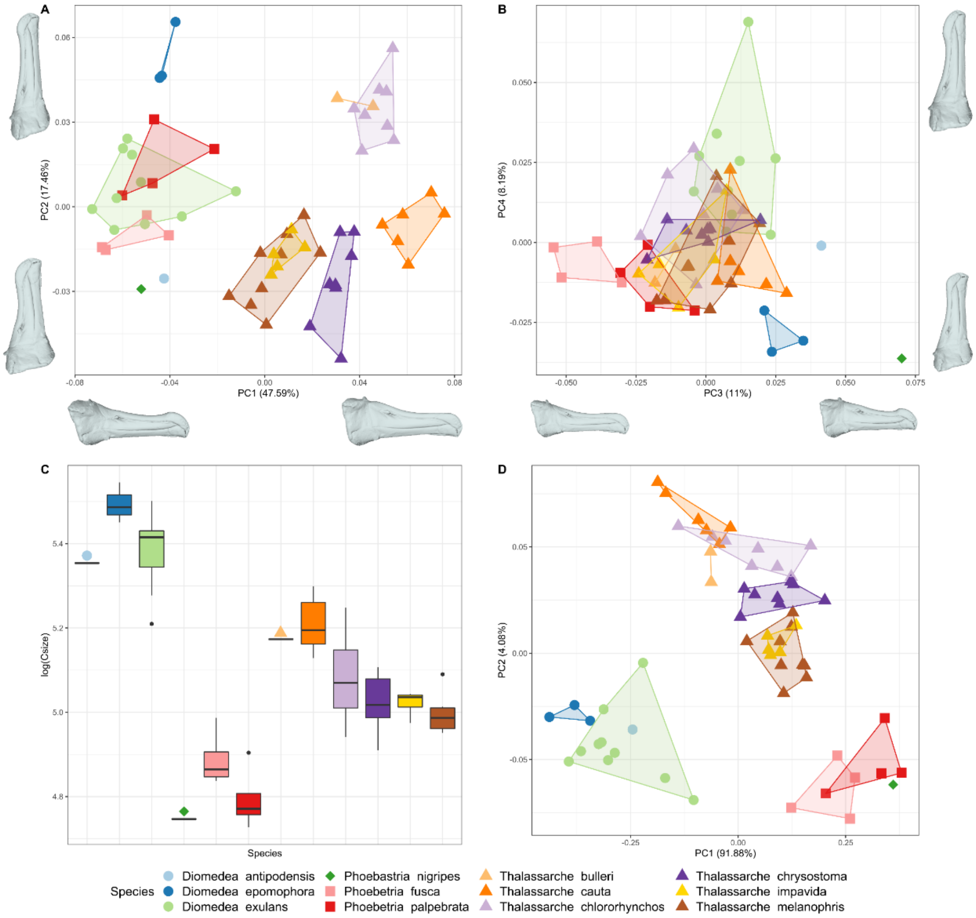

Figure 3.3: Shape and Size. A) Morphospace of first two principal components with convex hulls around species B) Morphospace of the third and fourth principal components with convex hulls around species C) Boxplot showing ranges of bill centroid size (key symbols used to identify bars where n=1 or n=2) D) First two axes of the Size-Shape morphospace based on the 13 landmarks and centroid size data.

When both size and shape are accounted for, all genera are clearly partitioned in morphospace (Figure 3.3D). Procrustes MANOVAs of shape and size against Species are both highly significant, with species means accounting for 90% of the variation in size and 79% of the variation in shape (p=0.001 for both tests, Figure 3.3A, B, C). Supplementary Material C contains the pairwise comparisons between species for both shape and size.

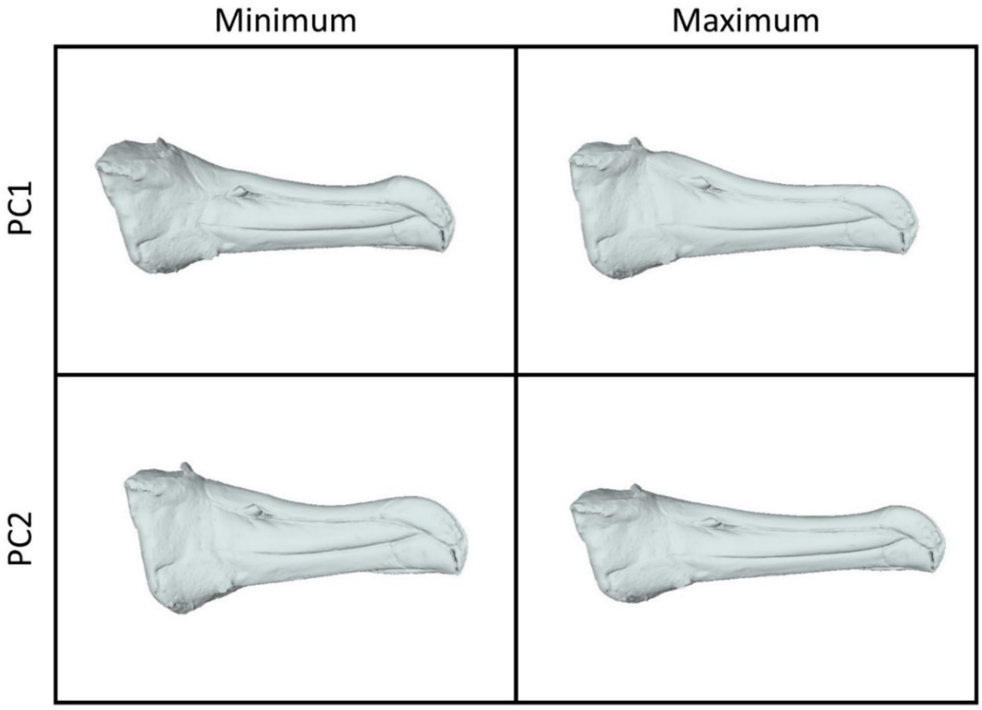

Figure 3.4: Relative Warps. Specimen B5348 (Campbell Albatross *Thalassarche impavida*) warped to the average shape and then to the extremes of Principal Component 1 & 2.

3.3.4.2 Evolution of bill shape in relation to ecology

Each Albatross species was assigned to one of three broad dietary categories: Omnivore, Invertivore & Vertebrate Fish Scavenger. Figure 3.5A shows these categorisations mapped onto the first two axes of the Principal Component space. Omnivores occupy positive PC1 space with both the more specialist diets (invertivores & fish-scavengers) occupying negative PC1 space. Both Omnivores and Invertivores are fully spread across PC2 with the Fish eating *Phoebastria* in the lower left quadrant.

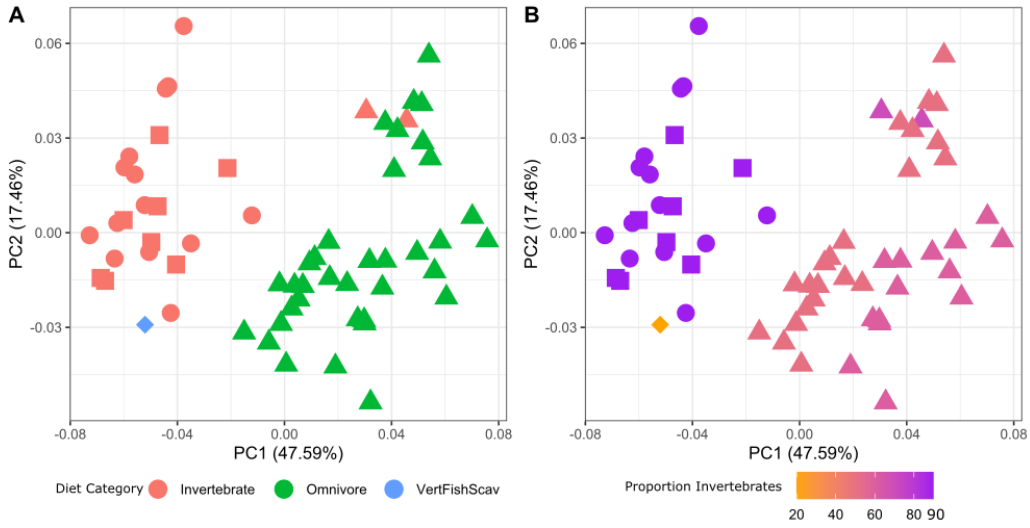

Figure 3.5: Diet. Both plots present first two PCA axes matching figure 4A with corresponding shapes mapping to Genera (Circle – *Diomedea*, Diamond – *Phoebastria*, Square – *Phoebetria*, Triangle – *Thalassarche*). A) Morphospace showing three discrete dietary categories: Invertivore, Omnivore, Fish & Scavenging B) Proportion of invertebrates in diet as given by the EltonTraits database

Overall, bill size and shape differ significantly among the three diet classes. Procrustes ANOVAs for shape and regular ANOVAs for size were both significant (shape: F= 18.092, p= 0.001, R^2= 0.38418; size: F= 5.6404, p=0.006, R^2= 0.16283). Pairwise comparisons of bill shape were all significant (Invertebrate:Omnivore p=0.001, Invertebrate:VertFishScav p=0.015, Omnivore:VertFishScav p=0.001); as were most pairwise comparisons of bill size (Invertebrate:Omnivore p=0.014, Invertebrate:VertFishScav p=0.010), with the exception of Omnivores and Fish Scavengers which did not differ significantly in size (p=0.172). When the proportions of diet are used, we find that bill shape and invertebrate diet proportion are significantly correlated based on an ANOVA test (F=20.235, p= 0.001, R^2=0.2553, Figure 3.5B), but has lower R^2 values than the coarse diet categorisation.

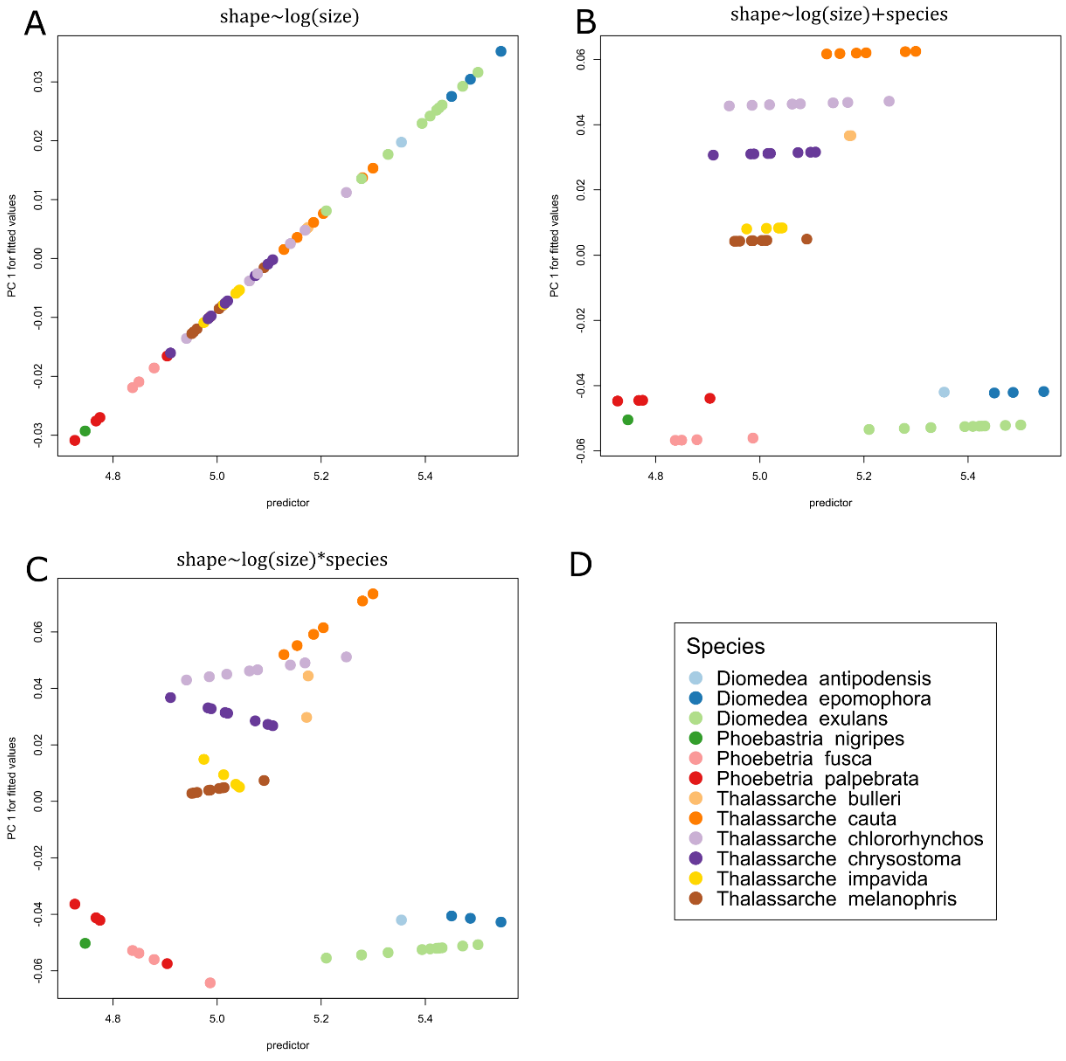

Figure 3.6: Comparison of three proposed allometric models predicting albatross bill shape. To test which allometric model best describes variation observed within albatross, three potential models (A-C). X-axis plots centroid size and y-axis plots Principal Component 1 of the fitted values of predicted shape (i.e., excluding the residuals) from the proposed regression. These panels are the equivalent of an R^2 equal to 1. A) Simple Allometric Model ($shape{\sim}Centroid\ Size$) where all taxa follow the same allometry vector B) Common Allometric Model ($shape{\sim}Centroid\ Size + species$) where the gradients of shape change are the same but the means are different (i.e. each species shares the same gradient but have different intercepts) C) Unique Allometric Model ($shape{\sim}Centroid\ Size * species$) where the gradients and intercepts for each species are different (i.e. inclusion of an interaction parameter) D) Legend for plots A-C

3.3.4.3 Allometric patterns within and between species

Allometry in geometric morphometrics uses linear models to predict shapes & construct shape change vectors using size and other covariates. In the simplest case, the predicted shape of an individual bill is dependent only on its size (Simple Allometric Model) whilst more complex models include predictions based on species assignment (Common Allometric Model) and allow interactions between covariates to produce different shape change vectors (Unique Allometric Model). We compared these three models, incorporating species means and associated interaction parameters alongside size, using a Homogeneity of Slopes test (described in the Methods and Materials and visualised in Figure 3.6). Positive and negative gradients in this context translate to having a certain vector of shape change associated with size and the steeper the gradient, the greater the shape variation with a unit change in size. We found that the Common Allometric Model (Figure 3.6B) produced a significant result when compared to the Simple Allometric Model (Figure 3.6A), yet there was not significant support to accept the Unique model (Figure 3.6C) (Simple vs Common; p=0.001 & Common vs Unique; p=0.266) (Supplementary Material D). This result translates to each species having a different predicted mean shape at a given centroid size, but the vector of shape change is common across all species with respect to size. The Common model accounts for ~80% of the variation with differences between species mean shapes explaining 10 time more than the size component (species: F=15.432, p= 0.001, R^2=0.726; size: F=15.926, p=0.001, R^2=0.068) (Supplementary Material D). The gradients of allometric shape change in the Common model are also very shallow indicating very small shape changes across the size ranges occupied by the albatross bills, approaching isometric growth (i.e., no shape change vector associated with size). Each species was subset and tested for significant allometry and only 2 species returned significant results (*Thalassarche impavida* - R^2= 0.527, p= 0.017, & *Thalassarche chrysostoma* - R^2= 0.328, p= 0.048). The test was repeated at the Genera level and both *Phoebetria* & *Thalassarche* have significant results (*Phoebetria* - R^2= 0.373, p= 0.013, & *Thalassarche* - R^2= 0.190, p= 0.001). In all of the significant results, the goodness of fit values were higher than in the Common model fit (R^2=0.068).

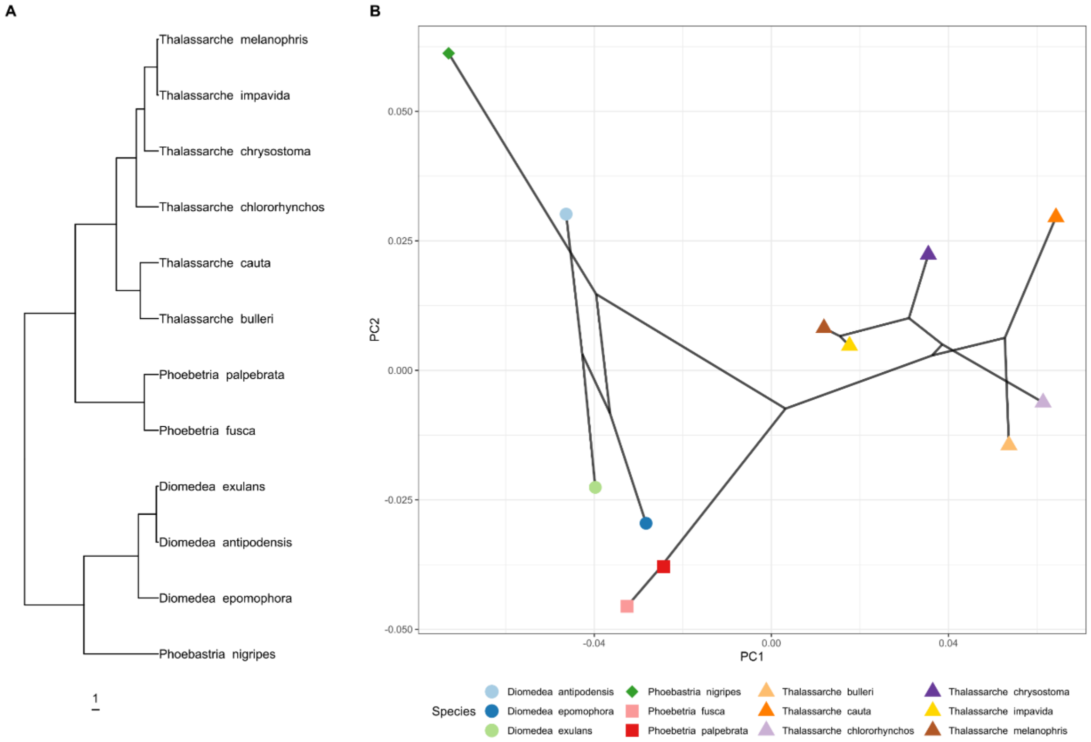

Figure 3.7: Phylogeny & Phylomorphospace. A) Scaled Albatross phylogeny used for analysis B) Phylomorphospace based on PCA analyses of species average bill shape. Colours and shapes match Figure 3.

3.3.4.4 Phylogenetic signal in species average shape

By averaging the bill shape for each species, we were able to understand the relative importance of phylogeny (Figure 3.7A) in driving the shape and size variation. Fitting Blomberg's K to both shape and size data returned statistically significant results for both (K= 0.29 & 1.10, p=0.001 & p=0.001, respectively). This implies that there is greater divergence in bill shape phylogenetically (compared to expectations under Brownian Motion), whereas bill size varies phylogenetically approximately as expected under Brownian Motion, i.e., more closely related taxa have relatively similarly sized bills, but greater than expected differences in shape. Another interpretation of the signal in shape is that the variance is found more within clades than between them. The K by p sequence shows that the first axis of shape has a remarkably high K value for that axis alone (K=1.9) but that is greatly reduced by the addition of subsequent axes (Table 3.2).

Table 3.2: K by p values. For each additional dimension, K is recalculated (K by p: i.e., 1, 1:2, 1:3) until all dimensions are included which matches the overall K value calculation.

# of axes	K Value
1	1.907207
2	0.601233
3	0.474638
4	0.427955
5	0.389136
6	0.354779
7	0.344101
8	0.339541
9	0.338771
10	0.297675
11	0.29136
12	0.29136

3.3.5 Discussion

3.3.5.1 Albatross bill size and shape variation

Here we show that albatross species are phenotypically divergent in both the shape and size of their bills. The majority of species and genera are clearly delineated by the first two principal components of the bill shape morphospace (Figure 3.3A), which together explain over 65% of bill shape variation. The bills of *Thalassarche impavida* (Campbell's albatross) and *Thalassarche melanophris* (Black-browed albatross) have complete overlap in both the shape and size-shape morphospaces (Figure 3.3A, 3.3C). *Thalassarche impavida* was historically considered a subspecies of *Thalassarche melanophris*, until it was elevated to a full species following genetic analyses (Burg & Croxall, 2001). Our finding reinforces the phenotypic similarity of the two taxa and is unsurprising given their shallow phylogenetic divergence (Burg & Croxall, 2001). Both the *Phoebetria species* (Sooty and Light-mantled albatross) overlap with *Diomedea exulans* (Wandering albatross) in shape morphospace. However, the inclusion of size into the morphospace (Figure 3.3D) completely separates the *Phoebetria* species from the *Diomedea* species, suggesting convergence in bill shape but divergence in size to occupy different foraging niches. This is achieved by eating proportionally sized prey, despite their dietary and range overlap in the South Atlantic and South Indian sections of the Southern Ocean between 40° and 60° South (Supplementary Material E) (Billerman et al., 2023; Ridoux, 1995; Xavier et al., 2003; Xavier & Croxall, 2007). This is reinforced by the results of the pairwise comparisons of shape and size between species. *Phoebetria palpebrata* is not statistically different in shape from any of the *Diomedea* species ($p>0.11$) but is significantly different in size ($p<0.01$) (Figure 3.3C, Supplementary Material C). The use of the bill for species identification seems well founded, with 50 of the 66 pairwise comparisons recovering a statistically significant difference in either shape or size or both. Of the comparisons that were non-significant, 10 included species that only had one or two individuals in the dataset. Where sample sizes were high, species were readily discernible by one or both features.

3.3.5.2 Diet as an explanatory factor for bill shape

We found that both extrinsic (diet) and intrinsic (size) factors are found to play a role in driving upper bill shape variation. Species, diet, and size are all statistically significant predictors of an individual's bill shape, with species the strongest predictor. Diet was also found to be a significant predictor of bill shape, particularly in the case of the differences between omnivores and invertivores.

Specialist invertivores and fish-scavengers dominate the negative PC1 region of the morphospace, with the generalist omnivores occupying the positive PC1 region (Figure 3.5A). When we break down the "generalist omnivore" category to consider the specific dietary proportions a slightly different pattern emerges. Taxa that consume a 50:50 split of invertebrates and fish sit in a valley between increasing invertebrate proportion; *Diomedea* & *Phoebetria* both consume high (90%) proportions of invertebrates at the negative PC1 extreme whilst *T. chrysostoma* & *T. cauta* show a much smaller increase (60%) in their invertebrate intake and occupy the lower right quadrant of the PC1-PC2 morphospace. One oddity is the position of the Black-footed Albatross (*Phoebastria nigripes*), here represented by a single individual. The Black-footed Albatross is a North Pacific species, and its dietary contents are known from a small number of studies, all indicating that a large proportion of its diet consists of flying fish eggs (Gould et al., 1997; Harrison et al., 1983). Therefore, whilst its diet consists of high proportions of fish (Figure 3.5A, B), the actual material being ingested is very different from the whole fish consumed by the *Thalassarche*. The other prominent exception is the position of the invertivore Buller's Albatross relative to the other invertivores. The morphospace shows a clear phylogenetic split between the *Thalassarche* genus and the other three included in the analyses. Therefore, the strength of phylogenetic conservatism may in this case be stronger than the extrinsic ecological pull to convergent morphologies, which has been documented in other specific bird groups but appears to be rarer at larger scales (Bright et al., 2016; Felice et al., 2019; E. T. Miller et al., 2017; Pigot et al., 2020).

3.3.5.3 Allometry

The influence of size on bill shape seems dependent on the taxonomic level, with both evolutionary & ontogenetic allometry signals being weak or sparse throughout the group. The results reiterate that of the intrinsic factors analysed here, species assignment is far more predictive than size. At the family level, based on the Homogeneity of Slopes testing, the Common Allometric Model best predicts bill shape, which implies that the shape change vector is shared across all species. This model however found that the predictive power of size was 10 times smaller than species assignment so despite both being significant predictors, the size signal is relatively weak. More interesting are the results from lower taxonomic ranks which point towards differing allometric patterns across the phylogeny. Only two species, *Thalassarche impavida* & *Thalassarche chrysostoma*, returned a significant allometric signal when each species was examined individually but when considering the genera level, two of the three Southern Ocean clades (*Thalassarche* & *Phoebetria*) had significant signals. This lack of signal in *Diomedea* alongside the shallow gradients of shape change found in the linear models points towards a predominantly isometric model of growth ontogenetically in the Great Albatross. Moreover, the predictive power of size in the allometric models decreases as the overall centroid size of the genera increases (Phoebetria R^2=0.373, Thalassarche R^2=0.190, Diomedea R^2=0.141 (non-significant)), suggesting that allometric constraint is stronger at smaller sizes.

3.3.5.4 Phenotypic differences mirror phylogenetic relationships

The strong phylogenetic patterns in Figure 3.7B and the K by p sequence point to deeper divergences in the past in terms of bill shape in Albatross. The large first K value in the sequence reflects the split at the root, seen in Figure 3.7B, delineating Genera on PC1. It suggests that the differences between genera are far more pronounced than those seen between species. Indeed, the Phylomorphospace (Figure 3.7B) shows how sister taxon are diverging in shape space, most likely through competitive displacement given range overlaps but other more distant related taxa are converging on common forms. This is most pronounced in between the *Diomedea* & *Phoebetria* species.

3.3.6 Conclusion

Here we have constructed one of the first 3D studies focussed on the Albatross compound bill. Despite being the largest seabirds, size is a relatively unimportant factor in the evolution of the albatross bill. Species means and coarse diet categorisation explain far more of the variation, as indicated by the ANOVA and Homogeneity of Slopes testing. We do find however that albatross species are indeed partitioning through differing shape and size to utilise similar resources, in this case invertivore specialists, whilst avoiding direct competition. The results show that both intrinsic and extrinsic factors should be considered when understanding morphological evolution. 3D data collection on at risk birds will be vital to understand their morphological adaptations and particularly in Albatross where the notion of a species is more complex.

3.3.7 Data Accessibility Statement

All data is available in the Supplementary Material A.

3.3.8 Acknowledgements

The authors would like to thank the curatorial team at TMAG for their assistance in providing specimens for the analyses and Julie McInnes for her advice on albatross diets. The authors acknowledge that TMAG is on the Country of the muwinina and murmirimina people, who did not survive British colonisation, and we pay our respects to the Tasmanian Aboriginal community. We honour the Aboriginal Elders past and present, and value the history, culture, and strength of the Tasmanian Aboriginal community.

3.3.9 Supplementary Material

Supplementary Material A: Classifiers and Covariates for each albatross individual.

Supplementary Material B: 3D Warped Mesh showcasing the shape variation on the first 4 principal components of Figure 3.3A & Figure 3.3B.

Supplementary Material C: Pairwise differences in bill shape and size between species. Upper half gives p-values from 1000 permutations in species assignment, with bold indicating significance. Lower half gives distance between species means.

Supplementary Material D: Homogeneity of Slopes and Procrustes ANOVA tests. p-values from 1000 permutations, with bold indicating significance.

Supplementary Material E: eBird Range Maps for Wandering, Sooty and Light-mantled Albatross.

3.4 Post-Commentary

This chapter adds to the growing literature surrounding morphological disparity that finds that there are several statistically significant covariates with shape, both intrinsic and extrinsic, across the avian clade (Bright et al., 2016; Cooney et al., 2017; Felice et al., 2019; Fröhlich et al., 2023; Navalón et al., 2019; Pigot et al., 2020). The difference here is that the homology of the bill can be studied in much greater detail thanks to the structure of the compound bill. While other studies with wider taxonomic scope have relied on landmark curves and meshes, here we are able to use the suture lines of the keratin plates to place type-I landmarks given the larger sample of homologous points, shown in Figure 3.1 of the manuscript.

Morphometric studies where shape is compared with different factors, either discrete categorisations or continuous measures, are inherently trying to measure the predictability of phenotypic evolution. The regressions performed in this chapter result in R^2 values, which measure the variation in shape explained by the independent factors. In a world where form-function relationships were infallible, diet could conceivably describe the entire variation in bill shape. Given that isn't the case, studies should endeavour to look at a range of intrinsic and extrinsic drivers of variation to ask questions about the contingent or deterministic nature of morphological disparity.

4 DIVING INTO A DEAD-END: ASYMMETRIC EVOLUTION OF DIVING DRIVES DIVERSITY AND DISPARITY SHIFTS IN WATERBIRDS

4.1 Opening Remarks

Evolution is fundamentally a stochastic process, but the resulting biodiversity seems to follow several patterns that would challenge that imperative. It could be argued that the finer the scale, the stronger the irreversibility; intrinsic features, such as genetic mutations, seem almost impossible to replicate completely in distantly related species (Dollo, 1893). Extrinsic features seem to reappear in a predicable fashion across macroevolutionary timescales, such as the evolution of the wing (Gleiss et al., 2011) or convergence in body shape & foraging strategies in secondarily marine tetrapods (Gutarra & Rahman, 2022; Kelley & Motani, 2015; Lindgren et al., 2010).

To complete the trifecta of macroevolutionary tenets, understanding niche adaptation is the most challenging, in part due to its slightly nebulous definition. Trying to characterise the ways in which organisms interact with the biotic and abiotic environment requires considerable amounts of data and thinking. By returning to the Venn diagram of Chapter 1 and investigating the overlapping regions between niche adaptation and its sister tenets, diversity, and disparity, so many intriguing questions can be asked, and we can assess the ways in which they are truly coupled.

Here, the focus is on a relatively qualifiable niche trait – diving. I considered the patterns of the evolution of diving across the entire Aequorlitornithes clade and whilst the categorisations are broad, the resolution of the signals found across waterbirds are striking. I then sought to understand diving's relative importance in driving phylogenetic diversity and morphological disparity. The overarching theme of this chapter is predictability: do traits evolve in a predictable fashion, does species diversification change in predictable ways and can we predict morphological traits from simple niche categorisations?

4.2 Authorship and Permissions

This declaration concerns the article entitled:			
Diving into a dead-end: Asymmetric evolution of diving drives diversity and disparity shifts in Waterbirds			
Publication status (tick one) **Draft manuscript** ☐ **Submitted** ☐ **In review** ☐ **Accepted** ☐ **Published** ☒			
Publication details (reference)	Tyler Joshua and Younger Jane L. 2022. Diving into a dead-end: asymmetric evolution of diving drives diversity and disparity shifts in waterbirds. Proc. R. Soc. B.2892022205620222056 http://doi.org/10.1098/rspb.2022.2056		
Copyright status (tick the appropriate statement) The material has been published with a CC-BY license ☒ The publisher has granted permission to replicate the material included here ☐			
Candidate's contribution to the paper (provide details, and also indicate as a percentage)	**J.T.**: conceptualization (lead), formal analysis, investigation, methodology, writing—original draft, writing—review and editing; **J.L.Y.**: conceptualization (supporting), supervision, writing—review and editing. Overall: J Tyler 90%, JL Younger 10%		
Statement from Candidate	This paper reports on original research I conducted during the period of my Higher Degree by Research candidature.		
Signed (Typed signature)	Joshua Tyler	**Date**	29 August 2023

4.3 Manuscript: Diving into a dead-end: Asymmetric evolution of diving drives disparity shifts in Waterbirds

4.3.1 Abstract

Diving is a relatively uncommon and highly specialised foraging strategy in birds, mostly observed within the Aequorlitornithes (waterbirds) by groups such as penguins, cormorants, and alcids. Three key diving techniques are employed within waterbirds: wing-propelled pursuit diving (e.g., penguins), foot-propelled pursuit diving (e.g., cormorants), and plunge diving (e.g., gannets). How many times diving evolved within waterbirds, whether plunge diving is an intermediate state between aerial foraging and submarine diving, and whether the transition to a diving niche is reversible are not known. Here we elucidate the evolutionary history of diving in waterbirds. We show that diving has been acquired independently at least fourteen times within waterbirds and this acquisition is apparently irreversible, in a striking example of asymmetric evolution. All three modes of diving have evolved independently, with no evidence for plunge diving as an intermediate evolutionary state. Net diversification rates differ significantly between diving vs. non-diving lineages, with some diving clades apparently prone to extinction. We find that body mass is evolving under multiple macroevolutionary regimes, with unique optima for each diving type with varying degrees of constraint. Our findings highlight the vulnerability of highly specialised lineages during the ongoing sixth mass extinction.

4.3.2 Introduction

The emergence of new foraging niches via key innovations can increase both diversity and disparity by releasing taxa from former constraints. Innovations that have opened new ecological opportunities have often resulted in adaptive radiations, for example in Darwin’s finches in the Galapagos (T. Bell et al., 2012; Navalón et al., 2020), cichlid fishes in East African lakes (Ronco et al., 2021; Seehausen,

2006) and within both placental and marsupial mammals throughout their evolution (Couzens & Prideaux, 2018; Grossnickle et al., 2019). Yet, there is inherent directionality in niche shifts resulting from key innovations (Heard & Hauser, 1995; A. H. Miller & Stroud, 2022). This dichotomy is a key theme in macroevolution. Dollo's law of irreversibility (Dollo, 1893), Cope's rule on body size (Rensch, 1948) and Ratchet mechanisms in macroevolution (M. A. Balisi & van Valkenburgh, 2020; Brocklehurst, 2019; D. Jablonski, 2020) are all examples of asymmetry in evolution, where the trajectories of trait evolution appear irreversible and directional over various time scales, from generations to epochs.

Given the new evolutionary pressures being applied to the world's biodiversity by climate change (IUCN, 2021), understanding if highly specialised taxa are evolutionarily "trapped" in their current niches is of great interest. Taxa with adaptive plasticity may be able to "weather the storm" of change, whilst those specialised taxa evolving under macroevolutionary ratchets may face higher risk due to their lower capacity for change. One example is within penguins where this scenario is already playing out, with generalist foraging gentoo penguins faring better than the sympatric krill-specialist chinstraps in terms of population size (H. J. Lynch et al., 2012). Moreover, the success of gentoos has translated into expansions of their range and recently posited speciation events (Clucas et al., 2014; Herman et al., 2020; H. J. Lynch et al., 2012; Tyler et al., 2020).

Aequorlitornithes are a group of waterbirds, covering 727 species across 11 avian orders. Whilst the higher-order taxonomic placement of these species has fluctuated in previous phylogenetic studies (Ericson et al., 2006; Hackett et al., 2008; Jetz et al., 2012), they were recovered as a single monophyletic clade in more recent analyses (Prum et al., 2015). They have a near global distribution and utilise habitats across the continents and oceans(Parkes & Austin, 1962). The group includes *Charadiiformes* (Shorebirds, Gulls, Terns, Woodcocks etc., n=369), *Ciconiiformes* (Storks & Openbills, n=19), *Eurypygiformes* (Sunbittern & Kagu, n=2), *Gaviiformes* (Loons, n=5), *Pelecaniformes* (Herons, Pelicans, Ibis, Bitterns etc, n=106), *Phaethontiformes* (Tropicbirds, n=3), *Phoenicopteriformes* (Flamingos, n=6), *Podicipediformes* (Grebes, n=19), *Procellariiformes* (Albatross, Petrels, Shearwaters etc, n=128), *Sphenisciformes* (Penguins, n=18) and *Suliformes* (Cormorants, Shags, Boobies etc, n=52)(Prum et al., 2015). Aequorlitornithes represents the largest clade of aquatic species within Aves, with other aquatic species appearing primarily within *Anseriformes* (Waterfowl), *Gruiformes* (Rails, Cranes, Moorhens etc.) and *Coraciiformes* (Kingfishers)(Parkes & Austin, 1962; Prum et al., 2015). Most of the Aequorlitornithes forage in marine, coastal, or freshwater environments, taking a range of prey from insects to fish. Several clades within Aequorlitornithes have evolved the ability to dive to target underwater prey.

Diving is a trait reliant on a suite of highly specialised morphological adaptations (Butler & Jones, 1997; Eliason et al., 2020; Felice & O'Connor, 2014; Pabst et al., 2016). As such, diving may represent a key innovation responsible for opening new ecological opportunity, while simultaneously underpinning an evolutionary ratchet dooming diving clades to decline. Diving as a foraging strategy in birds is relatively uncommon and several studies have focused on the evolution of the strategy in specific taxonomic groups (e.g. penguins (Cole et al., 2022), *Charadriiformes* (Smith & Clarke, 2012), loons & grebes(Clifton et al., 2018), dippers (Smith et al., 2022), kingfishers (Crandell et al., 2019), *Hesperornithiformes* (A. Bell & Chiappe, 2022)). Many of these groups are found within Aequorlitornithes and several different diving techniques have evolved, including pursuit diving (wing and foot propelled) and plunge diving, with other taxa occupying various non-diving niches.

Here, we used recent high-resolution phylogenies and trait simulation techniques to explore the evolution of diving across all waterbirds. Specifically, we address the following hypotheses: 1) That the evolution of diving in waterbirds is asymmetric and transitions and reversions are rare; 2) Diving represents a key innovation resulting in higher rates of speciation and diversification; and 3) Diving represents a release from former ecological constraints and results in shifts in body mass.

4.3.3 Materials & Methods

4.3.3.1 Phylogenetic framework

The analyses are based on a composite tree of all birds with 100% species coverage, following the process implemented in Cooney et al (2017), in which the family-level genomic backbone of Prum et al (2015) and the within-family topologies of the maximum clade credibility (MCC) tree of the Hackett backbone (Hackett et al., 2008; Jetz et al., 2012) are combined producing a younger branching topology than previous hypotheses (Ericson et al., 2006; Hackett et al., 2008; Jetz et al., 2012). This composite tree was used as it returns a monophyletic clade of waterbirds, *Aequorlitornithes*, comprising 727 species. The composite tree was trimmed to this clade using the *extract.clade* function in *ape* (Paradis et al., 2004), which was then used in subsequent analyses.

4.3.3.2 Trait assignments and covariates

Taxa were assigned to a broad foraging niche (non-diving or diving, herein the 2-state system) and a detailed foraging niche (non-diving, plunge diving, pursuit foot diving or pursuit wing diving, herein the 4-state system). These assignments represent the foraging strategy primarily utilised by each species and were based on the foraging niches provided in Pigot et al (2020). Here, we take any species listed as using the "Aquatic plunge" or "Aquatic dive" foraging niche to be diving in the 2-state system. These were then classified into plunge diving, pursuit foot diving and pursuit wing diving in the 4-state system. Cases where small numbers of species were listed as "Aquatic surface" or "Aquatic aerial" within primarily "Aquatic plunge" clades were checked individually in Birds of the World (Parkes & Austin, 1962) to determine if plunge diving was also utilised by these taxa, and those taxa that fully submerge from plunge diving were recategorized. Any "Generalists" of the families *Laridae & Procellaridae* that fully submerge from plunging were also re-assigned to the plunge diving category. All assignments can be found in Supplementary Material B which includes the 2-state, 4-state and original Pigot foraging niches. IUCN extinction risk categories were obtained from the IUCN Redlist (IUCN, 2021), to investigate correlations with extinction risk. Primary dietary categorisation (Plant/Seed, Omnivore, Invertebrate, and Vertebrate/Fish/Scavenging) and body mass ($\log_{10}$ scaled from original measurement in grams) for each taxon were taken from the EltonTraits 1.0 database (Wilman et al., 2014).

4.3.3.3 Model support using the Akaike information criterion (AIC)

To determine the best model from each model set in the subsequent elements of analysis, we use the Akaike information criterion in order to rank models based on fit (Burnham et al., 2011). The AIC score is calculated as:

$$AIC = -2\ln(L) + 2K$$

where L is the likelihood, given as the probability of the data given the model, and K is the number of free parameters.

To measure the relative support for each model *i*, we calculated the ΔAIC value:

$$\Delta AIC = AIC_i - AIC_{min}$$

where AIC_{min} is the smallest AIC score. Models that have a ΔAIC of less than 2 should be considered as having substantial support, those between 2 & 7 have minimal support and those greater than 7 have no support. All models with $\Delta AIC < 2$ are reported and interpreted.

We finally calculated the AIC weight based on the AIC scores:

$$w_i = \frac{\exp\left(-\frac{1}{2}\Delta AIC_i\right)}{\sum_{j=1}^{J} \exp\left(-\frac{1}{2}\Delta AIC_j\right)}$$

where J is the number of models being assessed. AIC weights sum to 1 and models with higher support have larger values.

4.3.3.4 Ancestral states of foraging niche

We estimated ancestral states of foraging niche using stochastic trait mapping as implemented in *phytools* in R (Bollback, 2006; R Core Team, 2022; Revell, 2012). To ascertain the best transition rate model, we used the fitMK function within *phytools* for a range of Markov models with differing patterns of discrete trait evolution. For the 2-state system, three models were compared: “equal rates” (where the transition rate between the two states are identical, “ER”), “all rates differ” (where the transition rate can vary dependent on direction, “ARD”) and “no reversion” (where the transition rate from diving to non-diving is explicitly set at zero).

Seven models were compared for the evolution of the 4-state system; three allowed transitions among all four states (“equal rates”, “symmetric”, “all rates differ”); a further three set the transition rate from any diving state to non-diving as zero (“no reversion equal rates”, “no reversion symmetric”, “no reversion all rates differ”); and a final model (“no reversions all”) where only transitions from non-diving to the diving states were allowed.

Predictive performance of the models was assessed using Akaike Information Criterion (AIC) weights. The best performing models for the 2-state and 4-state systems were then simulated using the *make.simmap* function in *phytools* with 100 replications. These trait maps were then summarised to generate a posterior estimate of the foraging niche state at each node, and to estimate the mean number of transitions between each state.

4.3.3.5 Influence of traits on speciation rate

Speciation rates (expected number of speciation events in the next time unit, in this case millions of years) were calculated for each taxon (*i*) on the phylogeny using tip-associated rates with the following equation:

$$DR_i = (\sum_{j=1}^{N_i} l_j \frac{1}{2^{j-1}})^{-1}$$

where N_i = number of edges on path from species *i* to the root and l_j = length of edge *j* (Jetz et al., 2012; Title & Rabosky, 2019). This metric represents the inverse of its mean equal splits measure for each species *i,* which is a measure of the expected waiting time per-lineage before another speciation event occurs. The DR statistic was chosen as the primary measure of speciation given its state independence, model-free nature, and ease for comparison across many categorisations(Title & Rabosky, 2019).

To examine the correlation of foraging niche and diet with speciation rate (*DR*) we carried out a phylogenetic ANOVA test (phylANOVA in *phytools*) with posthoc Holm correction for multiple comparisons and eta squared (η^2) measures for effect size.

4.3.3.6 Influence of traits on net diversification rate

To test trait-dependence of the net diversification rate across the phylogeny, we applied binary state speciation and extinction (BiSSE

(Fitzjohn et al., 2009)) and hidden state speciation and extinction (HiSSE (Beaulieu & O'Meara, 2016)) methods. The BiSSE framework is a model-based approach to estimate the influence of a single binary trait on diversification rate, whereas the HiSSE framework is a BiSSE extension that can also account for hidden states (i.e., unmeasured traits). We modelled seven scenarios, based on the 2-state (diving vs. non-diving) system: 1. a dull null where net diversification rate is equal across the tree; 2. a BiSSE model where the net diversification rate is dependent solely on the diving state; 3. a model where the net diversification rate is only dependent on the hidden state (a null model for the BiSSE), 4. a HiSSE model including the diving state and a hidden state where net diversification is dependent on both states (i.e. 4 regimes); 5. a HiSSE model including the diving state and a hidden state only for non-diving (i.e. 3 regimes); 6. a HiSSE model including the diving state and a hidden state only for diving (i.e. 3 regimes) and 7. a null version of model 4 where the parameters are estimated only for hidden states (i.e. 4 regimes) . In all models, we allowed both turnover and extinction fraction to be estimated per regime and set all transitions between hidden states to equal probabilities. The model fits were assessed using AIC weights. State assignment probabilities for the best fitting model are given in Supplementary Material C for each taxon.

4.3.3.7 Modelling continuous trait evolution

Body mass distribution comparisons with foraging strategy used a phylogenetic ANOVA test (phylANOVA in *phytools*) with posthoc Holm correction for multiple comparisons and eta squared (η^2) measures for effect size.

To test if the tempo and mode of body size evolution was influenced by diving, we fit a series of macroevolutionary diffusion models to the comparative body mass dataset mapped onto the SIMMAP niche trees based on the ancestral state reconstructions for both the 2- & 4-state systems (Bollback, 2006; Felsenstein, 1973, 1985; Hansen, 1997; Revell, 2012). In total 14 models were fit using the *fitContinuous* and *OUwie* functions from the *GEIGER* and *OUwie* R packages (Beaulieu et al., 2012; Harmon et al., 2008): four regime independent models (BM1, OU1, EB, Trend) and five regime dependent models (BMS, OUM, OUMA, OUMV, OUMVA) which were run for both the 2-state and 4-state systems. Relative support for each model was assessed using the associated AIC weights Phylogenetic half-life was calculated by dividing log(2) by the calculated alpha parameter and indicated the amount of time for the trait value to decay half the distance towards the trait optima (Beaulieu et al., 2012). To test if flightless taxa were having an impact on the results, we also ran the 5 regime dependent models again with flightless taxa in their own regime (i.e., non-diving, diving, flightless). Included taxa were all species within family Spheniscidae, *Nannopterum harrisi*, *Podiceps taczanowskii*, and *Rollandia microptera*.

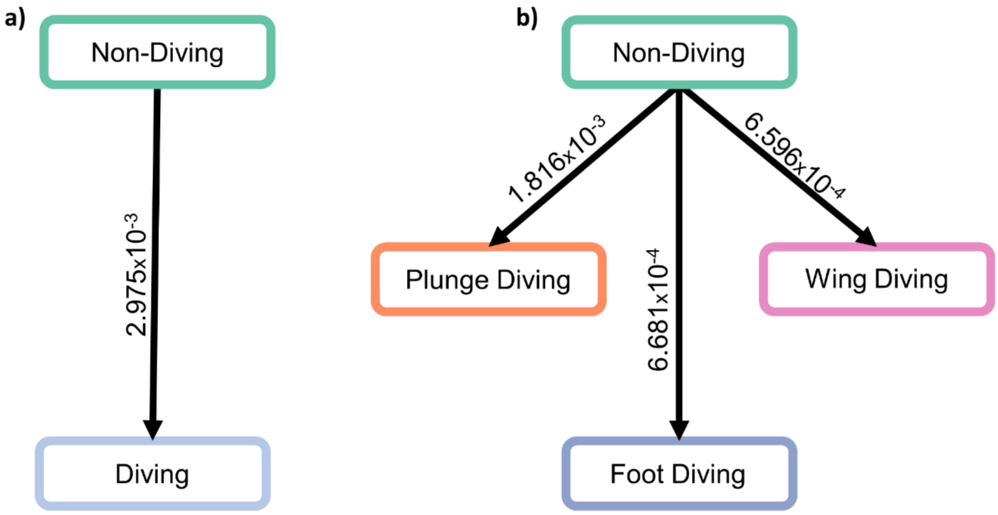

Figure 4.1: Transition Rate Models for the evolution of diving. Results from the fitMK models for a) 2-state system (No Reversion Model) and b) 4-state system (No Reversion Model). Values on arrows indicate transition rates. Both best fit models are asymmetric & unidirectional, with a transition rate of zero for diving to non-diving.

4.3.4 Results

4.3.4.1 Asymmetry of the evolution of diving

To assess whether the evolution of diving in waterbirds is asymmetric, we estimated the number of transitions to/from a diving niche. The 727 species of waterbird were each assigned to one of four diving traits (4-state system): non-diving, plunge diving, pursuit foot diving, and pursuit wing diving. These four states were also reduced to a binary system of non-diving vs. diving (2-state system). A suite of Markov models of discrete trait evolution were compared, ranging from equal transition rates among all traits to an All Rates Differ (ARD) model (Bollback, 2006; Revell, 2012).

In the 2-state system, both the No Reversion & ARD models of evolution had high support based on AICc weight (0.71 & 0.26, Table 4.1) and converged on the same solution whereby the transition rate from diving to non-diving was zero, with a transition rate towards diving of 2.97×10^{-3} (Figure 4.1a). Our ancestral state reconstructions recovered an average of 14 (95% HPD: 13-15) independent transitions to diving with no reversions (Figure 4.2).

Table 4.1: Mk model fits for 2-state system. Ordered by AIC weight. Transition rate given per million years.

Model Rank	Model Name	AIC Weight	ΔAIC	Non-Diving to Diving Rate	Diving to Non-Diving Rate
1	NR	0.7075	0	2.97×10^{-3}	0.00
2	ARD	0.2603	2	2.97×10^{-3}	0.00
3	ER	0.0323	6.17	2.38×10^{-3}	2.38×10^{-3}

In the 4-state system, the highest support (AIC weight 0.43, Table 4.2) was for a No Reversion All model which set the transition rate from diving states to non-diving and between diving states as zero. The remaining rates for transitions from non-diving to plunge diving, foot diving and wing diving were found to be 1.82×10^{-3}, 6.68×10^{-4} and 6.60×10^{-4}

respectively (Figure 4.1b, Supplementary Material A). Under this model the Ancestral State reconstructions found an average of 14 transitions among diving states within waterbirds: 8 from non-diving to plunge diving (95% HPD: 8-9); 3 from non-diving to pursuit foot diving (95% HPD: 3-3) and 3 from non-diving to pursuit wing diving (95% HPD: 3-4) (Figure 4.3; Table 4.3). The No Reversion Equal Rates model is also well supported (AIC weight 0.37, ΔAIC=0.30). Both models do not allow reversions back to non-diving, but the latter model allows for transitions between diving forms. Under this second model, the Ancestral State reconstructions find that the average number of transitions from non-diving to pursuit foot diving is unchanged (3; 95% HPD: 2-4), as is the number from non-diving to pursuit wing diving (3; 95% HPD: 2-4). The only difference in transitions between the two models is a reduction in non-diving to plunge diving transitions from 8 to 7 (95% HPD: 7-9), and the introduction of a single transition from pursuit foot diving to plunge diving (95% HPD: 0-2). The total number of transitions remains the same between the two models.

Table 4.2: Mk model fits for 4-state system. Ordered by AIC weight. Transition rates provided in Supplementary A.

Model Rank	Model Name	AIC Weight	ΔAIC	Log-likelihood
1	NR ALL	0.4306	0	-82.94
2	NR ER	0.3698	0.3045	-85.09
3	ER	0.1386	2.2668	-86.07
4	NR SYM	0.0430	4.6069	-82.24
5	SYM	0.0153	6.6719	-83.27
6	NR ARD	0.0025	10.2296	-82.05
7	ARD	0.0001	16.2296	-82.05

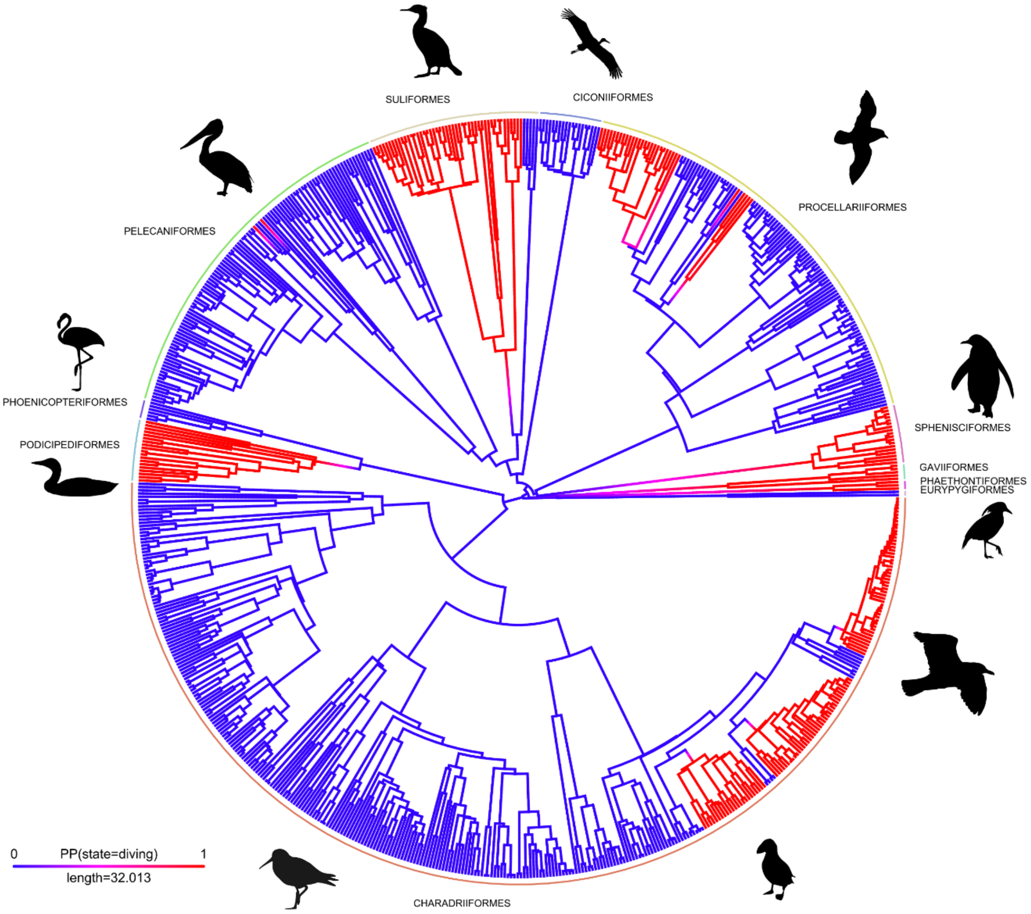

Figure 4.2: Multiple, convergent acquisitions of diving within Aequorlitornithes. Ancestral state reconstructions for the 2-State System: diving (red) vs. non-diving (blue). Our analyses recovered an average of 13.6 independent transitions to diving with no reversions, based on 100 simulations. Diving evolved convergently in 8 of the 11 Orders within Aequorlitornithes. Avian Orders are shown around circumference.

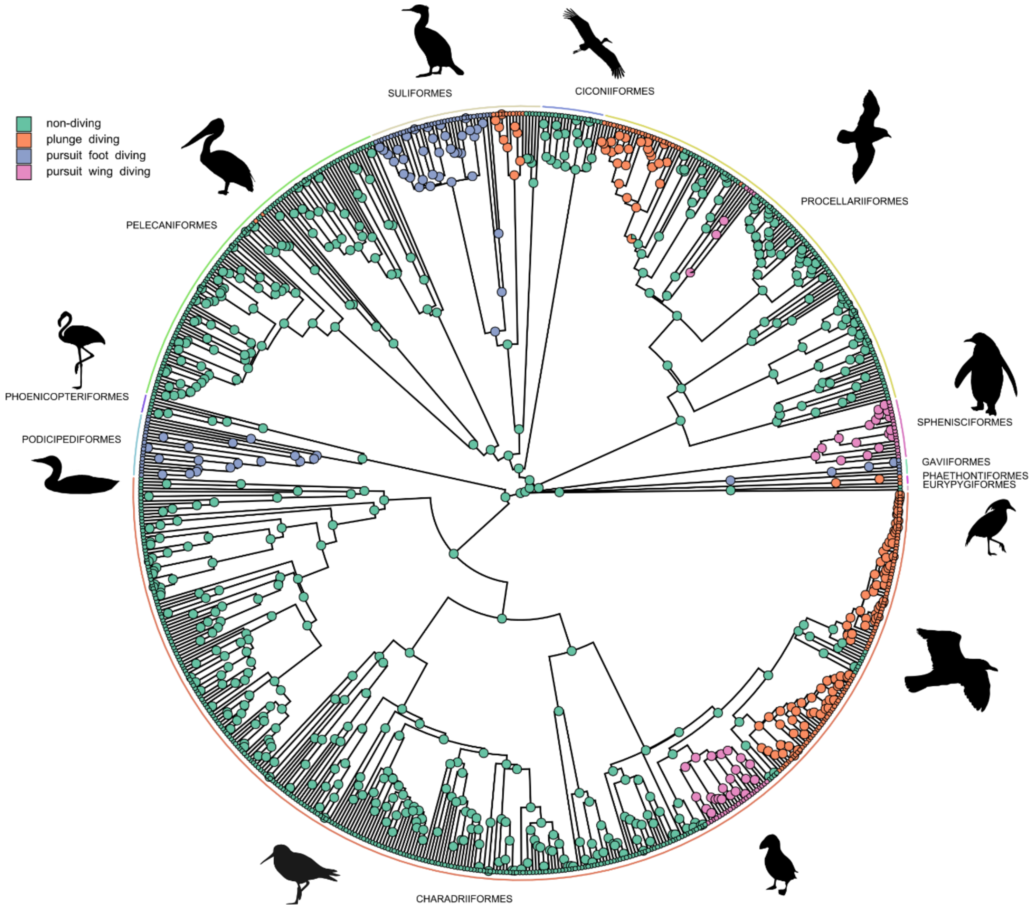

Figure 4.3: The evolution of diving niche in waterbirds. Ancestral state reconstruction for the 4-State System (non-diving, foot diving, wing diving, plunge diving) using the No Reversions All model. Pie charts on the internal nodes represent the proportion of assignment to each state over the 100 simulations. Our analyses recovered an average of 8, 3 & 3 independent transitions to plunge diving, pursuit foot diving and pursuit wing diving respectively, based on 100 simulations. Avian Orders shown around circumference.

Table 4.3: Average number of transitions between foraging niches in the 4-state system. Table reads row to column. Based on 100 SIMMAP simulations.

from	Non-diving	Plunge diving	Foot diving	Wing diving
Non-diving	NA	8.25	3.00	3.06
Plunge diving	0	NA	0	0
Foot diving	0	0	NA	0
Wing diving	0	0	0	NA

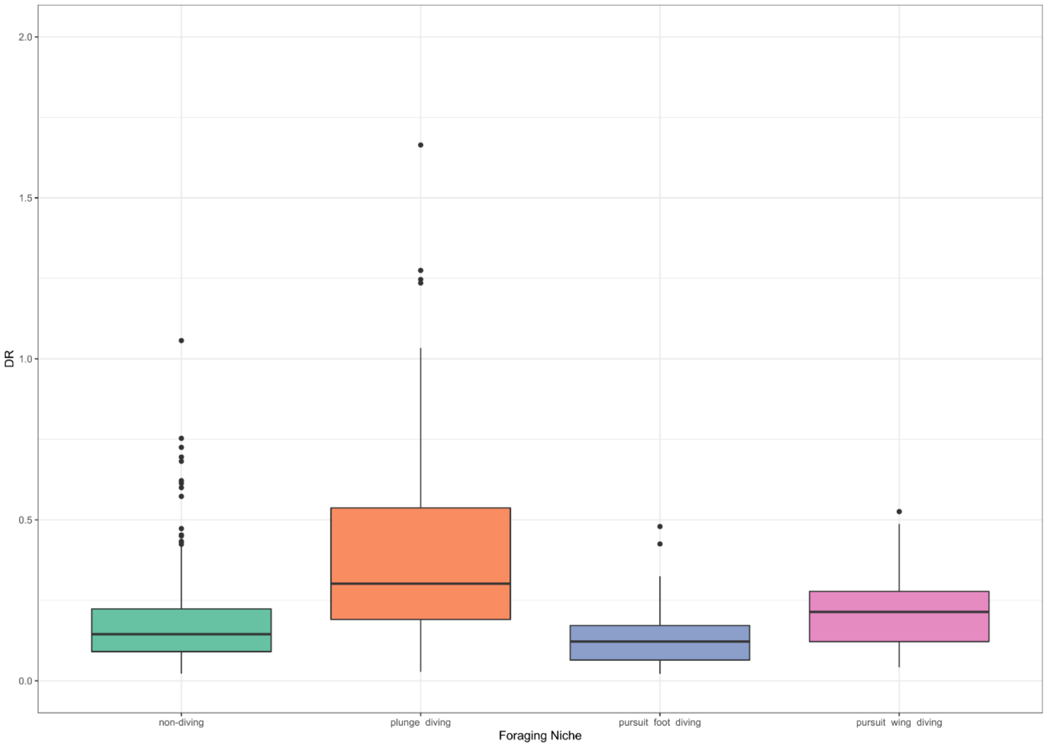

Figure 4.4: Speciation rate (DR) comparisons between diving niches. Diving taxa had a slightly higher speciation rates on average compared to non-diving taxa, but all phylogenetically corrected comparisons were statistically non-significant. Y-axis is truncated and 10 species with DR>2 are not shown for clarity (all within plunge diving niche). Taxon distribution: non-diving: 491, plunge diving: 130, pursuit foot diving: 61 & pursuit wing diving: 45. See Figure 3 & Supplementary Material B for Foraging Niche classifications.

4.3.4.2 Net diversification rates are correlated with foraging traits.

Speciation & diversification rates across the waterbird phylogeny were calculated to determine whether diving represents a key innovation facilitating a higher speciation or diversification rate. Tip rates (DR) were used as they provide a species-level metric that can be compared across the tree (Jetz et al., 2012; Title & Rabosky, 2019). We found that diving taxa have higher average speciation rates (DR) than non-diving taxa (diving: mean = 0.598, median = 0.245; non-diving: mean = 0.183, median = 0.145). This difference was significant based on a standard ANOVA, but non-significant using a phyloANOVA method ($p=4.97 \times 10^{-12}$ and $p=0.219$, $\eta^2=0.06$), attributable to the clustered nature of the diving on the phylogeny within certain orders. Only the standard ANOVA across the 4-state system was highly significant ($p=4.97 \times 10^{-12}$, $\eta^2=0.14$) with the phylogenetic ANOVA and pairwise t-tests producing non-significant results (Figure 4.4). When comparing speciation between the four dietary categories (Plant/Seed, Omnivore, Invertebrate, and Vertebrate/Fish/Scavenging), there were no significant differences in DR using a phyloANOVA method with a Holm posthoc correction (p=1.00 for all corrected pairwise comparisons).

HiSSE (Hidden State Speciation & Extinction) models allow for transitions between niches and net diversification rates within niches to be jointly estimated, providing a further method to understand the role of niche within speciation & extinction (Beaulieu & O'Meara, 2016; Fitzjohn et al., 2009). Simulations find strong support for the HiSSE Full model (speciation rates & extinction rates depend on both the diving character and a hidden character) (AIC weights ~ 1) (Table 4.4). Of the four regimes recovered, both non-diving regimes have positive net diversification (0A: 1.06×10^{-1} & 0B: 4.69×10^{-3}) whilst the diving regimes have a positive and a negative rate (1A: 1.06×10^{-1} &1B: -1.97×10^{-2}) (Figure 4.5, See Supplementary Material B for hidden state assignment probabilities).

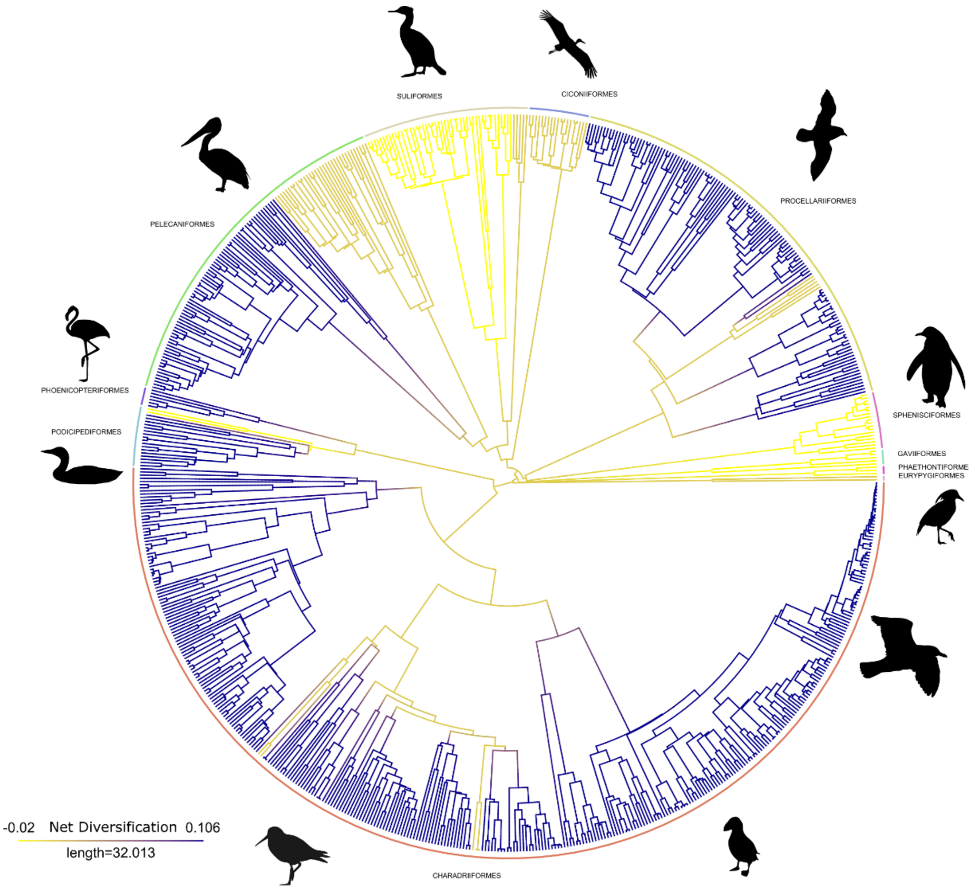

Figure 4.5: Net Diversification shifts between diving niches. Based on the HiSSE Full model (allowing for 2 defined states – non-diving (0) and diving (1); and 2 hidden states - A & B), there are 4 regimes with an associated net diversification rate (given as speciation rate minus extinction rate). The non-diving regimes both have positive rates (0A: $1.06x10^{-1}$ & 0B: $4.69x10^{-3}$) whilst the diving regimes have a positive and a negative rate (1A: $1.06x10^{-1}$ &1B: $-1.97x10^{-2}$). Avian Orders shown around circumference.

Table 4.4: HiSSE Model Results. Number of regimes corresponds to the sum of given and hidden states (i.e., for HiSSE Full there are two diving states, 0 & 1, and two hidden states, A & B).

Model Rank	Model Name	# of regimes	AIC Weight	ΔAIC
1	HiSSE Full	4	~1	0
2	HiSSE Null	4	0	178.6
3	BiSSE Null	2	0	246.2
4	HiSSE Non-Diving	3	0	568.8
5	HiSSE Diving	3	0	1579.3
6	BiSSE	2	0	2718.3
7	Dull Null	1	0	2836.5

4.3.4.3 Shifts in morphology following the evolution of diving

Body mass is a key morphological character and has been shown to dominate disparity signals in birds (Pigot et al., 2020). In the 2-state system, the standard ANOVA, not phylogenetic ANOVA, testing finds highly significant differences in mass distributions ($p=1.85 \times 10^{-10}$ & $p=0.219$, $\eta^2=0.05$) with diving birds occupying a heavier range. In the 4-state system, pairwise t-tests find significant differences between several states (p-values: non-diving – foot diving: 4.3×10^{-12}, non-diving – wing diving: 1.5×10^{-6}, plunge diving – foot diving: 1.9×10^{-6}, plunge diving – wing diving: 1.6×10^{-3}) but non-significant results when phylogeny is considered (Figure 4.6).

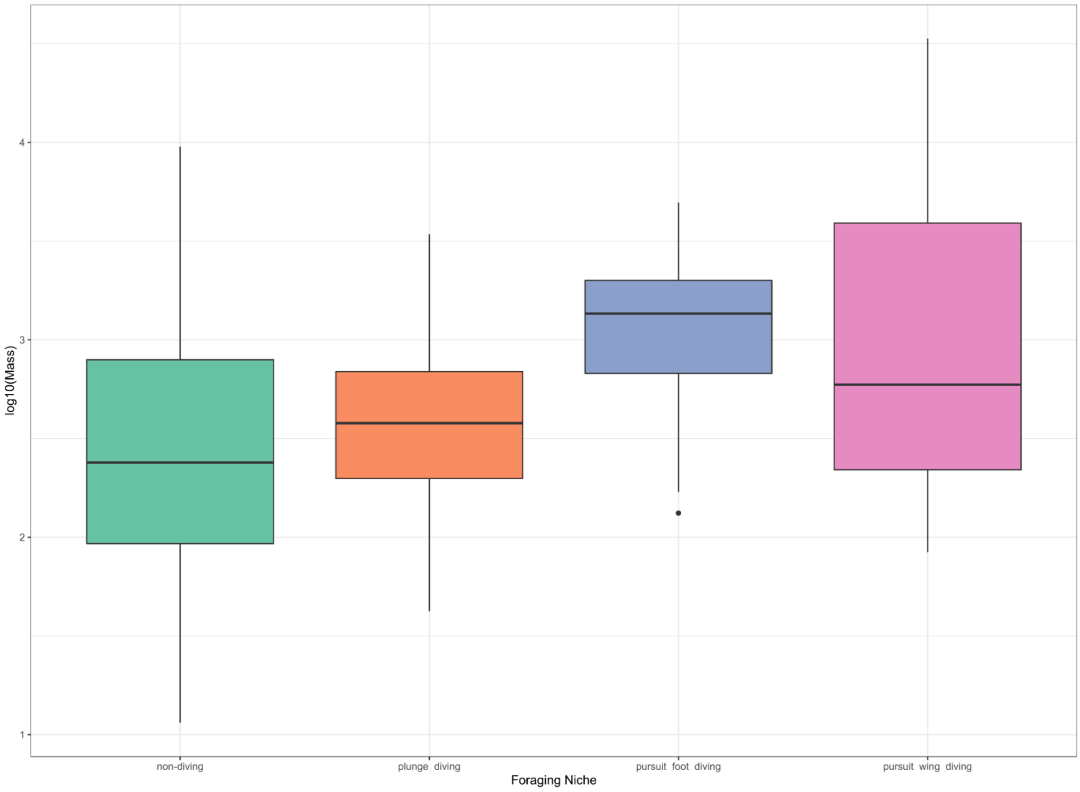

Figure 4.6: Body size comparisons between diving niches. Values shown are log$_{10}$(mass). Taxon distribution: non-diving: 491, plunge diving: 130, pursuit foot diving: 61 & pursuit wing diving: 45. See Figure 3 & Supplementary Material B for Foraging Niche classifications.

We considered the evolution of body mass on the phylogeny using multiple diffusion models of continuous trait evolution (covering both Brownian Motion and Ornstein-Uhlenbeck processes), grouping taxa according to both the 2-state and 4-state systems (Beaulieu et al., 2012; Felsenstein, 1973, 1985; Hansen, 1997; Harmon et al., 2008). Using AIC weights, the best fitting models for body mass evolution is OUMVA using the 4-state system (AIC weight= 0.98). The OUMVA model fits differing optima, alpha and variance parameters to each regime. These results correspond to wing diving birds having the heaviest body mass optima (θ=4.58) followed by foot divers (θ=3.00), with non-divers and plunge-divers having similarly small optima (θ=2.76 & 2.74, respectively). Both the alpha and variance parameters describe movement towards and around the trait optima. Plunge divers have the largest alpha and smallest variance of the 4 regimes (0.103 & 4.48x10^{-6}) with others having more intermediate values: non-diving: 0.025 & 0.024; foot diving: 0.044 & 0.005; and wing diving: 0.015 & 0.019. The alpha parameter can be converted into the phylogenetic half-life which indicates the strength of decay towards the optima. Wing divers have the longest half-life (46.1 Ma), compared to non-diving (27.7 Ma), foot diving (15.8 Ma), and plunge diving (6.71 Ma) (See Supplementary Material C for full results). Simpler models where only certain parameters were free had significantly lower support.

4.3.5 Discussion

Here, we show that the evolution of diving is irreversible in waterbirds. Transitions from non-diving to diving have occurred multiple times within modern Aequorlitornithes, but according to our analyses this is always a unidirectional acquisition. The evolution of diving therefore represents a macroevolutionary ratchet, i.e., repeated evolution towards a specialism from which reversion is not predicted. These ratchet patterns have been repeatedly found in the evolution of mammalian carnivores(M. Balisi et al., 2018; M. A. Balisi & van Valkenburgh, 2020; Brocklehurst, 2019; Strathmann, 1978), but here we develop one of the first large scale examples in birds, using the case of diving in waterbirds.

Furthermore, based on the most highly supported model of evolution (No Reversions All), we find that plunge diving is most likely not a required intermediate state between ariel and submarine flight, but rather all three modes of diving have evolved independently and convergently across the phylogeny. Diving has evolved in 8 of the 11 Avian Orders within Aequorlitornithes, with 14 unique transition events. Five of these transitions occurred on stems leading to Orders (*Podicipediformes, Suliformes, Sphenisciformes, Gaviiformes, Phaethontifomes*), whilst the other nine transitions are deeply nested within Orders (twice within *Pelecaniformes*, four times within *Procellariiformes* and three times within *Charadriiformes*). In the alternate model of evolution (No Reversions ER), all but 1 of the 14 transitions are unambiguously an acquisition of diving by a non-diving ancestor. Our discrete trait modelling predicts a single transition between diving niches (pursuit foot diving to plunge diving, within the *Suliformes*), however, this transition is only predicted in 87% of simulations, with the remaining 13% favouring a non-diving ancestor. Given the paucity of Orders where multiple diving niches have evolved and the lack of other transitions among diving niches, the result within Suliformes should be viewed with some caution.

We find evidence that the evolution of diving influences net diversification rather than speciation rates within Aequorlitornithes, yet diving does not appear to be a key innovation promoting speciation via ecological release (Heard & Hauser, 1995; A. H. Miller & Stroud, 2022). This may be because, whilst diving provides birds with access to a new environment, the aquatic niche is already partially occupied, e.g., by marine mammal, reptile, and fish lineages(Bestley et al., 2020; Halsey et al., 2006).

Our results indicate that some diving clades are experiencing negative net diversification (i.e., extinction rates larger than speciation rates). Of the 236 diving taxa included in the analysis, 75 (32%) were assigned to this negative diversification regime, including 72% of pursuit foot divers, 40% of pursuit wing divers, and 10% of plunge divers. The results from our hidden state models support the idea that diving is a partial driver of diversification shifts, with the HiSSE model indicating that there are other traits underpinning diversification regimes within waterbirds. It appears that the interaction between the diving state and the hidden state is the key driver rather than diving alone. This is reinforced by all taxa in hidden state A, irrespective of foraging strategy, having an equivalent diversification rate, which effectively reduces the four regimes to three, indicating that the hidden state is an important factor. Further studies incorporating wider behavioural, ecological, or environmental trait data may help elucidate these hidden drivers of speciation shifts in Aequorlitornithes.

Our analysis of phenotypic patterns shows that pursuit diving taxa are evolving towards larger body masses, with different optima for each diving strategy, whilst plunge diving and non-diving taxa have a similar smaller optimum. This is consistent with our understanding of diving physiology, in which larger body sizes seem to be selected for in diving birds and mammals, allowing for longer dive durations and deeper depths due to reduced metabolic rates, greater oxygen storage, and greater insulation (Cook et al., 2013; Halsey et al., 2006; Verberk et al., 2020). Moreover, our models show considerably more constraint on plunge diving taxa compared to non-diving and pursuit diving lineages, in terms of both the variance in body size and strength of selection towards the optimum. Essentially, the selective pressure for birds that rely on plunge diving for foraging to have body sizes around the optima is more intense than the selective pressure on size for other strategies, which may relate to the specific biomechanical requirements for plunge diving (Chang et al., 2016; Crandell et al., 2019; Eliason et al., 2020).

The possibility that diving taxa may be evolutionarily “trapped” in their current niches does not bode well for the long-term survival of these lineages. According to the IUCN Red List of Threatened Species (IUCN, 2021), 156 (21.5%) of the 727 Aequorlitornithes species are already listed as either Vulnerable, Endangered, or Critically Endangered. When considering diving taxa experiencing negative diversification specifically, that proportion rises to 32% (24 of 75 taxa). It remains to be seen whether diving specialists will be able shift their foraging niches in response to emerging evolutionary pressures, given the unidirectionality in the evolution of diving we have shown here.

4.3.6 Conclusion

The evolution of diving in Aequorlitornithes has occurred multiple times independently across the clade and is accompanied by a shift in morphological optima towards heavier body masses for pursuit divers and an increase in constraint on the range of body masses occupied by plunge divers especially. The shifts in discrete and continuous traits reflect macroevolutionary ratchets, with an inherent directionality and lack of reversals. These patterns, alongside the convergence on strategy and form, point towards evolutionary processes that favour the exploration of new forms and functions rather than a return to an ancestral state. However, these are associated with changes in net diversification rate and point towards a pattern of species filling moving niches in an adaptive landscape rather than exploring all options. With many diving taxa at risk as marine prey resources decline, this result reiterates the need to protect waterbirds globally.

4.3.7 Data Accessibility Statement

All data available either in original publications cited or in the Supplementary Material including R code used for analysis. Package Versions: R (4.1.2), OUwie (2.6), hisse (2.1.6), geiger (2.0.7), phytools (1.1-7), ape (5.6-2), ggplot2 (3.3.5), tidyverse (1.3.1).

4.3.8 Supplementary Material

Supplementary Material A: Transition rate matrices for the 4-state system.

Supplementary Material B: Data matrix containing all species used in analyses alongside categorisations and covariates.

Supplementary Material C: Results from body mass modelling including all parameter estimates.

Supplementary Material D: Phylogeny used for all analyses.

4.4 Post-Commentary

By applying the latest in modelling techniques, the simulation results uncover deep patterns within the waterbird clade and some surprising results on the coupled nature of macroevolutionary features, in this case, niche and diversification. However, it should be noted that modelling of speciation and extinction rate may be influenced by the inclusion of fossils. In the Aequorlitornithes, there is an imbalance and general paucity of fossil examples. For example, there are at least 40 known penguin fossil species, outnumbering extant taxa by almost 2:1 (Ksepka et al., 2006, 2023; Livezey, 1989). This abundance of Sphenisciformes is directly related to the preservation potential of their much denser bones in contrast to most flighted pelagic species. Therefore, this work should be seen as a first step in understanding the evolution of foraging niches within waterbirds and the addition of fossils could give an interesting perspective to the timings and rates of diversification within the group.

5 DISCUSSION

5.1 Chapter Syntheses

Chapter 1 explored the core tenets of macroevolution, proposing three primary areas of interest: phylogenetic diversity, morphological disparity, and niche adaptation. It went on to detail the connected and overlapping nature of each tenet and how their influence on each other manifests. From a taxonomic perspective, Seabirds represent a novel group to investigate these pillars as they contain abundant species diversity, an extraordinary range of morphologies and occupy niches found across avian evolution.

Chapter 2 further elucidated the topic of phylogenetic diversity and introduced the range of species concepts used to try and quantify biodiversity. Gentoo penguins had previously been suggested as harbouring hidden and cryptic biodiversity based on genetic evidence. Gentoos were therefore prime candidates for an integrative taxonomic approach combining genetics, morphometrics and ecological evidence to determine if they are indeed multiple species. DNA evidence found that populations formed monophyletic clades and these groupings were delineated by phenotypic measures of the bill, flippers, and legs. This combination of evidence led to the recommendation of elevating three gentoo subspecies to species level (*P. papua, P. ellsworthi, P. taeniata*) and the designation of a fourth species (*P. poncetii*).

Chapter 3 investigated a wider taxonomic group of seabirds, the albatrosses, and utilised a 3D dataset of rhamphothecae to understand intrinsic and extrinsic drivers of morphological evolution. The compound bill presented a novel opportunity to place homologous landmarks across the upper bill of twelve different species and test correlations with size and diet. Both were found to have statistically significant relationships with shape, but species assignment was the strongest predictor, highlighting an interesting use of bill shape in species identification. Despite the deep connection with size as the largest seabirds, the allometric signal is relatively weak and the associated shape change approaches isometry. In a phylogenetic context, the primary axis of bill shape variation is dominated by a strong phylogenetic signal separating genera that subsides as further axes are included. The outcome of the study emphasizes the need to look at many intrinsic and extrinsic factors when determining drivers of shape and size variation.

Finally, **Chapter 4** examined the evolution of phenotypes and niches, in particular the evolution of diving. This foraging strategy is used across birds but is found most frequently within waterbirds (Aequorlitornithes). Using ancestral state reconstructions, diving was found to have evolved at least 14 times independently across the waterbird phylogeny and there are no reversions to non-diving once this niche is occupied. The coupled nature of macroevolution was then further tested by assessing whether the evolution of diving affected diversity or disparity. Diversification modelling found that net diversification rates differed significantly and recovered a 3-rate system where some diving birds had negative rates. Moreover, disparity was also found to be connected to foraging niche as body mass in each diving type (pursuit wing, pursuit foot, plunge) was found to be evolving under differing levels of constraint. The asymmetry and diversification results are particularly significant, given the ongoing sixth mass extinction.

5.2 Can we untangle the macroevolutionary tenets?

The purpose of this thesis was to explore the interplay between macroevolutionary tenets and understand their impact on the evolution of seabirds. Each chapter has aimed to answer simple questions: How many species of penguin are there? How do Albatross bills differ? How many times has diving evolved? The surprising outcome of these analyses has been the complex nature of the answers. The complexity comes from the need to appreciate all aspects of the core tenets, highlighted in Figure 1.1 as the central overlapping region of the Venn diagram. It is evident that understanding the interaction between diversity, disparity and niche produce remarkably compelling patterns and results. None of the questions asked in each of the analysis chapters would have been soluble without following the tangled nature of macroevolution. This seems to hold true for a range of taxonomic scales, from the intra-specific analysis into gentoo diversity to the family level disparity analysis into albatross bills to the multi-order scale of diving within Aequorlitornithes. Macroevolutionary patterns must be viewed holistically, and hypotheses and analyses should be designed appreciating all the complexities and nuances of the core tenets.

5.3 Limitations & Future Work

Chapters 2, 3 & 4 present thorough analyses which explore macroevolution at a range of taxonomic scopes within seabirds. There are however several additional avenues of research that would overcome some of the limitations herein.

5.3.1 Phylogenetic hypotheses

Since the start of the 21st century, there have been a multitude of phylogenies constructed covering some or all avian species. Each of these phylogenetic hypotheses have key features and characteristics that differentiate them from one another. When studying the total waterbird clade, as in Chapter 4, the incongruence is even larger, with some trees finding a monophyletic group for all waterbirds

(Aequorlitornithes)(Prum et al., 2015) while others find varying degrees of para- & polyphyly (Ericson et al., 2006; Hackett et al., 2008; Jetz et al., 2012). At the smaller scales, Chapters 2 & 3 show that species numbers within individual families are in flux. Given the need to incorporate phylogenetic information into macroevolutionary studies, further work must be done on the refinement of clade-level avian trees. Seabirds are notorious for constantly being in phylogenetic flux (Ferrer Obiol et al., 2023; Friesen, 2015; Penhallurick, 2012; Penhallurick & Wink, 2004; Pertierra et al., 2020; Tyler et al., 2020), which is precisely why they are so fascinating to study. The results in Chapter 4 were a striking example of asymmetrical directionality within evolution but was very dependent on the phylogenetic structure and positions of diving birds. Future work in this area would be grounded in understanding the inter-specific relationships of waterbirds at all scales. Techniques used in Chapter 2 can be readily applied to other seabird groups, particularly those which have large representation in museum collections. Whilst birds are rare, in that a pan-avian phylogeny exists, it currently represents one of the rate-limiters to future macroevolutionary analyses.

5.3.2 Morphometric and niche datasets

Each of the three data chapters of this thesis involved collecting or collating new datasets, primarily based on phenotypes and ecomorphs. Birds have been a particular focus of the research community in recent years, with numerous large-scale morphological datasets being produced (Cooney et al., 2017; Felice et al., 2019; Pigot et al., 2020; Tobias et al., 2022). One large limitation that has plagued the analyses in this thesis has been the inability to travel to collect data due to the pandemic. As the taxonomic scope increased with each chapter, so did the required dataset size, which limited which traits could be focussed on. Utilisation of museum collections is vital for macroevolutionary studies like those included in this thesis. Concerted efforts by the international community to create specimen databases allow for greater species inclusion in studies and can help guide research questions based on specimen availability (Johnson et al., 2023). When thinking back to the three Macroevolutionary tenets framed in this thesis and the questions surrounding them, we can only answer questions with sufficient data.

5.3.3 The Fossil Record

The work presented here has focussed exclusively on extant taxa and ultrametric phylogenies. This was done primarily due to the imbalance of fossil data across seabirds and lack of access to fossil specimens due to the pandemic. More intuitively, the inclusion of fossils changes the very nature of the questions being asked. Our analysis into the evolution of diving does not include fossils due to the imperfect nature of assigning foraging ecologies to incomplete specimens that cannot be actively observed, a theme commonly discussed when considering form-function relationships (Benton, 2010; Hickman, 1988). Furthermore, the problems and differences in phylogenetic hypotheses for extant seabirds becomes even more acute when we try to include fossil taxa based purely on morphology, resulting in greater uncertainty within analyses. As we develop better statistical techniques to account for uncertainty in phylogenetic analyses, a key area for growth is incorporating fossil data into ecomorphological studies, particularly those where the available trait data from skeletal morphology only partially informs the character states.

5.4 Conclusion

The application of modelling within macroevolution has seen a rebirth in the last decade. Datasets of increasing size and dimensionality are being constructed for swathes of the tree of life, providing greater resolution and detail to test long held theories. The biodiversity we see today is a result of the interplays between phylogenetic diversity, morphological disparity, and niche adaptation. Within seabirds, the notion of a species has always been controversial and here we show that the application of morphometric and phenotypic analyses can shine a light on species level diversity. With the advent of higher and higher dimension datasets covering all aspects of phenotype, studies of morphological disparity can test fine scale form-function relationships. The avian bill remains a key area of study and the work on albatross here adds to that rich body of literature by finding that both extrinsic and intrinsic factors drive shape variation to varying degrees. Niche adaptation has always been a complex field, combining so many different aspects of evolutionary biology. By utilising the latest modelling techniques, the evolution of foraging niches can be teased apart by understanding how they appear and to what extent they influence diversity and disparity. In the case of waterbirds, a surprising asymmetry in the evolution of diving points towards increased specialisation and the risk of extinction. These results paint seabird macroevolution in a new light, uncovering new evidence of strongly coupled evolution of diversity, disparity, and niche. With studies investigating the tenets of macroevolution being published daily, we must endeavour to ensure that all aspects of macroevolution are considered as even simple questions result in complex answers.

REFERENCES

Abbott, C. L., Double, M. C., Gales, R., Baker, G. B., Lashko, A., Robertson, C. J. R., & Ryan, P. G. (2006). Molecular provenance analysis for shy and white-capped albatrosses killed by fisheries interactions in Australia, New Zealand, and South Africa. *Conservation Genetics*, *7*(4), 531–542. https://doi.org/10.1007/s10592-005-9064-y

Adams, D. C. (2014). A generalized K statistic for estimating phylogenetic signal from shape and other high-dimensional multivariate data. *Systematic Biology*, *63*(5), 685–697. https://doi.org/10.1093/sysbio/syu030

Adams, D. C., & Collyer, M. L. (2018). Multivariate Phylogenetic Comparative Methods: Evaluations, Comparisons, and Recommendations. *Systematic Biology*, *67*(1), 14–31. https://doi.org/10.1093/sysbio/syx055

Adams, D. C., & Otárola-Castillo, E. (2013). Geomorph: An r package for the collection and analysis of geometric morphometric shape data. *Methods in Ecology and Evolution*, *4*(4), 393–399. https://doi.org/10.1111/2041-210X.12035

Agisoft. (2022). *Agisoft Metashape Standard (Version 2.0.0)*.

Anderson, S. C., & Ruxton, G. D. (2020). The evolution of flight in bats: a novel hypothesis. *Mammal Review*, *50*(4), 426–439.

Baken, E. K., Collyer, M. L., Kaliontzopoulou, A., & Adams, D. C. (2021). geomorph v4.0 and gmShiny: Enhanced analytics and a new graphical interface for a comprehensive morphometric experience. *Methods in Ecology and Evolution*, *12*(12), 2355–2363. https://doi.org/10.1111/2041-210X.13723

Baldwin, S. P., Oberholser, H. C., Worley, L. G., & Valentine, J. M. (1931). *Measurements of birds,: Vol. v.2 (1931)*. https://www.biodiversitylibrary.org/item/122689

Balisi, M. A., & van Valkenburgh, B. (2020). Iterative evolution of large-bodied hypercarnivory in canids benefits species but not clades. *Communications Biology*, *3*(1), 461. https://doi.org/10.1038/s42003-020-01193-9

Balisi, M., Casey, C., & van Valkenburgh, B. (2018). Dietary specialization is linked to reduced species durations in North American fossil canids. *Royal Society Open Science*, *5*(4), 171861. https://doi.org/10.1098/rsos.171861

Bardua, C., Felice, R. N., Watanabe, A., Fabre, A. C., & Goswami, A. (2019). A practical guide to sliding and surface semilandmarks in morphometric analyses. *Integrative Organismal Biology*, *1*(1). https://doi.org/10.1093/iob/obz016

Barrowclough, G. F., Cracraft, J., Klicka, J., & Zink, R. M. (2016). How many kinds of birds are there and why does it matter? *PLoS ONE*, *11*(11), 1–15. https://doi.org/10.1371/journal.pone.0166307

Baumgart, S. L., Sereno, P. C., & Westneat, M. W. (2021). Wing Shape in Waterbirds: Morphometric Patterns Associated with Behavior, Habitat, Migration, and Phylogenetic Convergence. *Integrative Organismal Biology*, *3*(1). https://doi.org/10.1093/iob/obab011

Baylis, A. M. M., Zuur, A. F., Brickle, P., & Pistorius, P. A. (2012). Climate as a driver of population variability in breeding Gentoo Penguins Pygoscelis papua at the Falkland Islands. *Ibis*, *154*(1), 30–41. https://doi.org/10.1111/j.1474-919X.2011.01179.x

Beaulieu, J. M., & O'Meara, B. C. (2016). Detecting hidden diversification shifts in models of trait-dependent speciation and extinction. *Systematic Biology*, *65*(4), 583–601. https://doi.org/10.1093/sysbio/syw022

Beaulieu, J. M., O'Meara, B. C., & MacOS, X. (2012). OUwie: analysis of evolutionary rates in an OU framework. *R Package Version*. http://cran.r-project.org/package=OUwie%5Cnpapers://e21e3140-ccc7-4142-911c-e74fc5ceecf7/Paper/p11062

Bell, A., & Chiappe, L. M. (2022). The Hesperornithiformes: A Review of the Diversity, Distribution, and Ecology of the Earliest Diving Birds. In *Diversity* (Vol. 14, Issue 4, p. 267). Multidisciplinary Digital Publishing Institute. https://doi.org/10.3390/d14040267

Bell, T., Darwin, C., Eyton, T. C., Fitzroy, R., Gould, E., Gould, J., Hawkins, B. W., Jenyns, L., Owen, R., & Waterhouse, G. R. (2012). The zoology of the voyage of H.M.S. Beagle, under the command of Captain Fitzroy, R.N., during the years 1832 to 1836. In *The zoology of the voyage of H.M.S. Beagle, under the command of Captain Fitzroy, R.N., during the years 1832 to 1836.: Vol. pt.2 (1838*. London, Published by Smith, Elder and Co., 65 Cornhill, 1839-1843. https://doi.org/10.5962/bhl.title.61217

Benton, M. J. (2010). Studying function and behavior in the fossil record. *PLoS Biology*, *8*(3), 1–5. https://doi.org/10.1371/journal.pbio.1000321

Bestley, S., Ropert-Coudert, Y., Bengtson Nash, S., Brooks, C. M., Cotté, C., Dewar, M., Friedlaender, A. S., Jackson, J. A., Labrousse, S., Lowther, A. D., McMahon, C. R., Phillips, R. A., Pistorius, P., Puskic, P. S., Reis, A. O. de A., Reisinger, R. R., Santos, M., Tarszisz, E., Tixier, P., … Wienecke, B. (2020). Marine Ecosystem Assessment for the Southern Ocean: Birds and Marine Mammals in a Changing Climate. In *Frontiers in Ecology and Evolution* (Vol. 8, p. 338). Frontiers Media S.A. https://doi.org/10.3389/fevo.2020.566936

Billerman, S. M., Keeney, B. K., Rodewald, P. G., & Schulenberg, T. S. (2023). *Birds of the World*. Cornell Laboratory of Ornithology, Ithaca, NY, USA.

Bingham, M. (1998). The distribution, abundance and population trends of gentoo, rockhopper and king penguins in the Falkland Islands. *Oryx*, *32*(3), 223–232. https://doi.org/10.1046/j.1365-3008.1998.d01-39.x

BirdLife International. (2018). *State of the world's birds: taking the pulse of the planet.*

Bollback, J. P. (2006). SIMMAP: Stochastic character mapping of discrete traits on phylogenies. *BMC Bioinformatics*, *7*(1), 1–7. https://doi.org/10.1186/1471-2105-7-88

Bost, C.-A., & Jouventin, P. (1990). Evolutionary Ecology of Gentoo Penguins (Pygoscelis papua). *Penguin Biology*, 85–112. https://doi.org/10.1016/b978-0-08-057106-5.50011-5

Bouckaert, R., Heled, J., Kühnert, D., Vaughan, T., Wu, C. H., Xie, D., Suchard, M. A., Rambaut, A., & Drummond, A. J. (2014). BEAST 2: A Software Platform for Bayesian Evolutionary Analysis. *PLoS Computational Biology*, *10*(4), e1003537. https://doi.org/10.1371/journal.pcbi.1003537

Bright, J. A., Marugán-Lobón, J., Cobb, S. N., & Rayfield, E. J. (2016). The shapes of bird beaks are highly controlled by nondietary factors. *Proceedings of the National Academy of Sciences of the United States of America*, *113*(19), 5352–5357. https://doi.org/10.1073/pnas.1602683113

Brocklehurst, N. (2019). Morphological evolution in therocephalians breaks the hypercarnivore ratchet. *Proceedings of the Royal Society B: Biological Sciences*, *286*(1900), 20190590. https://doi.org/10.1098/rspb.2019.0590

Brooke, M. (2004). *Albatrosses and petrels across the world*. Oxford University Press.

Bryant, D., Bouckaert, R., Felsenstein, J., Rosenberg, N. A., & Roychoudhury, A. (2012). Inferring species trees directly from biallelic genetic markers: Bypassing gene trees in a full coalescent analysis. *Molecular Biology and Evolution*, *29*(8), 1917–1932. https://doi.org/10.1093/molbev/mss086

Burg, T. M., & Croxall, J. P. (2001). Global relationships amongst black-browed and grey-headed albatrosses: analysis of population structure using mitochondrial DNA and microsatellites. *Molecular Ecology*, *10*(11), 2647–2660. https://doi.org/10.1046/j.0962-1083.2001.01392.x

Burg, T. M., & Croxall, J. P. (2004). Global population structure and taxonomy of the wandering albatross species complex. *Molecular Ecology*, *13*(8), 2345–2355.

Burnham, K. P., Anderson, D. R., & Huyvaert, K. P. (2011). AIC model selection and multimodel inference in behavioral ecology: some background, observations, and comparisons. *Behavioral Ecology and Sociobiology*, *65*(1), 23–35. https://doi.org/10.1007/s00265-010-1029-6

Burress, E. D., & Muñoz, M. M. (2022). Ecological Opportunity from Innovation, not Islands, Drove the Anole Lizard Adaptive Radiation. *Systematic Biology*, *71*(1), 93–104. https://doi.org/10.1093/sysbio/syab031

Burton, M. G. P., Benson, R. B. J., & Field, D. J. (2023). Direct quantification of skeletal pneumaticity illuminates ecological drivers of a key avian trait. *Proceedings of the Royal Society B*, *290*(1995), 20230160.

Butler, P. J., & Jones, D. R. (1997). Physiology of diving of birds and mammals. *Physiological Reviews*, *77*(3), 837–899. https://doi.org/10.1152/physrev.1997.77.3.837

Cadotte, M. W., Carscadden, K., & Mirotchnick, N. (2011). Beyond species: functional diversity and the maintenance of ecological processes and services. *Journal of Applied Ecology*, *48*(5), 1079–1087.

Cadotte, M. W., Dinnage, R., & Tilman, D. (2012). Phylogenetic diversity promotes ecosystem stability. *Ecology*, *93*(sp8), S223--S233.

Chang, B., Croson, M., Straker, L., Gart, S., Dove, C., Gerwin, J., & Jung, S. (2016). How seabirds plunge-dive without injuries. *Proceedings of the National Academy of Sciences of the United States of America*, *113*(43), 12006–12011. https://doi.org/10.1073/PNAS.1608628113/SUPPL_FILE/PNAS.1608628113.SM02.MOV

Cherel, Y., & Klages, N. (1998). A review of the food of albatrosses. *Albatross Biology and Conservation. Surrey Beatty \& Sons, Chipping Norton*, 113–136.

Clarke, M., Thomas, G. H., & Freckleton, R. P. (2017). Trait evolution in adaptive radiations: Modeling and measuring interspecific competition on phylogenies. *American Naturalist*, *189*(2), 121–137. https://doi.org/10.1086/689819

Clavel, J., & Morlon, H. (2017). Accelerated body size evolution during cold climatic periods in the Cenozoic. *Proceedings of the National Academy of Sciences of the United States of America*, *114*(16), 4183–4188. https://doi.org/10.1073/pnas.1606868114

Clements, J. F., Schulenberg, T. S., Iliff, M. J., Billerman, S. M., Fredericks, T. A., Sullivan, B. L., & Wood, C. L. (2019). *The eBird/Clements Checklist of Birds of the World: v2019*. https://www.birds.cornell.edu/clementschecklist/download/

Clifton, G. T., Carr, J. A., & Biewener, A. A. (2018). Comparative hindlimb myology of foot-propelled swimming birds. *Journal of Anatomy*, *232*(1), 105–123. https://doi.org/10.1111/joa.12710

Clucas, G. V., Dunn, M. J., Dyke, G., Emslie, S. D., Naveen, R., Polito, M. J., Pybus, O. G., Rogers, A. D., & Hart, T. (2014). A reversal of fortunes: Climate change 'winners' and 'losers' in Antarctic Peninsula penguins. *Scientific Reports*, *4*(1), 5024. https://doi.org/10.1038/srep05024

Clucas, G. V., Younger, J. L., Kao, D., Emmerson, L., Southwell, C., Wienecke, B., Rogers, A. D., Bost, C. A., Miller, G. D., Polito, M. J., Lelliott, P., Handley, J., Crofts, S., Phillips, R. A., Dunn, M. J., Miller, K. J., & Hart, T. (2018). Comparative population genomics reveals key barriers to dispersal in Southern Ocean penguins. *Molecular Ecology*, *27*(23), 4680–4697. https://doi.org/10.1111/mec.14896

Cole, T. L., Zhou, C., Fang, M., Pan, H., Ksepka, D. T., Fiddaman, S. R., Emerling, C. A., Thomas, D. B., Bi, X., Fang, Q., Ellegaard, M. R., Feng, S., Smith, A. L., Heath, T. A., Tennyson, A. J. D., Borboroglu, P. G., Wood, J. R., Hadden, P. W., Grosser, S., … Zhang, G. (2022). Genomic insights into the secondary aquatic transition of penguins. *Nature Communications*, *13*(1), 3912. https://doi.org/10.1038/s41467-022-31508-9

Collyer, M. L., & Adams, D. C. (2018). RRPP: An R package for fitting linear models to high-dimensional data using residual randomization. In *Methods in Ecology and Evolution* (Vol. 9, Issue 2, pp. 1772–1779).

Collyer, M. L., & Adams, D. C. (2019). *RRPP: Linear Model Evaluation with Randomized Residuals in a Permutation Procedure. R package version 0.4.0.* https://cran.r-project.org/package=RRPP

Cook, T. R., Lescroël, A., Cherel, Y., Kato, A., & Bost, C. A. (2013). Can Foraging Ecology Drive the Evolution of Body Size in a Diving Endotherm? *PLoS ONE*, *8*(2), e56297. https://doi.org/10.1371/journal.pone.0056297

Cooney, C. R., Bright, J. A., Capp, E. J. R., Chira, A. M., Hughes, E. C., Moody, C. J. A., Nouri, L. O., Varley, Z. K., & Thomas, G. H. (2017). Mega-evolutionary dynamics of the adaptive radiation of birds. *Nature*, *542*(7641), 344–347. https://doi.org/10.1038/nature21074

Cornwell, W., & Nakagawa, S. (2017). Phylogenetic comparative methods. *Current Biology*, *27*(9), R333–R336. https://doi.org/https://doi.org/10.1016/j.cub.2017.03.049

Couzens, A. M. C., & Prideaux, G. J. (2018). Rapid Pliocene adaptive radiation of modern kangaroos. *Science*, *362*(6410), 72–75. https://doi.org/10.1126/science.aas8788

Coyne, J. A. (2007). Sympatric speciation. *Current Biology*, *17*(18), R787--R788.

Cracraft, J. (1983). Species Concepts and Speciation Analysis. In *Current Ornithology* (pp. 159–187). Springer US. https://doi.org/10.1007/978-1-4615-6781-3_6

Crandell, K. E., Howe, R. O., & Falkingham, P. L. (2019). Repeated evolution of drag reduction at the air–water interface in diving kingfishers. *Journal of the Royal Society Interface*, *16*(154). https://doi.org/10.1098/rsif.2019.0125

Crofts, S., & Stanworth, A. (2019). Falkland Islands seabird monitoring programme annual report 2018/2019 (SMP26). *Falklands Conservation, Stanley.*, *2019*(June), 0–45.

Croxall, J. P., & Prince, P. A. (1980). Food, feeding ecology and ecological segregation of seabirds at South Georgia. *Biological Journal of the Linnean Society*, *14*(1), 103–131. https://doi.org/10.1111/j.1095-8312.1980.tb00101.x

Darwin, C. (1859). *On the Origin of Species by Means of Natural Selection*. John Murray.

de Brito, V., Betancur-R, R., Burns, M. D., Buser, T. J., Conway, K. W., Fontenelle, J. P., Kolmann, M. A., McCraney, W. T., Thacker, C. E., & Bloom, D. D. (2022). Patterns of Phenotypic Evolution Associated with Marine/Freshwater Transitions in Fishes. *Integrative and Comparative Biology*, *62*(2), 406–423. https://doi.org/10.1093/icb/icac085

de Dinechin, M., Dobson, F. S., Zehtindjiev, P., Metcheva, R., Couchoux, C., Martin, A., Quillfeldt, P., & Jouventin, P. (2012). The biogeography of Gentoo Penguins (Pygoscelis papua). *Canadian Journal of Zoology*, *90*(3), 352–360. https://doi.org/10.1139/Z2012-016

De Queiroz, K. (2007). Species concepts and species delimitation. *Systematic Biology*, *56*(6), 879–886. https://doi.org/10.1080/10635150701701083

Devictor, V., Mouillot, D., Meynard, C., Jiguet, F., Thuiller, W., & Mouquet, N. (2010). Spatial mismatch and congruence between taxonomic, phylogenetic and functional diversity: the need for integrative conservation strategies in a changing world. *Ecology Letters*, *13*(8), 1030–1040.

Dias, M. P., Martin, R., Pearmain, E. J., Burfield, I. J., Small, C., Phillips, R. A., Yates, O., Lascelles, B., Borboroglu, P. G., & Croxall, J. P. (2019). Threats to seabirds: A global assessment. *Biological Conservation*, *237*, 525–537. https://doi.org/10.1016/j.biocon.2019.06.033

Dickson, B. V., & Pierce, S. E. (2019). Functional performance of turtle humerus shape across an ecological adaptive landscape. *Evolution*, *73*(6), 1265–1277. https://doi.org/10.1111/evo.13747

Dickson, B. V., Sherratt, E., Losos, J. B., & Pierce, S. E. (2017). Semicircular canals in Anolis lizards: Ecomorphological convergence and ecomorph affinities of fossil species. *Royal Society Open Science*, *4*(10), 170058. https://doi.org/10.1098/rsos.170058

Dollo, L. (1893). Les lois de l'évolution. *Bul. Soc. Belge Géol. Pal. Hydr*, *7*, 164–166.

Dunn, M. J., Forcada, J., Jackson, J. A., Waluda, C. M., Nichol, C., & Trathan, P. N. (2019). A long-term study of gentoo penguin (Pygoscelis papua) population trends at a major Antarctic tourist site, Goudier Island, Port Lockroy. *Biodiversity and Conservation*, *28*(1), 37–53. https://doi.org/10.1007/s10531-018-1635-6

Dunn, M. J., Jackson, J. A., Adlard, S., Lynnes, A. S., Briggs, D. R., Fox, D., & Waluda, C. M. (2016). Population size and decadal trends of three penguin species nesting at Signy Island, South Orkney Islands. *PLoS ONE*, *11*(10), e0164025. https://doi.org/10.1371/journal.pone.0164025

Eliason, C. M., Straker, L., Jung, S., & Hackett, S. J. (2020). Morphological innovation and biomechanical diversity in plunge-diving birds. *Evolution*, *74*(7), 1514–1524. https://doi.org/10.1111/evo.14024

Elton, C. S. (2001). *Animal ecology*. University of Chicago Press.

Ericson, P. G. P., Zuccon, D., Ohlson, J. I., Johansson, U. S., Alvarenga, H., & Prum, R. O. (2006). Higher-level phylogeny and morphological evolution of tyrant flycatchers, cotingas, manakins, and their allies (Aves: Tyrannida). *Molecular Phylogenetics and Evolution*, *40*(2), 471–483. https://doi.org/10.1016/j.ympev.2006.03.031

Faith, D. P. (1992). Conservation evaluation and phylogenetic diversity. *Biological Conservation*, *61*(1), 1–10. https://doi.org/https://doi.org/10.1016/0006-3207(92)91201-3

Felice, R. N., & Goswami, A. (2018). Developmental origins of mosaic evolution in the avian cranium. *Proceedings of the National Academy of Sciences of the United States of America*, *115*(3), 555–560. https://doi.org/10.1073/pnas.1716437115

Felice, R. N., & O'Connor, P. M. (2014). Ecology and caudal skeletal morphology in birds: The convergent evolution of pygostyle shape in underwater foraging taxa. *PLoS ONE*, *9*(2), e89737. https://doi.org/10.1371/journal.pone.0089737

Felice, R. N., Tobias, J. A., Pigot, A. L., & Goswami, A. (2019). Dietary niche and the evolution of cranial morphology in birds. *Proceedings of the Royal Society B: Biological Sciences*, *286*(1897), 20182677. https://doi.org/10.1098/rspb.2018.2677

Felsenstein, J. (1973). Maximum likelihood estimation of evolutionary trees from continuous characters. *American Journal of Human Genetics*, *25*(5), 471–492.

Felsenstein, J. (1985). Phylogenies and the comparative method. *American Naturalist*, *125*(1), 1–15. https://doi.org/10.1086/284325

Fennessy, J., Bidon, T., Reuss, F., Kumar, V., Elkan, P., Nilsson, M. A., Vamberger, M., Fritz, U., & Janke, A. (2016). Multi-locus Analyses

Reveal Four Giraffe Species Instead of One. *Current Biology*, *26*(18), 2543–2549. https://doi.org/10.1016/j.cub.2016.07.036

Fennessy, J., Bock, F., Tutchings, A., Brenneman, R., & Janke, A. (2013). Mitochondrial DNA analyses show that Zambia's South Luangwa Valley giraffe (Giraffa camelopardalis thornicrofti) are genetically isolated. *African Journal of Ecology*, *51*(4), 635–640. https://doi.org/10.1111/AJE.12085

Ferrer Obiol, J., Herranz, J. M., Paris, J. R., Whiting, J. R., Rozas, J., Riutort, M., & González-Solís, J. (2023). Species delimitation using genomic data to resolve taxonomic uncertainties in a speciation continuum of pelagic seabirds. *Molecular Phylogenetics and Evolution*, *179*(October 2022). https://doi.org/10.1016/j.ympev.2022.107671

Fitzjohn, R. G., Maddison, W. P., & Otto, S. P. (2009). Estimating trait-dependent speciation and extinction rates from incompletely resolved phylogenies. *Systematic Biology*, *58*(6), 595–611. https://doi.org/10.1093/sysbio/syp067

Fitzpatrick, B. M., Fordyce, J. A., & Gavrilets, S. (2009). Pattern, process and geographic modes of speciation. *Journal of Evolutionary Biology*, *22*(11), 2342–2347.

Foote, M. (1997). The evolution of morphological diversity. *Annual Review of Ecology and Systematics*, *28*(1), 129–152. https://doi.org/10.1146/annurev.ecolsys.28.1.129

Forster, J. R. (1781). *Indische Zoologie oder systematische Beschreibungen seltener und unbekannter Thiere aus Indien*. Johann Jacob Gebauer.

Friesen, V. L. (2015). Speciation in seabirds: why are there so many species…and why aren't there more? *Journal of Ornithology*, *156*(1), 27–39. https://doi.org/10.1007/s10336-015-1235-0

Frugone, M. J., López, M. E., Segovia, N. I., Cole, T. L., Lowther, A., Pistorius, P., Dantas, G. P. M., Petry, M. V., Bonadonna, F., Trathan, P., Polanowski, A., Wienecke, B., Bi, K., Wang-Claypool, C. Y., Waters, J. M., Bowie, R. C. K., Poulin, E., & Vianna, J. A. (2019). More than the eye can see: Genomic insights into the drivers of genetic differentiation in Royal/Macaroni penguins across the Southern Ocean. *Molecular Phylogenetics and Evolution*, *139*(July). https://doi.org/10.1016/j.ympev.2019.106563

Fröhlich, A., Kotowska, D., Rafałand, M., & Symonds, M. R. E. (2023). Allometry reveals trade-offs between Bergmann's and Allen's rules, and different avian adaptive strategies for thermoregulation. *Nature Communications*, *14*(1), 1101.

Garamszegi, L. Z. (2014). *Modern phylogenetic comparative methods and their application in evolutionary biology: concepts and practice*. Springer.

Gearty, W., O'Meara, B., Berv, J., Ballen, G. A., Ferreira, D., Lapp, H., Schmitz, L., Smith, M. R., Upham, N. S., & Nations, J. A. (2022). *{CRAN} Task View: Phylogenetics*.

Gill, F., Donsker, D., & Rasmussen, P. (2021). *IOC world bird list*. IOC.

Gleiss, A. C., Jorgensen, S. J., Liebsch, N., Sala, J. E., Norman, B., Hays, G. C., Quintana, F., Grundy, E., Campagna, C., Trites, A. W., & others. (2011). Convergent evolution in locomotory patterns of flying and swimming animals. *Nature Communications*, *2*(1), 352.

Gómez, R. O., & Lois-Milevicich, J. (2021). Why the long beak? Phylogeny, convergence, feeding ecology, and evolutionary allometry shaped the skull of the Giant Cowbird Molothrus oryzivorus (Icteridae). *Journal of Morphology*, *282*(11), 1587–1603. https://doi.org/10.1002/jmor.21408

Goswami, A., Milne, N., & Wroe, S. (2011). Biting through constraints: Cranial morphology, disparity and convergence across living and fossil carnivorous mammals. *Proceedings of the Royal Society B: Biological Sciences*, *278*(1713), 1831–1839. https://doi.org/10.1098/rspb.2010.2031

Goswami, A., Watanabe, A., Felice, R. N., Bardua, C., Fabre, A. C., & Polly, P. D. (2019). High-Density Morphometric Analysis of Shape and Integration: The Good, the Bad, and the Not-Really-a-Problem. *Integrative and Comparative Biology*, *59*(3), 669–683. https://doi.org/10.1093/icb/icz120

Gould, P., Ostrom, P., & Walker, W. (1997). Trophic relationships of albatrosses associated with squid and large-mesh drift-net fisheries in the North Pacific Ocean. *Canadian Journal of Zoology*, *75*(4), 549–562.

Grinnell, J. (1917). The niche-relationships of the California Thrasher. *The Auk*, *34*(4), 427–433.

Grossnickle, D. M., Smith, S. M., & Wilson, G. P. (2019). Untangling the Multiple Ecological Radiations of Early Mammals. *Trends in Ecology and Evolution*, *34*(10), 936–949. https://doi.org/10.1016/j.tree.2019.05.008

Guillerme, T., Cooper, N., Brusatte, S. L., Davis, K. E., Jackson, A. L., Gerber, S., Goswami, A., Healy, K., Hopkins, M. J., Jones, M. E. H., Lloyd, G. T., O'Reilly, J. E., Pate, A., Puttick, M. N., Rayfield, E. J., Saupe, E. E., Sherratt, E., Slater, G. J., Weisbecker, V., … Donoghue, P. C. J. (2020). Disparities in the analysis of morphological disparity. *Biology Letters*, *16*(7). https://doi.org/10.1098/rsbl.2020.0199

Guillerme, T., Puttick, M. N., Marcy, A. E., & Weisbecker, V. (2020). Shifting spaces: Which disparity or dissimilarity measurement best summarize occupancy in multidimensional spaces? *Ecology and Evolution*, *10*(14), 7261–7275. https://doi.org/10.1002/ece3.6452

Gutarra, S., & Rahman, I. A. (2022). The locomotion of extinct secondarily aquatic tetrapods. *Biological Reviews*, *97*(1), 67–98.

Hackett, S. J., Kimball, R. T., Reddy, S., Bowie, R. C. K., Braun, E. L., Braun, M. J., Chojnowski, J. L., Cox, W. A., Han, K. L., Harshman, J., Huddleston, C. J., Marks, B. D., Miglia, K. J., Moore, W. S., Sheldon, F. H., Steadman, D. W., Witt, C. C., & Yuri, T. (2008). A phylogenomic study of birds reveals their evolutionary history. *Science*, *320*(5884), 1763–1768. https://doi.org/10.1126/science.1157704

Halsey, L. G., Blackburn, T. M., & Butler, P. J. (2006). A comparative analysis of the diving behaviour of birds and mammals. *Functional Ecology*, *20*(5), 889–899. https://doi.org/10.1111/j.1365-2435.2006.01170.x

Hansen, T. F. (1997). Stabilizing selection and the comparative analysis of adaptation. *Evolution*, *51*(5), 1341–1351. https://doi.org/10.1111/j.1558-5646.1997.tb01457.x

Hansen, T. F., & Martins, E. P. (1996). Translating Between Microevolutionary Process and Macroevolutionary Patterns: The Correlation Structure of Interspecific Data. *Evolution*, *50*(4), 1404. https://doi.org/10.2307/2410878

Harmon, L. J., Weir, J. T., Brock, C. D., Glor, R. E., & Challenger, W. (2008). GEIGER: Investigating evolutionary radiations. *Bioinformatics*, *24*(1), 129–131. https://doi.org/10.1093/bioinformatics/btm538

Harrison, C. S., Hida, T. S., & Seki, M. P. (1983). Hawaiian seabird feeding ecology. *Wildlife Monographs*, 3–71.

Heard, S. B., & Hauser, D. L. (1995). Key evolutionary innovations and their ecological mechanisms. *Historical Biology*, *10*(2), 151–173. https://doi.org/10.1080/10292389509380518

Herman, R., Borowicz, A., Lynch, M., Trathan, P., Hart, T., & Lynch, H. (2020). Update on the global abundance and distribution of breeding Gentoo Penguins (Pygoscelis papua). *Polar Biology*, *43*(12), 1947–1956. https://doi.org/10.1007/s00300-020-02759-3

Hickcox, R. P., Jara, M., Deacon, L. A. K., Harvey, L. P., & Pincheira-Donoso, D. (2019). Global terrestrial distribution of penguins (Spheniscidae) and their conservation by protected areas. *Biodiversity and Conservation*, *28*(11), 2861–2876. https://doi.org/10.1007/s10531-019-01801-z

Hickman, C. S. (1988). Analysis of form and function in fossils. *American Zoologist*, *28*(2), 775–793.

Hieronymus, T. L., & Witmer, L. M. (2010). Homology and Evolution of Avian Compound Rhamphothecae. *The Auk*, *127*(3), 590–604. https://doi.org/10.1525/AUK.2010.09122

Hindell, M. A., Reisinger, R. R., Ropert-Coudert, Y., Hückstädt, L. A., Trathan, P. N., Bornemann, H., Charrassin, J.-B., Chown, S. L., Costa, D. P., Danis, B., Lea, M.-A., Thompson, D., Torres, L. G., Van de Putte, A. P., Alderman, R., Andrews-Goff, V., Arthur, B., Ballard, G., Bengtson, J., … Raymond, B. (2020). Tracking of marine predators to protect Southern Ocean ecosystems. *Nature*, *580*(7801), 87–92. https://doi.org/10.1038/s41586-020-2126-y

Holt, R. D. (2009). Bringing the Hutchinsonian niche into the 21st century: Ecological and evolutionary perspectives. *Proceedings of the National Academy of Sciences*, *106*(supplement_2), 19659–19665. https://doi.org/10.1073/pnas.0905137106

Hopkins, M. J., & Gerber, S. (2021). *Morphological Disparity*. https://doi.org/10.1007/978-3-319-32979-6_132

Hosner, P. A., Campillo, L. C., Andersen, M. J., Sánchez-González, L. A., Oliveros, C. H., Urriza, R. C., & Moyle, R. G. (2018). An integrative species delimitation approach reveals fine-scale endemism and substantial unrecognized avian diversity in the Philippine Archipelago. *Conservation Genetics*, *19*(5), 1153–1168. https://doi.org/10.1007/s10592-018-1085-4

Howard, R., Moore, A., & others. (1991). *A complete checklist of the birds of the world.* (Issue Ed. 2). Academic Press Ltd.

Howell, S. N. G., & Zufelt, K. (2019). Oceanic Birds of the World. In *Oceanic Birds of the World*. Princeton University Press. https://doi.org/10.2307/j.ctvg254dg

Hughes, E. C., Edwards, D. P., & Thomas, G. H. (2022). The homogenization of avian morphological and phylogenetic diversity under the global extinction crisis. *Current Biology*, *32*(17), 3830-3837.e3. https://doi.org/https://doi.org/10.1016/j.cub.2022.06.018

Hutchinson, G. E. (1957). Concluding Remarks. *Cold Spring Harbor Symposia on Quantitative Biology*, 22, 415–427.

IUCN. (2021). *The IUCN Red List of Threatened Species.* Version 2021. 1.

Jablonski, B. (1984). Distribution, numbers and breeding preferences of penguins in the region of the Admiralty Bay (King George Island, South Shetland Islands) in the season 1979/1980. *Polish Polar Research*, *5*(1–2), 5–16.

Jablonski, D. (2017a). Approaches to Macroevolution: 1. General Concepts and Origin of Variation. *Evolutionary Biology*, *44*(4), 427–450. https://doi.org/10.1007/s11692-017-9420-0

Jablonski, D. (2017b). Approaches to Macroevolution: 2. Sorting of Variation, Some Overarching Issues, and General Conclusions. *Evolutionary Biology*, *44*(4), 451–475. https://doi.org/10.1007/s11692-017-9434-7

Jablonski, D. (2020). Developmental bias, macroevolution, and the fossil record. *Evolution and Development*, *22*(1–2), 103–125. https://doi.org/10.1111/ede.12313

Jetz, W., Thomas, G. H., Joy, J. B., Hartmann, K., & Mooers, A. O. (2012). The global diversity of birds in space and time. *Nature*, *491*(7424), 444–448. https://doi.org/10.1038/nature11631

Johnson, K. R., Owens, I. F. P., & Group, the G. C. (2023). A global approach for natural history museum collections. *Science*, *379*(6638), 1192–1194. https://doi.org/10.1126/SCIENCE.ADF6434

Jombart, T. (2008). Adegenet: A R package for the multivariate analysis of genetic markers. *Bioinformatics*, *24*(11), 1403–1405. https://doi.org/10.1093/bioinformatics/btn129

Jombart, T., & Ahmed, I. (2011). adegenet 1.3-1: New tools for the analysis of genome-wide SNP data. *Bioinformatics*, *27*(21), 3070–3071. https://doi.org/10.1093/bioinformatics/btr521

Jonathan Davies, T., Meiri, S., Barraclough, T. G., & Gittleman, J. L. (2007). Species co-existence and character divergence across carnivores. *Ecology Letters*, *10*(2), 146–152. https://doi.org/10.1111/j.1461-0248.2006.01005.x

Juáres, M. A., Casaux, R., Negrete, J., Rios, A., Castillo, M., Coria, N. R., & Santos, M. M. (2020). Update of the population size and breeding performance of gentoo penguins (Pygoscelis papua) at Stranger Point/Cabo Funes, South Shetland Islands. *Polar Biology*, *43*(2), 123–129. https://doi.org/10.1007/s00300-019-02614-0

Kass, R. E., & Raftery, A. E. (1995). Bayes factors. *Journal of the American Statistical Association*, *90*(430), 773–795. https://doi.org/10.1080/01621459.1995.10476572

Kassambara, A., & Mundt, F. (2020). Package ‘factoextra’: Extract and visualize the results of multivariate data analyses. In *CRAN- R Package* (p. 84).

Kear, J. (2005). *Birds Families of the World: Ducks, Geese, and Swans*. Oxford University Press (OUP).

Kelley, N. P., & Motani, R. (2015). Trophic convergence drives morphological convergence in marine tetrapods. *Biology Letters*, *11*(1), 20140709.

Kemp, F. (2003). Modern Applied Statistics with S,. In *Journal of the Royal Statistical Society: Series D (The Statistician)* (Fourth, Vol. 52, Issue 4). Springer. https://doi.org/10.1046/j.1467-9884.2003.t01-19-00383_22.x

Kikinis, R., Pieper, S. D., & Vosburgh, K. G. (2014). 3D Slicer: A Platform for Subject-Specific Image Analysis, Visualization, and Clinical Support. In F. A. Jolesz (Ed.), *Intraoperative Imaging and Image-Guided*

Therapy (pp. 277–289). Springer New York. https://doi.org/10.1007/978-1-4614-7657-3_19

Kleynhans, E. J., Jolles, A. E., Bos, M. R. E., & Olff, H. (2011). Resource partitioning along multiple niche dimensions in differently sized African savanna grazers. *Oikos*, *120*(4), 591–600. https://doi.org/10.1111/j.1600-0706.2010.18712.x

Klingenberg, C. P. (2016). Size, shape, and form: concepts of allometry in geometric morphometrics. *Development Genes and Evolution*, *226*(3), 113–137. https://doi.org/10.1007/s00427-016-0539-2

Ksepka, D. T., Bertelli, S., & Giannini, N. P. (2006). The phylogeny of the living and fossil Sphenisciformes (penguins). *Cladistics*, *22*(5), 412–441.

Ksepka, D. T., Field, D. J., Heath, T. A., Pett, W., Thomas, D. B., Giovanardi, S., & Tennyson, A. J. D. (2023). Largest-known fossil penguin provides insight into the early evolution of sphenisciform body size and flipper anatomy. *Journal of Paleontology*, 1–20.

Leaché, A. D., Fujita, M. K., Minin, V. N., & Bouckaert, R. R. (2014). Species delimitation using genome-wide SNP Data. *Systematic Biology*, *63*(4), 534–542. https://doi.org/10.1093/sysbio/syu018

Lean, C., & Maclaurin, J. (2016). The value of phylogenetic diversity. *Biodiversity Conservation and Phylogenetic Systematics: Preserving Our Evolutionary Heritage in an Extinction Crisis*, 19–37.

Lescroël, A., & Bost, C. A. (2006). Recent decrease in gentoo penguin populations at Iles Kerguelen. *Antarctic Science*, *18*(2), 171–174. https://doi.org/10.1017/S0954102006000198

Levy, H., Clucas, G. V., Rogers, A. D., Leaché, A. D., Ciborowski, K. L., Polito, M. J., Lynch, H. J., Dunn, M. J., & Hart, T. (2016). Population structure and phylogeography of the Gentoo Penguin (Pygoscelis papua) across the Scotia Arc. *Ecology and Evolution*, *6*(6), 1834–1853. https://doi.org/10.1002/ece3.1929

Lindgren, J., Caldwell, M. W., Konishi, T., & Chiappe, L. M. (2010). Convergent evolution in aquatic tetrapods: insights from an exceptional fossil mosasaur. *PloS One*, *5*(8), e11998.

Livezey, B. C. (1989). Morphometric patterns in Recent and fossil penguins (Aves, Sphenisciformes). *Journal of Zoology*, *219*(2), 269–307. https://doi.org/10.1111/j.1469-7998.1989.tb02582.x

Lönnberg, E. (1904). *On the homologies of the different pieces of the compound rhamphotheca of birds*.

Losos, J. B. (2011). Convergence, adaptation, and constraint. *Evolution*, *65*(7), 1827–1840.

Lowi-Merri, T. M., Benson, R. B. J., Claramunt, S., & Evans, D. C. (2021). The relationship between sternum variation and mode of locomotion in birds. *BMC Biology*, *19*(1), 1–23. https://doi.org/10.1186/s12915-021-01105-1

Lynch, H. J., Naveen, R., Trathan, P. N., & Fagan, W. F. (2012). Spatially integrated assessment reveals widespread changes in penguin populations on the Antarctic Peninsula. *Ecology*, *93*(6), 1367–1377. https://doi.org/10.1890/11-1588.1

Lynch, M. A., & Lynch, H. J. (2017). Variation in the ecstatic display call of the Gentoo Penguin (Pygoscelis papua) across regional geographic scales. *Auk*, *134*(4), 894–902. https://doi.org/10.1642/AUK-17-4.1

Marugán-Lobón, J., Nebreda, S. M., Navalón, G., & Benson, R. B. J. (2022). Beyond the beak: Brain size and allometry in avian craniofacial evolution. *Journal of Anatomy*, *240*(2), 197–209. https://doi.org/10.1111/joa.13555

Marx, F. G., & Fordyce, R. E. (2015). Baleen boom and bust: a synthesis of mysticete phylogeny, diversity and disparity. *Royal Society Open Science*, *2*(4), 140434.

Mathews, G. M. (1927). Systema avium Australasianarum: A systematic list of the birds of the Australasian region. In *Systema avium*

Australasianarum. British Ornithologists' Union. https://doi.org/10.5962/bhl.title.152920

McCurry, M. R., Evans, A. R., Fitzgerald, E. M. G., Adams, J. W., Clausen, P. D., & McHenry, C. R. (2017). The remarkable convergence of skull shape in crocodilians and toothed whales. *Proceedings of the Royal Society B: Biological Sciences*, *284*(1850), 9–11. https://doi.org/10.1098/rspb.2016.2348

McInnes, J. C., Alderman, R., Lea, M. A., Raymond, B., Deagle, B. E., Phillips, R. A., Stanworth, A., Thompson, D. R., Catry, P., Weimerskirch, H., Suazo, C. G., Gras, M., & Jarman, S. N. (2017). High occurrence of jellyfish predation by black-browed and Campbell albatross identified by DNA metabarcoding. *Molecular Ecology*, *26*(18), 4831–4845. https://doi.org/10.1111/MEC.14245

McInnes, J. C., Raymond, B., Phillips, R. A., Jarman, S. N., Lea, M.-A., & Alderman, R. (2016). A review of methods used to analyse albatross diets—assessing priorities across their range. *ICES Journal of Marine Science*, *73*(9), 2125–2137.

McMahon, K. W., Michelson, C. I., Hart, T., McCarthy, M. D., Patterson, W. P., & Polito, M. J. (2019). Divergent trophic responses of sympatric penguin species to historic anthropogenic exploitation and recent climate change. *Proceedings of the National Academy of Sciences of the United States of America*, *116*(51), 25721–25727. https://doi.org/10.1073/pnas.1913093116

Meirmans, P. G., & Van Tienderen, P. H. (2004). GENOTYPE and GENODIVE: Two programs for the analysis of genetic diversity of asexual organisms. *Molecular Ecology Notes*, *4*(4), 792–794. https://doi.org/10.1111/j.1471-8286.2004.00770.x

Miller, A. H., & Stroud, J. T. (2022). Novel Tests of the Key Innovation Hypothesis: Adhesive Toepads in Arboreal Lizards. *Systematic Biology*, *71*(1), 139–152. https://doi.org/10.1093/sysbio/syab041

Miller, E. T., Wagner, S. K., Harmon, L. J., & Ricklefs, R. E. (2017). Radiating despite a lack of character: ecological divergence among closely related, morphologically similar honeyeaters (Aves: Meliphagidae) co-occurring in arid Australian environments. *The American Naturalist*, *189*(2), E14--E30.

Minelli, A. (2019). Biodiversity, Disparity and Evolvability. *History, Philosophy and Theory of the Life Sciences*, *24*, 233–246. https://doi.org/10.1007/978-3-030-10991-2_11/COVER

Münkemüller, T., Lavergne, S., Bzeznik, B., Dray, S., Jombart, T., Schiffers, K., & Thuiller, W. (2012). How to measure and test phylogenetic signal. *Methods in Ecology and Evolution*, *3*(4), 743–756. https://doi.org/10.1111/j.2041-210X.2012.00196.x

Murphy, R. C. (1947). A New Zonal Race of the Gentoo Penguin. *The Auk*, *64*(3), 454–455. https://doi.org/10.2307/4080392

Nations, J. A., Heaney, L. R., Demos, T. C., Achmadi, A. S., Rowe, K. C., & Esselstyn, J. A. (2019). A simple skeletal measurement effectively predicts climbing behaviour in a diverse clade of small mammals. *Biological Journal of the Linnean Society*, *128*(2), 323–336. https://doi.org/10.1093/biolinnean/blz085

Nations, J. A., Mount, G. G., Morere, S. M., Achmadi, A. S., Rowe, K. C., & Esselstyn, J. A. (2021). Locomotory mode transitions alter phenotypic evolution and lineage diversification in an ecologically rich clade of mammals. *Evolution*, *75*(2), 376–393. https://doi.org/10.1111/evo.14156

Navalón, G., Bjarnason, A., Griffiths, E., & Benson, R. B. J. (2022). Environmental signal in the evolutionary diversification of bird skeletons. *Nature*, 1–6.

Navalón, G., Bright, J. A., Marugán-Lobón, J., & Rayfield, E. J. (2019). The evolutionary relationship among beak shape, mechanical advantage, and feeding ecology in modern birds*. *Evolution*, *73*(3), 422–435. https://doi.org/10.1111/evo.13655

Navalón, G., Marugán-Lobón, J., Bright, J. A., Cooney, C. R., & Rayfield, E. J. (2020). The consequences of craniofacial integration for the adaptive radiations of Darwin's finches and Hawaiian honeycreepers. *Nature Ecology and Evolution*, *4*(2), 270–278. https://doi.org/10.1038/s41559-019-1092-y

Nunn, G. B., Cooper, J., Jouventin, P., Robertson, C. J. R., & Robertson, G. G. (1996). Evolutionary relationships among extant albatrosses (Procellariiformes: Diomedeidae) established from complete cytochrome-b gene sequences. *The Auk*, *113*(4), 784–801.

Pabst, D. A., McLellan, W. A., & Rommel, S. A. (2016). How to build a deep diver: The extreme morphology of mesoplodonts. *Integrative and Comparative Biology*, *56*(6), 1337–1348. https://doi.org/10.1093/icb/icw126

Paradis, E., Claude, J., & Strimmer, K. (2004). APE: Analyses of phylogenetics and evolution in R language. *Bioinformatics*, *20*(2), 289–290. https://doi.org/10.1093/bioinformatics/btg412

Parkes, K. C., & Austin, O. L. (1962). Birds of the World. In S. M. Billerman, B. K. Keeney, P. G. Rodewald, & T. S. Schulenberg (Eds.), *Bird-Banding* (Vol. 33, Issue 2). Cornell Laboratory of Ornithology. https://doi.org/10.2307/4510938

Pascoe, P., McInnes, J. C., Lashko, A., Robinson, S., Achurch, H., Salton, M., Alderman, R., & Carmichael, N. (2020). Trends in gentoo penguin (Pygoscelis papua) breeding population size at Macquarie Island. *Polar Biology*, *43*(7), 877–886. https://doi.org/10.1007/s00300-020-02697-0

Penhallurick, J. (2012). The number of albatross (Diomedeidae) species. *The Open Ornithology Journal*, *5*(1).

Penhallurick, J., & Wink, M. (2004). Analysis of the taxonomy and nomenclature of the Procellariiformes based on complete nucleotide sequences of the mitochondrial cytochrome b gene. *Emu*, *104*(2), 125–147.

Pertierra, L. R., Segovia, N. I., Noll, D., Martinez, P. A., Pliscoff, P., Barbosa, A., Aragón, P., Raya Rey, A., Pistorius, P., Trathan, P., Polanowski, A., Bonadonna, F., Le Bohec, C., Bi, K., Wang-Claypool, C. Y., González-Acuña, D., Dantas, G. P. M., Bowie, R. C. K., Poulin, E., & Vianna, J. A. (2020). Cryptic speciation in gentoo penguins is driven by geographic isolation and regional marine conditions: Unforeseen vulnerabilities to global change. *Diversity and Distributions*, *26*(8), 958–975. https://doi.org/10.1111/ddi.13072

Petalas, C., Lazarus, T., Lavoie, R. A., Elliott, K. H., & Guigueno, M. F. (2021). Foraging niche partitioning in sympatric seabird populations. *Scientific Reports*, *11*(1), 2493. https://doi.org/10.1038/s41598-021-81583-z

Peters, J. L. (1935). Check-List of Birds of the World. In *Nature* (Vol. 135, Issue 3416, pp. 603–603). https://doi.org/10.1038/135603d0

Pigot, A. L., Sheard, C., Miller, E. T., Bregman, T. P., Freeman, B. G., Roll, U., Seddon, N., Trisos, C. H., Weeks, B. C., & Tobias, J. A. (2020). Macroevolutionary convergence connects morphological form to ecological function in birds. *Nature Ecology and Evolution*, *4*(2), 230–239. https://doi.org/10.1038/s41559-019-1070-4

Piro, A. (2022). Comparative morphology of the compound rhamphotheca of tubenosed seabirds (order Procellariiformes). *Zoologischer Anzeiger*, *299*, 176–188. https://doi.org/10.1016/j.jcz.2022.05.012

Prager, E. M., & Wilson, A. C. (1975). Slow evolutionary loss of the potential for interspecific hybridization in birds: a manifestation of slow regulatory evolution. *Proceedings of the National Academy of Sciences of the United States of America*, *72*(1), 200–204. https://doi.org/10.1073/pnas.72.1.200

Prum, R. O., Berv, J. S., Dornburg, A., Field, D. J., Townsend, J. P., Lemmon, E. M., & Lemmon, A. R. (2015). A comprehensive phylogeny of birds (Aves) using targeted next-generation DNA sequencing. *Nature*, *526*(7574), 569–573. https://doi.org/10.1038/nature15697

Pulido-Santacruz, P., Aleixo, A., & Weir, J. T. (2018). Morphologically cryptic amazonian bird species pairs exhibit strong postzygotic reproductive isolation. *Proceedings of the Royal Society B: Biological Sciences*, *285*(1874), 20172081. https://doi.org/10.1098/rspb.2017.2081

R Core Team. (2022). *R: A Language and Environment for Statistical Computing*.

Ratcliffe, N., & Trathan, P. (2012). A review of the diet and at-sea distribution of penguins breeding within the CAMLR convention area. *CCAMLR Science*, *19*, 1–40.

Reilly, P. N., & Kerle, J. A. (1981). A study of the Gentoo penguin Pygoscelis papua. *Notornis*, *28*, 189–202.

Rensch, B. (1948). Histological changes correlated with evolutionary changes of body size. *Evolution*, *2*(3), 218–230. https://doi.org/10.1111/j.1558-5646.1948.tb02742.x

Revell, L. J. (2012). phytools: An R package for phylogenetic comparative biology (and other things). *Methods in Ecology and Evolution*, *3*(2), 217–223. https://doi.org/10.1111/j.2041-210X.2011.00169.x

Ridoux, V. (1995). The diets and dietary segregation of seabirds at the subantarctic Crozet Islands. *Oceanographic Literature Review*, *12*(42), 1128.

Ripley, D., & Mayr, E. (1943). Systematics and the Origin of Species. *Bird-Banding*, *14*(3), 89. https://doi.org/10.2307/4509787

Robertson, C. J. R. (1998). Towards a new taxonomy for albatrosses. *Albatross Biology and Conservation*, 13–19.

Ronco, F., Matschiner, M., Böhne, A., Boila, A., Büscher, H. H., El Taher, A., Indermaur, A., Malinsky, M., Ricci, V., Kahmen, A., Jentoft, S., & Salzburger, W. (2021). Drivers and dynamics of a massive adaptive radiation in cichlid fishes. *Nature*, *589*(7840), 76–81. https://doi.org/10.1038/s41586-020-2930-4

Rothier, P. S., Fabre, A.-C., Clavel, J., Benson, R. B. J., & Herrel, A. (2023). Mammalian forelimb evolution is driven by uneven proximal-to-distal morphological diversity. *Elife*, *12*, e81492.

Sangster, G., & Mayr, G. (2021). Feraequornithes: A name for the clade formed by Procellariiformes, Sphenisciformes, Ciconiiformes, Suliformes and Pelecaniformes (Aves). *Vertebrate Zoology*, *71*, 49–53. https://doi.org/10.3897/vz.71.e61728

Sausner, J., Torres-Mura, J. C., Robertson, J., & Hertel, F. (2016). Ecomorphological differences in foraging and pattering behavior among storm-petrels in the eastern Pacific Ocean. *Auk*, *133*(3), 397–414. https://doi.org/10.1642/AUK-15-158.1

Sauve, D., Divoky, G., & Friesen, V. L. (2019). Phenotypic plasticity or evolutionary change? An examination of the phenological response of an arctic seabird to climate change. *Functional Ecology*, *33*(11), 2180–2190. https://doi.org/10.1111/1365-2435.13406

Schweizer, M., Hertwig, S. T., & Seehausen, O. (2014). Diversity versus disparity and the role of ecological opportunity in a continental bird radiation. *Journal of Biogeography*, *41*(7), 1301–1312.

Seehausen, O. (2006). African cichlid fish: A model system in adaptive radiation research. *Proceedings of the Royal Society B: Biological Sciences*, *273*(1597), 1987–1998. https://doi.org/10.1098/rspb.2006.3539

Sheard, C., Neate-Clegg, M. H. C., Alioravainen, N., Jones, S. E. I., Vincent, C., MacGregor, H. E. A., Bregman, T. P., Claramunt, S., & Tobias, J. A. (2020). Ecological drivers of global gradients in avian dispersal inferred from wing morphology. *Nature Communications*, *11*(1), 1–27. https://doi.org/10.1038/s41467-020-16313-6

Singh, A., Gupta, S. K., Alström, P., Mohan, D., Hooper, D. M., Kumar, R. S., Bhatt, D., Singh, P., & Price, T. D. (2020). Taxonomy of cryptic species in the Cyornis rubeculoides complex in the Indian subcontinent. *Ibis*, *162*(3), 924–935. https://doi.org/10.1111/ibi.12735

Smith, N. A., & Clarke, J. A. (2012). Endocranial Anatomy of the Charadriiformes: Sensory System Variation and the Evolution of Wing-Propelled Diving. *PLoS ONE*, *7*(11), e49584. https://doi.org/10.1371/journal.pone.0049584

Smith, N. A., Koeller, K. L., Clarke, J. A., Ksepka, D. T., Mitchell, J. S., Nabavizadeh, A., Ridgley, R. C., & Witmer, L. M. (2022). Convergent evolution in dippers (Aves, Cinclidae): The only wing-propelled diving songbirds. *Anatomical Record*, *305*(7), 1563–1591. https://doi.org/10.1002/ar.24820

Soberón, J. (2007). Grinnellian and Eltonian niches and geographic distributions of species. *Ecology Letters*, *10*(12), 1115–1123. https://doi.org/10.1111/J.1461-0248.2007.01107.X

Srivastava, D. S., Cadotte, M. W., MacDonald, A. A. M., Marushia, R. G., & Mirotchnick, N. (2012). Phylogenetic diversity and the functioning of ecosystems. *Ecology Letters*, *15*(7), 637–648.

Stamatakis, A. (2014). RAxML version 8: A tool for phylogenetic analysis and post-analysis of large phylogenies. *Bioinformatics*, *30*(9), 1312–1313. https://doi.org/10.1093/bioinformatics/btu033

Stankowski, S., & Ravinet, M. (2021). Quantifying the use of species concepts. *Current Biology*, *31*(9), R428–R429. https://doi.org/10.1016/J.CUB.2021.03.060

Steell, E. M., Nguyen, J. M. T., Benson, R. B. J., & Field, D. J. (2023). Comparative anatomy of the passerine carpometacarpus helps illuminate the early fossil record of crown Passeriformes. *Journal of Anatomy*, *242*(3), 495–509.

Stonehouse, B. (1970). Geographic Variation in Gentoo Penguins Pygoscelis Papua. *Ibis*, *112*(1), 52–57. https://doi.org/10.1111/j.1474-919X.1970.tb00075.x

Strathmann, R. R. (1978). Progressive Vacating of Adaptive Types During the Phanerozoic. *Evolution*, *32*(4), 907. https://doi.org/10.2307/2407503

Title, P. O., & Rabosky, D. L. (2019). Tip rates, phylogenies and diversification: What are we estimating, and how good are the estimates? *Methods in Ecology and Evolution*, *10*(6), 821–834. https://doi.org/10.1111/2041-210X.13153

Tobias, J. A., Sheard, C., Pigot, A. L., Devenish, A. J. M., Yang, J., Sayol, F., Neate-Clegg, M. H. C., Alioravainen, N., Weeks, T. L., Barber, R. A., Walkden, P. A., MacGregor, H. E. A., Jones, S. E. I., Vincent, C., Phillips, A. G., Marples, N. M., Montaño-Centellas, F. A., Leandro-Silva, V., Claramunt, S., … Schleuning, M. (2022). AVONET: morphological, ecological and geographical data for all birds. *Ecology Letters*, *25*(3), 581–597. https://doi.org/10.1111/ele.13898

Tyler, J., Bonfitto, M. T., Clucas, G. V., Reddy, S., & Younger, J. L. (2020). Morphometric and genetic evidence for four species of gentoo penguin. *Ecology and Evolution*, *10*(24), 13836–13846. https://doi.org/10.1002/ece3.6973

Uyeda, J. C., Zenil-Ferguson, R., & Pennell, M. W. (2018). Rethinking phylogenetic comparative methods. *Systematic Biology*, *67*(6), 1091–1109. https://doi.org/10.1093/sysbio/syy031

Valen, L. Van. (1971). Adaptive Zones and the Orders of Mammals. *Evolution*, *25*(2), 420–428.

Van Oordt, F., Torres-Mura, J. C., & Hertel, F. (2018). Ecomorphology and foraging behaviour of Pacific boobies. *Ibis*, *160*(2), 313–326. https://doi.org/10.1111/ibi.12545

Verberk, W. C. E. P., Calosi, P., Brischoux, F., Spicer, J. I., Garland, T., & Bilton, D. T. (2020). Universal metabolic constraints shape the evolutionary ecology of diving in animals. *Proceedings of the Royal Society B: Biological Sciences*, *287*(1927), 20200488. https://doi.org/10.1098/rspb.2020.0488

Vianna, J. A., Noll, D., Dantas, G. P. M., Petry, M. V., Barbosa, A., González-Acuña, D., Le Bohec, C., Bonadonna, F., & Poulin, E. (2017). Marked phylogeographic structure of Gentoo penguin reveals an ongoing diversification process along the Southern Ocean. *Molecular Phylogenetics and Evolution*, *107*, 486–498. https://doi.org/10.1016/j.ympev.2016.12.003

Volkman, N. J., & Trivelpiece, W. (1981). Nest-Site Selection Among Adelie, Chinstrap and Gentoo Penguins in Mixed Species Rookeries. *Wilson Bulletin*, *93*(2), 243–248.

von Linnaeus, C. (1735). *Systema naturae; sive, Regna tria naturae: systematice proposita per classes, ordines, genera \& species*. Haak.

Wakefield, E. D., Phillips, R. A., & Matthiopoulos, J. (2014). Habitat-mediated population limitation in a colonial central-place forager: the sky is not the limit for the black-browed albatross. *Proceedings of the Royal Society B: Biological Sciences*, *281*(1778), 20132883.

Wakefield, E. D., Phillips, R. A., Matthiopoulos, J., Fukuda, A., Higuchi, H., Marshall, G. J., & Trathan, P. N. (2009). Wind field and sex constrain the flight speeds of central-place foraging albatrosses. *Ecological Monographs*, *79*(4), 663–679.

Wang, X., & Clarke, J. A. (2014). Phylogeny and forelimb disparity in waterbirds. *Evolution*, *68*(10), 2847–2860. https://doi.org/10.1111/evo.12486

Warham, J. (1977). Wing loadings, wing shapes, and flight capabilities of procellariiformes. *New Zealand Journal of Zoology*, *4*(1), 73–83. https://doi.org/10.1080/03014223.1977.9517938

Watanabe, A., Fabre, A. C., Felice, R. N., Maisano, J. A., Müller, J., Herrel, A., & Goswami, A. (2019). Ecomorphological diversification in squamates from conserved pattern of cranial integration. *Proceedings of the National Academy of Sciences of the United States of America*, *116*(29), 14688–14697. https://doi.org/10.1073/pnas.1820967116

Watanuki, Y., Wanless, S., Harris, M., Lovvorn, J. R., Miyazaki, M., Tanaka, H., & Sato, K. (2006). Swim speeds and stroke patterns in wing-propelled divers: A comparison among alcids and a penguin. *Journal of Experimental Biology*, *209*(7), 1217–1230. https://doi.org/10.1242/jeb.02128

Weimerskirch, H., Bartle, J. A., Jouventin, P., & Stahl, J. C. (1988). Foraging ranges and partitioning of feeding zones in three species of southern albatrosses. *The Condor*, *90*(1), 214–219.

Weir, B. S., & Cockerham, C. C. (1984). Estimating F-Statistics for the Analysis of Population Structure. *Evolution*, *38*(6), 1358. https://doi.org/10.2307/2408641

Wilman, H., Belmaker, J., Simpson, J., de la Rosa, C., Rivadeneira, M. M., & Jetz, W. (2014). EltonTraits 1.0: Species-level foraging attributes of the world’s birds and mammals. *Ecology*, *95*(7), 2027–2027. https://doi.org/10.1890/13-1917.1

Winter, M., Devictor, V., & Schweiger, O. (2013). Phylogenetic diversity and nature conservation: where are we? *Trends in Ecology \& Evolution*, *28*(4), 199–204.

Winter, S., Fennessy, J., & Janke, A. (2018). Limited introgression supports division of giraffe into four species. *Ecology and Evolution*, *8*(20), 10156–10165.

Woehler, E. J. (1994). The Distribution and Abundance of Antarctic and Subantarctic Penguins. Eric J. Woehler (Compiler). 1993. Cambridge: Scientific Committe on Antarctic Research. 76 p, illustrated, soft cover. ISBN 0-948277-14-9. £10.00; US$16.00. *Polar Record*, *30*(172), 66–66. https://doi.org/10.1017/s0032247400021197

Woehler, E. J., Cooper, J., Croxall, J. P., Fraser, W. R., Kooyman, G. L., Miller, G. D., Nel, D. C., Patterson, D. L., Peter, H. U., Ribic, C. A., Salwicka, K., Trivelpiece, W. Z., & Weimerskirch, H. (2001). A statistical assessment of the status and trends of Antarctic and subantarctic seabirds. Report on SCAR BBS Workshop on Southern Ocean seabird populations. *Scientific Committee for Antarctic Research, Cambridge*.

Xavier, J. C., & Croxall, J. P. (2007). Predator–prey interactions: why do larger albatrosses eat bigger squid? *Journal of Zoology*, *271*(4), 408–417. https://doi.org/https://doi.org/10.1111/j.1469-7998.2006.00224.x

Xavier, J. C., Croxall, J. P., Trathan, P. N., & Rodhouse, P. G. (2003). Inter-annual variation in the cephalopod component of the diet of the wandering albatross, Diomedea exulans, breeding at Bird Island, South Georgia. *Marine Biology*, *142*(3), 611–622.

Yamasaki, T., Aoki, S., & Tokita, M. (2018). Allometry and integration do not strongly constrain beak shape evolution in large-billed (Corvus macrorhynchos) and carrion crows (Corvus corone). *Ecology and Evolution*, *8*(20), 10057–10066. https://doi.org/https://doi.org/10.1002/ece3.4440

Younger, J. L., Dempster, P., Nyári, Á. S., Helms, T. O., Raherilalao, M. J., Goodman, S. M., & Reddy, S. (2019). Phylogeography of the Rufous Vanga and the role of bioclimatic transition zones in promoting speciation within Madagascar. *Molecular Phylogenetics and Evolution*, *139*(January), 106535. https://doi.org/10.1016/j.ympev.2019.106535

Younger, J. L., Strozier, L., Maddox, J. D., Nyári, Á. S., Bonfitto, M. T., Raherilalao, M. J., Goodman, S. M., & Reddy, S. (2018). Hidden diversity of forest birds in Madagascar revealed using integrative taxonomy. *Molecular Phylogenetics and Evolution*, *124*(September 2017), 16–26. https://doi.org/10.1016/j.ympev.2018.02.017

Zelditch, M. L., Ye, J., Mitchell, J. S., & Swiderski, D. L. (2017). Rare ecomorphological convergence on a complex adaptive landscape: Body size and diet mediate evolution of jaw shape in squirrels (Sciuridae). *Evolution*, *71*(3), 633–649. https://doi.org/10.1111/evo.13168

APPENDIX A: SUPPLEMENTARY MATERIAL FOR CHAPTER 2

Supplementary Material can be found at https://onlinelibrary.wiley.com/doi/full/10.1002/ece3.6973 in the supporting information section.

Table S1: Table recording all gentoo specimens analysed and the averaged trait measures. Acronyms: CL – culmen length; BWB – bill width at base; BH – bill height; BWG – bill width at gonys angle; RL – radius length; ML – manus length; TML – tarsus length; MTL – middle toe length.

Collection	sex	Accession	Lineage	CL_Average	BWB_Average	BH_Average	BWG_Average	FW_Average	RL_Average	ML_Average	TML_Average	MTL_Average
AMNH	Male	445212	FALK	60.33	20.87	15.74	9.17	52.83	58.31	138.03	37.14	77.83
AMNH	Unknown	525830	FALK	55.80	13.56	14.89	6.72	51.14	52.97	124.47	34.39	70.61
AMNH	Male	445210	FALK	60.16	18.47	15.91	9.25	53.37	58.07	136.02	33.21	75.77
AMNH	Unknown	525829	FALK	51.21	17.27	16.38	10.23	53.36	58.72	130.86	33.00	74.19
AMNH	Male	445211	FALK	60.92	23.42	19.08	10.23	55.37	63.79	136.30	36.35	78.81
AMNH	Male	445204	FALK	62.25	19.87	17.46	9.46	54.50	59.35	135.29	35.24	76.63
AMNH	Male	445209	FALK	58.61	19.47	17.34	9.03	51.63	58.32	135.74	38.12	77.39
Tring	Unknown	No Accession - Label text (38, Tail 7/8)	FALK	66.32	19.39	19.47	10.86	55.83	57.89	144.46	39.66	64.58
Tring	Unknown	Unlabelled	FALK	48.92	15.55	16.55	9.88	51.70	55.58	134.52	38.23	64.31
AMNH	Unknown	442642	KERG	55.17	15.21	14.57	8.13	53.45	55.68	133.40	31.15	73.41
AMNH	Male	525824	KERG	56.25	17.71	15.10	8.74	47.61	54.49	119.66	31.14	68.43
AMNH	Unknown	442459	KERG	53.28	14.75	14.22	7.78	52.97	54.37	128.20	31.53	71.37
Tring	Unknown	80.11.18.772	KERG	57.76	16.80	16.49	9.07	51.35	56.26	128.59	36.63	63.11
Tring	Unknown	41.782	KERG	49.62	16.58	15.81	8.24	48.97	46.58	114.15	29.42	50.95
Tring	Unknown	80.11. 18. 773	KERG	58.20	16.09	14.57	8.30	52.13	52.03	124.27	31.84	58.29
Tring	Unknown	90.5. 5. 4	KERG	50.95	13.73	14.62	7.98	50.85	52.45	124.89	30.68	60.46
Tring	Unknown	80.11.18.771	KERG	50.43	13.64	15.05	7.51	50.51	55.25	128.98	32.56	63.11
AMNH	Unknown	525827	SGI	53.11	16.54	12.79	8.80	49.78	51.62	130.17	32.55	71.45
AMNH	Male	435822	SGI	53.75	16.97	16.45	10.22	57.65	56.12	130.05	34.04	73.40
AMNH	Unknown	525826	SGI	52.86	15.09	14.80	8.50	53.90	53.78	130.79	32.33	72.30
AMNH	Male	132463	SGI	62.14	16.60	17.24	9.32	54.94	56.85	134.83	35.73	75.80
AMNH	Female	439823	SGI	40.46	13.69	11.68	6.71	47.09	49.91	124.79	28.54	67.75
AMNH	Female	132465	SGI	57.20	18.07	16.32	9.53	54.15	56.05	129.08	35.65	73.59
AMNH	Female	269638	SGI	51.88	16.89	13.91	9.03	46.52	50.04	130.73	31.25	70.67
AMNH	Male	132462	SGI	59.85	18.27	17.07	9.88	54.53	55.48	139.50	36.75	77.24
AMNH	Male	132464	SGI	53.93	15.22	16.91	9.05	55.85	53.13	132.69	32.94	72.92
AMNH	Male	435821	SGI	48.92	14.71	13.95	7.78	53.92	50.91	130.70	31.39	71.00
Tring	Male	1914.3. 8. 8	SGI	53.04	17.71	15.25	7.89	52.36	50.05	126.93	34.68	63.06
Tring	Female	3. 8. 7	SGI	54.29	19.66	14.90	9.35	53.37	48.08	129.61	33.79	61.78
Tring	Male	1914. 3. 8. 6	SGI	58.99	20.51	15.69	8.70	52.90	52.87	126.47	36.93	60.87
AMNH	Male	196165	SSHWAP	50.00	16.67	17.32	8.80	54.34	54.77	126.72	32.87	71.45
AMNH	Unknown	442416	SSHWAP	42.02	17.29	12.89	7.78	46.93	46.27	110.07	30.20	62.18
AMNH	Unknown	442412	SSHWAP	51.33	19.20	15.17	8.39	52.59	49.93	116.28	32.91	66.37
AMNH	Unknown	442414	SSHWAP	44.85	14.79	14.06	8.63	46.48	46.52	111.66	30.89	63.02
AMNH	Unknown	442415	SSHWAP	47.22	17.06	12.59	7.99	47.84	47.91	113.54	30.99	64.15
AMNH	Female	775712	SSHWAP	48.49	16.43	15.49	8.82	49.90	49.29	111.77	31.15	64.07
Tring	Female	1940.12. 7. 7	SSHWAP	45.57	15.28	14.47	8.71	48.12	47.31	114.35	27.31	56.47
Tring	Male	1924. 5. 8. 43	SSHWAP	48.47	15.50	15.38	8.35	51.06	49.18	116.93	31.84	56.64
Tring	Female	1924. 5. 8. 44	SSHWAP	47.92	13.88	13.69	8.06	51.92	48.90	117.06	32.76	54.73

Table S2: ANOVAs of sex within lineage for each measured trait. Acronyms: CL – culmen length; BWB – bill width at base; BH – bill height; BWG – bill width at gonys angle; RL – radius length; ML – manus length; TML – tarsus length; MTL – middle toe length.

CL	Df	Sum Sq	Mean Sq	F value	Pr(>F)
Lineage	3	0.197093	0.065698	8.732751	**0.000278**
Lineage:Sex	6	0.049799	0.0083	1.103248	0.384344
Residuals	29	0.218171	0.007523	NA	NA

BWB	Df	Sum Sq	Mean Sq	F value	Pr(>F)
Lineage	3	0.143004	0.047668	3.96145	**0.017537**
Lineage:Sex	6	0.161791	0.026965	2.240944	0.067343
Residuals	29	0.348955	0.012033	NA	NA

BH	Df	Sum Sq	Mean Sq	F value	Pr(>F)
Lineage	3	0.123044	0.041015	5.372653	**0.004578**
Lineage:Sex	6	0.105385	0.017564	2.300778	0.061349
Residuals	29	0.221386	0.007634	NA	NA

BWG	Df	Sum Sq	Mean Sq	F value	Pr(>F)
Lineage	3	0.087944	0.029315	2.550286	0.075047
Lineage:Sex	6	0.014018	0.002336	0.203259	0.973022
Residuals	29	0.333346	0.011495	NA	NA

FW	Df	Sum Sq	Mean Sq	F value	Pr(>F)
Lineage	3	0.026972	0.008991	4.62484	**0.009201**
Lineage:Sex	6	0.033866	0.005644	2.903401	**0.024275**
Residuals	29	0.056377	0.001944	NA	NA

RL	Df	Sum Sq	Mean Sq	F value	Pr(>F)
Lineage	3	0.135504	0.045168	17.02449	**1.44E-06**
Lineage:Sex	6	0.024287	0.004048	1.525684	2.05E-01
Residuals	29	0.07694	0.002653	NA	NA

ML	Df	Sum Sq	Mean Sq	F value	Pr(>F)
Lineage	3	0.128514	0.042838	30.50751	**4.15E-09**
Lineage:Sex	6	0.012573	0.002096	1.492364	2.16E-01
Residuals	29	0.040721	0.001404	NA	NA

TML	Df	Sum Sq	Mean Sq	F value	Pr(>F)
Lineage	3	0.114041	0.038014	8.258069	**0.000401**
Lineage:Sex	6	0.021177	0.00353	0.766757	0.602056
Residuals	29	0.133494	0.004603	NA	NA

MTL	Df	Sum Sq	Mean Sq	F value	Pr(>F)
Lineage	3	0.175294	0.058431	7.785509	**0.000582**
Lineage:Sex	6	0.0614	0.010233	1.363503	0.262292
Residuals	29	0.21765	0.007505	NA	NA

Table S3: Confusion Matrices for Linear Discriminant Analysis: a) without cross-validation; b) with cross validation

a)		Predicted Group			
		FALK	KERG	SGI	SSHWAP
Actual Group	FALK	8	1	0	0
	KERG	0	7	0	1
	SGI	1	0	12	0
	SSHWAP	1	0	0	8

b)		Predicted Group			
		FALK	KERG	SGI	SSHWAP
Actual Group	FALK	6	1	2	0
	KERG	1	5	1	1
	SGI	4	1	8	0
	SSHWAP	1	2	0	6

APPENDIX B: SUPPLEMENTARY MATERIAL FOR CHAPTER 3

Supplementary Material A: Classifiers and Covariates for each albatross individual.

Supplementary Material B: 3D Warped Mesh showcasing the shape variation on the first 4 principal components of Figure 3A & Figure 3B.

Supplementary Material C: Pairwise differences in bill shape and size between species. Upper half gives p-values from 1000 permutations in species assignment, with bold indicating significance. Lower half gives distance between species means.

Supplementary Material D: Homogeneity of Slopes and Procrustes ANOVA tests. p-values from 1000 permutations, with bold indicating significance.

Supplementary Material E: eBird Range Maps for Wandering, Sooty and Light-mantled Albatross.

Supplementary Material A: Classifiers and Covariates for each albatross individual.

id	Specimen	Genus_species	Genus	Species	Growth	IUCN	Diet_Inv	Diet_Vfish	Diet_Scav	Diet_5Cat
B1857	Diomedea_melanophris_B1857_6244	Thalassarche_melanophris	Thalassarche	melanophris	Adult	EN	50	50	0	Omnivore
B3305	Phoebetria_palpebrata_B3305	Phoebetria_palpebrata	Phoebetria	palpebrata	Adult	NT	90	10	0	Invertebrate
B3306	Phoebetria_palpebrata_B3306	Phoebetria_palpebrata	Phoebetria	palpebrata	Adult	NT	90	10	0	Invertebrate
B3366	Diomedea_chlororhynchos_B3366	Thalassarche_chlororhynchos	Thalassarche	chlororhynchos	Adult	EN	50	50	0	Omnivore
B4297	Diomedea_exulans_B4297	Diomedea_exulans	Diomedea	exulans	Chick	VU	90	10	0	Invertebrate
B4361	Phoebetria_palpebrata_B4361	Phoebetria_palpebrata	Phoebetria	palpebrata	Adult	NT	90	10	0	Invertebrate
B4371	Diomedea_chlororhynchos_B4371	Thalassarche_chlororhynchos	Thalassarche	chlororhynchos	Adult	EN	50	50	0	Omnivore
B4694	Phoebetria_palpebrata_B4694	Phoebetria_palpebrata	Phoebetria	palpebrata	Adult	NT	90	10	0	Invertebrate
B4695	Diomedea_antipodensis_B4695	Diomedea_antipodensis	Diomedea	antipodensis	Adult	VU	90	10	0	Invertebrate
B4797	Diomedea_bulleri_B4797	Thalassarche_bulleri	Thalassarche	bulleri	Adult	NT	70	30	0	Invertebrate
B4827	Diomedea_bulleri_B4827	Thalassarche_bulleri	Thalassarche	bulleri	Adult	NT	70	30	0	Invertebrate
B4978	Phoebetria_fusca_B4978	Phoebetria_fusca	Phoebetria	fusca	Adult	EN	90	10	0	Invertebrate
B5009	Phoebetria_fusca_B5009	Phoebetria_fusca	Phoebetria	fusca	Immature	EN	90	10	0	Invertebrate
B5010	Phoebetria_fusca_B5010	Phoebetria_fusca	Phoebetria	fusca	Adult	EN	90	10	0	Invertebrate
B5050	Phoebetria_fusca_B5050	Phoebetria_fusca	Phoebetria	fusca	Adult	EN	90	10	0	Invertebrate
B5056	Thalassarche_melanophris_B5056	Thalassarche_melanophris	Thalassarche	melanophris	Immature	EN	50	50	0	Omnivore
B5057	Thalassarche_chlororhynchos_B5057	Thalassarche_chlororhynchos	Thalassarche	chlororhynchos	Adult	EN	50	50	0	Omnivore
B5061	Thalassarche_melanophris_B5061	Thalassarche_melanophris	Thalassarche	melanophris	Adult	EN	50	50	0	Omnivore
B5075	Thalassarche_melanophris_B5075	Thalassarche_melanophris	Thalassarche	melanophris	Immature	EN	50	50	0	Omnivore
B5078	Thalassarche_chlororhynchos_B5078	Thalassarche_chlororhynchos	Thalassarche	chlororhynchos	Immature	EN	50	50	0	Omnivore
B5085	Thalassarche_melanophris_B5085	Thalassarche_melanophris	Thalassarche	melanophris	Immature	EN	50	50	0	Omnivore
B5091	Thalassarche_chlororhynchos_B5091	Thalassarche_chlororhynchos	Thalassarche	chlororhynchos	Immature	EN	50	50	0	Omnivore
B5095	Thalassarche_melanophris_B5095	Thalassarche_melanophris	Thalassarche	melanophris	Immature	EN	50	50	0	Omnivore
B5096	Thalassarche_melanophris_B5096	Thalassarche_melanophris	Thalassarche	melanophris	Adult	EN	50	50	0	Omnivore
B5099	Thalassarche_melanophris_B5099	Thalassarche_melanophris	Thalassarche	melanophris	Immature	EN	50	50	0	Omnivore
B5103	Thalassarche_chlororhynchos_B5103	Thalassarche_chlororhynchos	Thalassarche	chlororhynchos	Immature	EN	50	50	0	Omnivore
B5110	Thalassarche_melanophris_B5110	Thalassarche_melanophris	Thalassarche	melanophris	Immature	EN	50	50	0	Omnivore
B5115	Thalassarche_melanophris_B5115	Thalassarche_melanophris	Thalassarche	melanophris	Immature	EN	50	50	0	Omnivore
B5120	Diomedea_epomorphora_B5120	Diomedea_epomophora	Diomedea	epomophora	Immature	VU	90	10	0	Invertebrate
B5159	Thalassarche_chrysostoma_B5159	Thalassarche_chrysostoma	Thalassarche	chrysostoma	Immature	VU	60	40	0	Omnivore
B5161	Thalassarche_chrysostoma_B5161	Thalassarche_chrysostoma	Thalassarche	chrysostoma	Immature	VU	60	40	0	Omnivore
B5168	Thalassarche_cauta_B5168	Thalassarche_cauta	Thalassarche	cauta	Adult	NT	60	40	0	Omnivore

B5170	Thalassarche_cauta_B5170	Thalassarche_cauta	Thalassarche	cauta	Immature	NT	60	40	0	Omnivore
B5173	Thalassarche_cauta_B5173	Thalassarche_cauta	Thalassarche	cauta	Adult	NT	60	40	0	Omnivore
B5174	Thalassarche_cauta_B5174	Thalassarche_cauta	Thalassarche	cauta	Adult	NT	60	40	0	Omnivore
B5175	Thalassarche_cauta_B5175	Thalassarche_cauta	Thalassarche	cauta	Immature	NT	60	40	0	Omnivore
B5179	Thalassarche_cauta_B5179	Thalassarche_cauta	Thalassarche	cauta	Adult	NT	60	40	0	Omnivore
B5254	Diomedea_exulans_B5254	Diomedea_exulans	Diomedea	exulans	Adult	VU	90	10	0	Invertebrate
B5255	Diomedea_exulans_B5255	Diomedea_exulans	Diomedea	exulans	Adult	VU	90	10	0	Invertebrate
B5256	Diomedea_exulans_B5256	Diomedea_exulans	Diomedea	exulans	Adult	VU	90	10	0	Invertebrate
B5257	Diomedea_exulans_B5257	Diomedea_exulans	Diomedea	exulans	Adult	VU	90	10	0	Invertebrate
B5259	Diomedea_exulans_B5259	Diomedea_exulans	Diomedea	exulans	Adult	VU	90	10	0	Invertebrate
B5260	Diomedea_epomorphora_B5260	Diomedea_epomophora	Diomedea	epomophora	Adult	VU	90	10	0	Invertebrate
B5261	Diomedea_exulans_B5261	Diomedea_exulans	Diomedea	exulans	Adult	VU	90	10	0	Invertebrate
B5262	Diomedea_exulans_B5262	Diomedea_exulans	Diomedea	exulans	Immature	VU	90	10	0	Invertebrate
B5263	Diomedea_exulans_B5263	Diomedea_exulans	Diomedea	exulans	Adult	VU	90	10	0	Invertebrate
B5264	Diomedea_exulans_B5264	Diomedea_exulans	Diomedea	exulans	Immature	VU	90	10	0	Invertebrate
B5270	Diomedea_epomorphora_B5270	Diomedea_epomophora	Diomedea	epomophora	Adult	VU	90	10	0	Invertebrate
B5273	Thalassarche_chrysostoma_B5273	Thalassarche_chrysostoma	Thalassarche	chrysostoma	Immature	VU	60	40	0	Omnivore
B5276	Thalassarche_chrysostoma_B5276	Thalassarche_chrysostoma	Thalassarche	chrysostoma	Immature	VU	60	40	0	Omnivore
B5281	Thalassarche_impavida_B5281	Thalassarche_impavida	Thalassarche	impavida	Adult	VU	50	50	0	Omnivore
B5286	Thalassarche_chlororhynchos_B5286	Thalassarche_chlororhynchos	Thalassarche	chlororhynchos	Immature	EN	50	50	0	Omnivore
B5288	Thalassarche_chrysostoma_B5288	Thalassarche_chrysostoma	Thalassarche	chrysostoma	Immature	VU	60	40	0	Omnivore
B5348	Thalassarche_impavida_B5348	Thalassarche_impavida	Thalassarche	impavida	Adult	VU	50	50	0	Omnivore
B5358	Thalassarche_impavida_B5358	Thalassarche_impavida	Thalassarche	impavida	Adult	VU	50	50	0	Omnivore
B5359	Thalassarche_impavida_B5359	Thalassarche_impavida	Thalassarche	impavida	Immature	VU	50	50	0	Omnivore
B5362	Thalassarche_chrysostoma_B5362	Thalassarche_chrysostoma	Thalassarche	chrysostoma	Adult	VU	60	40	0	Omnivore
B5370	Thalassarche_impavida_B5370	Thalassarche_impavida	Thalassarche	impavida	Adult	VU	50	50	0	Omnivore
B5379	Thalassarche_chrysostoma_B5379	Thalassarche_chrysostoma	Thalassarche	chrysostoma	Adult	VU	60	40	0	Omnivore
B5384	Thalassarche_chrysostoma_B5384	Thalassarche_chrysostoma	Thalassarche	chrysostoma	Adult	VU	60	40	0	Omnivore
B5386	Thalassarche_chlororhynchos_B5386	Thalassarche_chlororhynchos	Thalassarche	chlororhynchos	Adult	EN	50	50	0	Omnivore
B5854	Diomedea_nigripes_B5854	Phoebastria_nigripes	Phoebastria	nigripes	Adult	EN	20	70	10	VertFishScav

Supplementary Material B: Warped mean mesh & mean wireframe to the extreme positions of Principal Component Axis 1, 2, 3 and 4.

PC1 **Max**

PC1 **Min**

PC2 **Max**

PC2 **Min**

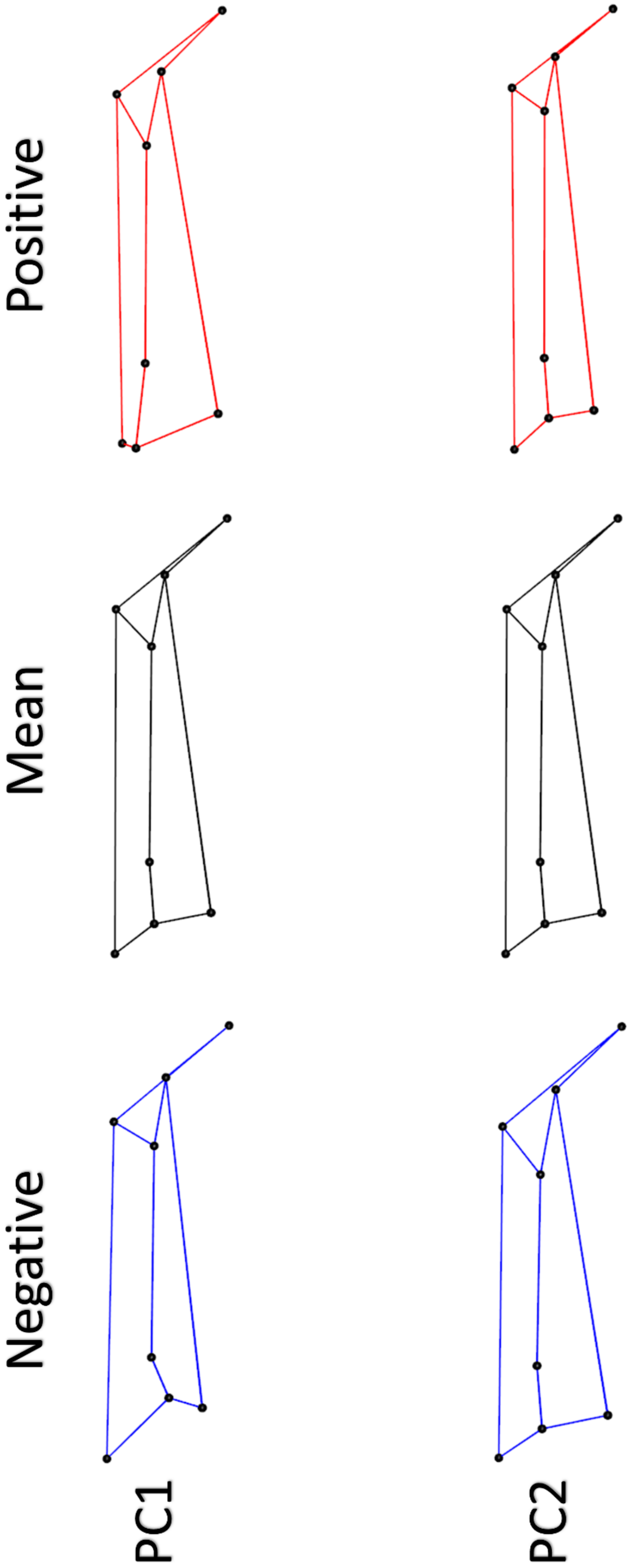
Positive
Mean
Negative
PC1
PC2

PC3 **Max**

PC3 **Min**

PC4 Max

PC4 Min

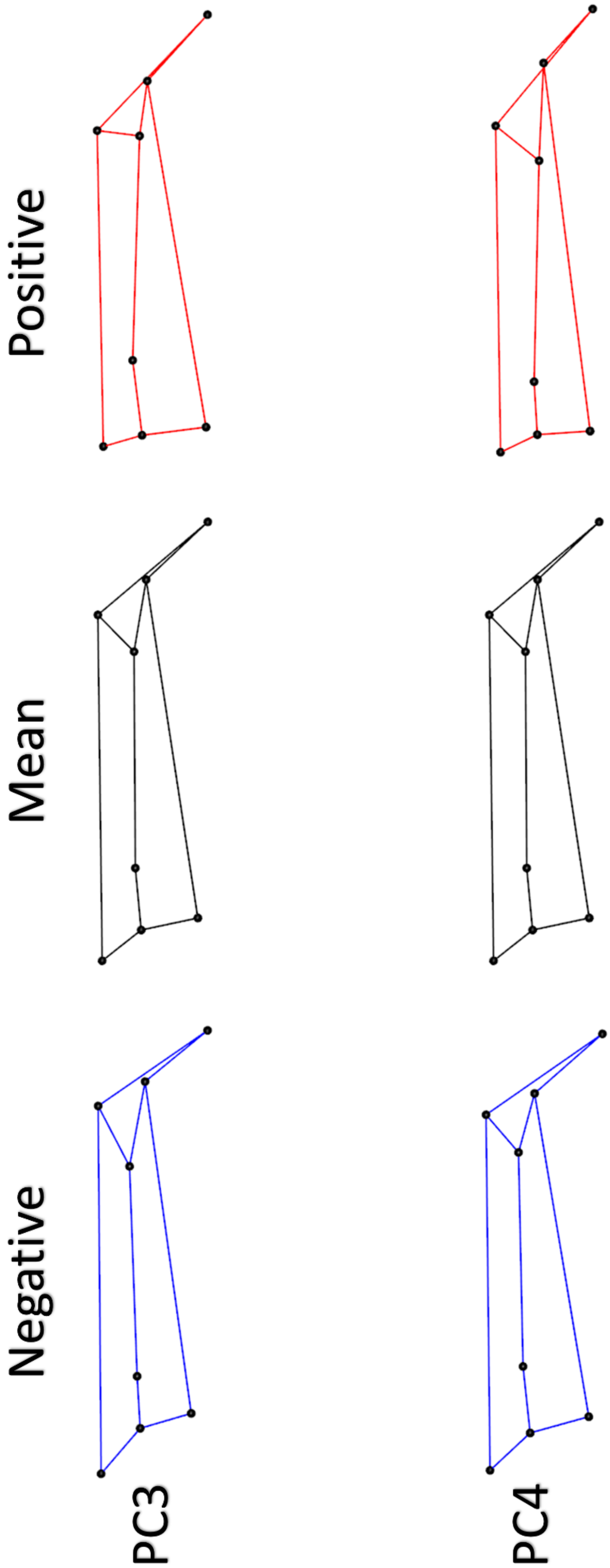
Positive
Mean
Negative
PC3
PC4

Supplementary Material C: Pairwise differences in bill shape and size between species. Upper half gives p-values from 1000 permutations in species assignment, with bold indicating significance. Lower half gives distance between species means. Additional table showing whether shape and/or size is a significant distinguisher between species.

SHAPE	Diomedea antipodensis	Diomedea epomophora	Diomedea exulans	Phoebastria nigripes	Phoebetria fusca	Phoebetria palpebrata	Thalassarche bulleri	Thalassarche cauta	Thalassarche chlororhynchos	Thalassarche chrysostoma	Thalassarche impavida	Thalassarche melanophris
Diomedea antipodensis		0.152	0.528	0.664	0.137	0.259	0.053	**0.018**	**0.005**	0.081	0.252	0.309
Diomedea epomophora	0.0960		**0.016**	**0.032**	**0.002**	0.119	**0.028**	**0.001**	**0.001**	**0.001**	**0.002**	**0.001**
Diomedea exulans	0.0621	0.0747		**0.015**	**0.019**	0.114	**0.001**	**0.001**	**0.001**	**0.001**	**0.004**	**0.001**
Phoebastria nigripes	0.0710	0.1154	0.1073		**0.005**	**0.019**	**0.001**	**0.001**	**0.001**	**0.003**	**0.011**	**0.008**
Phoebetria fusca	0.0946	0.1009	0.0663	0.1292		0.417	**0.001**	**0.001**	**0.001**	**0.001**	**0.012**	**0.002**
Phoebetria palpebrata	0.0814	0.0655	0.0511	0.1149	0.0440		**0.039**	**0.001**	**0.001**	**0.001**	0.058	**0.020**
Thalassarche bulleri	0.1197	0.1011	0.1054	0.1507	0.1137	0.0892		0.133	0.795	0.097	0.190	**0.049**
Thalassarche cauta	0.1167	0.1229	0.1191	0.1482	0.1334	0.1157	0.0672		**0.036**	0.082	**0.031**	**0.013**
Thalassarche chlororhynchos	0.1231	0.1062	0.1068	0.1535	0.1221	0.0985	0.0339	0.0559		**0.008**	**0.005**	**0.001**
Thalassarche chrysostoma	0.0924	0.1179	0.0935	0.1261	0.0995	0.0902	0.0702	0.0486	0.0652		0.500	0.252
Thalassarche impavida	0.0799	0.0986	0.0739	0.1172	0.0775	0.0661	0.0652	0.0645	0.0694	0.0326		0.940
Thalassarche melanophris	0.0749	0.0953	0.0716	0.1137	0.0780	0.0671	0.0761	0.0648	0.0761	0.0354	0.0192	

SIZE	Diomedea antipodensis	Diomedea epomophora	Diomedea exulans	Phoebastria nigripes	Phoebetria fusca	Phoebetria palpebrata	Thalassarche bulleri	Thalassarche cauta	Thalassarche chlororhynchos	Thalassarche chrysostoma	Thalassarche impavida	Thalassarche melanophris
Diomedea antipodensis		0.579	0.904	**0.021**	**0.043**	**0.009**	0.462	0.531	0.245	0.16	0.173	0.116
Diomedea epomophora	0.1400		0.441	**0.001**	**0.001**	**0.001**	0.087	0.058	**0.004**	**0.001**	**0.003**	**0.001**
Diomedea exulans	0.0331	0.10695		**0.001**	**0.001**	**0.001**	0.184	0.087	**0.001**	**0.001**	**0.004**	**0.001**
Phoebastria nigripes	0.6075	0.74756	0.64061		0.549	0.849	0.094	**0.02**	0.144	0.229	0.237	0.269
Phoebetria fusca	0.4657	0.60576	0.49881	0.14180		0.522	0.111	**0.008**	0.111	0.287	0.335	0.374
Phoebetria palpebrata	0.5608	0.70079	0.59384	0.04677	0.09504		**0.029**	**0.001**	**0.026**	0.078	0.098	0.103
Thalassarche bulleri	0.1807	0.32070	0.21375	0.42686	0.28506	0.38010		0.844	0.593	0.388	0.366	0.288
Thalassarche cauta	0.1457	0.28570	0.17875	0.46187	0.32006	0.41510	0.03500		0.262	0.079	0.138	**0.039**
Thalassarche chlororhynchos	0.2737	0.41377	0.30683	0.33379	0.19198	0.28702	0.09308	0.12808		0.584	0.612	0.401
Thalassarche chrysostoma	0.3297	0.46973	0.36278	0.27784	0.13603	0.23107	0.14903	0.18403	0.05595		0.985	0.764
Thalassarche impavida	0.3326	0.47267	0.36572	0.27490	0.13309	0.22813	0.15197	0.18697	0.05889	0.00294		0.823
Thalassarche melanophris	0.3589	0.49893	0.39198	0.24863	0.10682	0.20186	0.17824	0.21324	0.08516	0.02921	0.02627	

SIGNIFICANT	Diomedea antipodensis	Diomedea epomophora	Diomedea exulans	Phoebastria nigripes	Phoebetria fusca	Phoebetria palpebrata	Thalassarche bulleri	Thalassarche cauta	Thalassarche chlororhynchos	Thalassarche chrysostoma	Thalassarche impavida	Thalassarche melanophris
Diomedea antipodensis		0	0	1	1	1	0	1	1	0	0	0
Diomedea epomophora			1	2	2	1	1	1	2	2	2	2
Diomedea exulans				2	2	1	1	1	2	2	2	2
Phoebastria nigripes					1	1	1	2	1	1	1	1
Phoebetria fusca						0	1	2	1	1	1	1
Phoebetria palpebrata							2	2	2	1	0	1
Thalassarche bulleri								0	0	0	0	1
Thalassarche cauta									1	0	1	2
Thalassarche chlororhynchos										1	1	1
Thalassarche chrysostoma											0	0
Thalassarche impavida												0
Thalassarche melanophris												

Supplementary Material D: Homogeneity of Slopes and Procrustes ANOVA tests. p-values from 1000 permutations, with bold indicating significance.

HOS Test between Simple & Common Allometry Models

	ResDf	Df	RSS	SS	MS	Rsq	F	Z	Pr(>F)
shape~log(Csize) (NULL)	59	1	0.226258			0			
shape~log(Csize)+species	48	11	0.049875	0.17638	0.016035	0.72644	15.432	9.7075	**0.001**
Total	60		0.242806						

HOS Test between Common & Unique Allometry Models

	ResDf	Df	RSS	SS	MS	Rsq	F	Z	Pr(>F)
shape~log(Csize)+species (NULL)	48	1	0.049875			0			
shape~log(Csize)+species+log(Csize):species	39	9	0.039622	0.010253	0.001139	0.042229	1.1214	0.61326	0.266
Total	60		0.242806						

Simple Allometry Procrustes ANOVA

	Df	SS	MS	Rsq	F	Z	Pr(>F)
log(Csize)	1	0.016548	0.016548	0.06815	4.3151	2.5612	**0.005**
Residuals	59	0.226258	0.003835	0.93185			
Total	60	0.242806					

Common Allometry Procrustes ANOVA

	Df	SS	MS	Rsq	F	Z	Pr(>F)
log(Csize)	1	0.016548	0.016548	0.06815	15.926	4.6158	**0.001**
species	11	0.176383	0.016035	0.72644	15.432	9.7075	**0.001**
Residuals	48	0.049875	0.001039	0.20541			
Total	60	0.242806					

Unique Allometry Procrustes ANOVA

	Df	SS	MS	Rsq	F	Z	Pr(>F)
log(Csize)	1	0.016548	0.016548	0.06815	16.2884	4.6493	**0.001**
species	11	0.176383	0.016035	0.72644	15.7832	10.0286	**0.001**
log(Csize):species	9	0.010253	0.001139	0.04223	1.1214	0.6133	0.266
Residuals	39	0.039622	0.001016	0.16318			
Total	60	0.242806					

Supplementary Material E: Range maps from eBird data for three albatross species of interest: Wandering Albatross (*Diomedea exulans*), Sooty Albatross (*Phoebetria fusca*) and Light-mantled Albatross (*Phoebetria palpebrata*). Images provided by eBird (www.ebird.org) and created 15th March 2023.

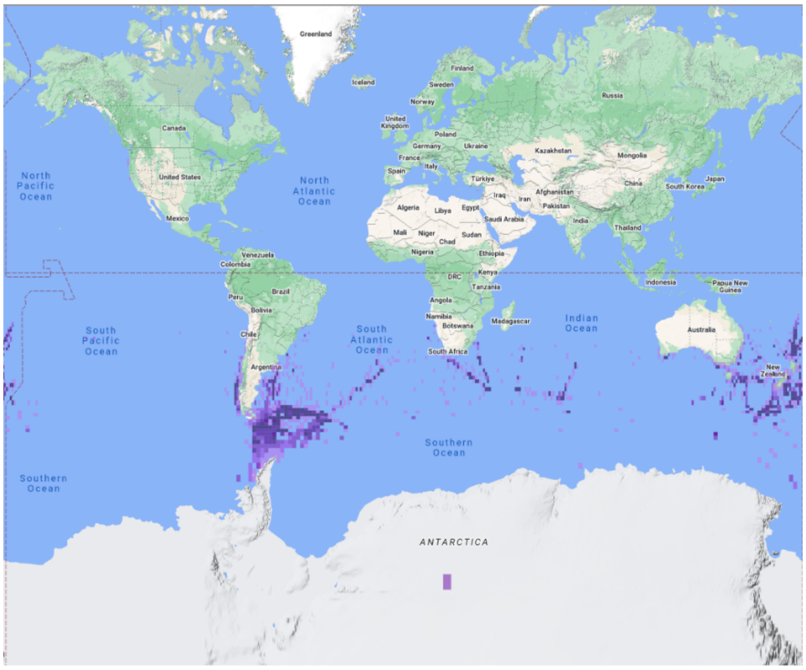

a) Wandering Albatross

b) Sooty Albatross

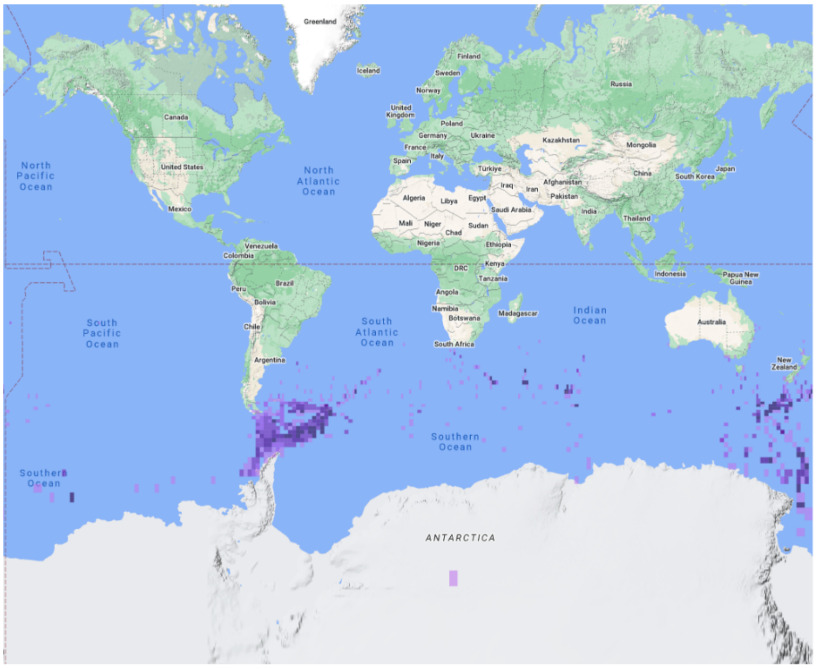

c) Light-mantled Albatross

APPENDIX C: SUPPLEMENTARY MATERIAL FOR CHAPTER 4

Supplementary Material can be found at the following reference: Tyler J, Younger JL. 2022 Diving into a dead-end: asymmetric evolution of diving drives diversity and disparity shifts in waterbirds. Figshare. (doi:10.6084/m9.figshare.c.6328047) (https://rs.figshare.com/collections/Supplementary_material_from_Diving_into_a_dead-end_asymmetric_evolution_of_diving_drives_diversity_and_disparity_shifts_in_waterbirds_/6328047)

Supplementary Material A: Transition rate matrices for the 4-state system. Note: All values given as 0 with no trailing decimals are values where the transition rate was set as zero a priori. In print & online.

Supplementary Material B: Data matrix containing all species used in analyses alongside categorisations and covariates. Online.

Supplementary Material C: Results from body mass modelling including all parameter estimates. In Print & Online.

Supplementary Material D: Phylogeny used for all analyses. Online.

Supplementary Material E: R Analysis Code. Online.

Supplementary Material A: Transition rate matrices for the 4-state system. Note: All values given as 0 with no trailing decimals are values where the transition rate was set as zero a priori.

Table A.1: ER model transition rates for 4-state system. Transition rate given per million years. ER - Transition rates between all states are equal.

	Non-Diving	Plunge Diving	Foot Diving	Wing Diving
Non-Diving	-0.002472	0.000824	0.000824	0.000824
Plunge Diving	0.000824	-0.002472	0.000824	0.000824
Foot Diving	0.000824	0.000824	-0.002472	0.000824
Wing Diving	0.000824	0.000824	0.000824	-0.002472

Table A.2: SYM model transition rates for 4-state system. Transition rate given per million years. SYM - Transition rates between each pair of states are equal.

	Non-Diving	Plunge Diving	Foot Diving	Wing Diving
Non-Diving	-0.002769	0.001587	0.000552	0.000630
Plunge Diving	0.001587	-0.002386	0.000799	0.000000
Foot Diving	0.000552	0.000799	-0.001352	0.000000
Wing Diving	0.000630	0.000000	0.000000	-0.000630

Table A.3: ARD model transition rates for 4-state system. Transition rate given per million years. ARD – Each transition rate is independent.

	Non-Diving	Plunge Diving	Foot Diving	Wing Diving
Non-Diving	-0.002964	0.001633	0.000668	0.000662
Plunge Diving	0.000000	0.000000	0.000000	0.000000
Foot Diving	0.000000	0.001278	-0.001278	0.000000
Wing Diving	0.000000	0.000000	0.000000	0.000000

Table A.4: NR ER model transition rates for 4-state system. Transition rate given per million years. NR ER - Transition rates between all states are equal except for those from diving niches to Non-Diving which are explicitly set to zero.

	Non-Diving	Plunge Diving	Foot Diving	Wing Diving
Non-Diving	-0.002641	0.000880	0.000880	0.000880
Plunge Diving	0	-0.001761	0.000880	0.000880
Foot Diving	0	0.000880	-0.001761	0.000880
Wing Diving	0	0.000880	0.000880	-0.001761

Table A.5: NR SYM model transition rates for 4-state system. Transition rate given per million years. SYM - Transition rates between each pair of states are equal except for those from diving niches to Non-Diving which are explicitly set to zero.

	Non-Diving	Plunge Diving	Foot Diving	Wing Diving
Non-Diving	-0.002975	0.001692	0.00062	0.000662
Plunge Diving	0	-0.00079	0.00079	0.000000
Foot Diving	0	0.00079	-0.00079	0.000000
Wing Diving	0	0.000000	0.000000	0.000000

Table A.6: NR ARD model transition rates for 4-state system. Transition rate given per million years. ARD – Each transition rate is independent except for those from diving niches to Non-Diving which are explicitly set to zero.

	Non-Diving	Plunge Diving	Foot Diving	Wing Diving
Non-Diving	-0.002964	0.001633	0.000668	0.000662
Plunge Diving	0	0.000000	0.000000	0.000000
Foot Diving	0	0.001278	-0.001278	0.000000
Wing Diving	0	0.000000	0.000000	0.000000

Table A.7: NR ALL model transition rates for 4-state system. Transition rate given per million years. NR ALL – Only the transitions away from Non-Diving to each of the Diving Niches are allowed to be non-zero.

	Non-Diving	Plunge Diving	Foot Diving	Wing Diving

Non-Diving	-0.003143	0.001816	0.000668	0.000660
Plunge Diving	0	0	0	0
Foot Diving	0	0	0	0
Wing Diving	0	0	0	0

Supplementary Material C: Results from body mass modelling including all parameter estimates.

Model Rank	Model	AIC Weights	deltaAIC	AIC Scores	Regimes	Parameters
1	OUMVA	9.87E-01	0.000	438.0	4 (non-diving, plunge, foot, wing)	non-diving σ2=0.024, θ=2.76, α=0.025 plunge diving σ2=4.48e-06, θ=2.74, α=0.103 foot diving σ2=0.005, θ=3.00, α=0.044 wing diving σ2=0.019, θ=4.58, α=0.015
2	OUMVA	1.28E-02	8.700	446.7	3 (non-diving, diving, flightless)	non-diving σ2=0.027, θ=2.64, α=0.039 diving σ2=0.007, θ=2.97, α=0.053 flightless σ2=0.005, θ=3.97, α=0.064
3	OUMVA	9.69E-05	18.500	456.5	2 (non-diving, diving)	non-diving σ2=0.027, θ=,2.64 α=0.038 diving σ2=0.012, θ=3.09, α=0.046
4	OUMA	5.23E-05	19.700	457.7	4 (non-diving, plunge, foot, wing)	non-diving σ2=0.026, θ=2.61, α=0.040 plunge diving σ2=0.026, θ=2.95, α=0.042 foot diving σ2=0.026, θ=3.09, α=0.031 wing diving σ2=0.026, θ=3.79, α=0.030
5	OUMV	1.35E-05	22.400	460.4	4 (non-diving, plunge, foot, wing)	non-diving σ2=0.027, θ=2.62, α=0.041 plunge diving σ2=0.030, θ=3.00, α=0.041 foot diving σ2=0.015, θ=3.02, α=0.041 wing diving σ2=0.014, θ=3.51, α=0.041
6	OUM	2.18E-06	26.100	464.1	3 (non-diving, diving, flightless)	non-diving σ2=0.026, θ=2.59, α=0.043 diving σ2=0.026, θ=2.92, α=0.043 flightless σ2=0.026, θ=4.69, α=0.043
7	OUMV	1.12E-06	27.400	465.4	3 (non-diving, diving, flightless)	non-diving σ2=0.028, θ=2.59, α=0.045 diving σ2=0.024, θ=2.93, α=0.045 flightless σ2=0.019, θ=4.64, α=0.045

8	OUM	5.85E-07	28.700	466.7	2 (non-diving, diving)	non-diving σ2=0.026, θ=2.60, a=0.042 diving σ2=0.026, θ=3.05, a=0.042
9	OUMV	4.95E-07	29.000	467.0	2 (non-diving, diving)	non-diving σ2=0.028, θ=2.60, a=0.043 diving σ2=0.028, θ=3.06, a=0.043
10	OUMA	2.73E-07	30.200	468.2	2 (non-diving, diving)	non-diving σ2=0.025, θ=2.61, a=0.041 diving σ2=0.025, θ=3.05, a=0.042
11	OUMA	1.62E-07	31.300	469.3	3 (non-diving, diving, flightless)	non-diving σ2=0.024, θ=2.62, a=0.036 diving σ2=0.024, θ=2.94, a=0.037 flightless σ2=0.024, θ=5.25, a=0.034
12	OUM	1.32E-07	31.700	469.7	4 (non-diving, plunge, foot, wing)	non-diving σ2=0.026, θ=2.61, a=0.042 plunge diving σ2=0.026, θ=2.98, a=0.042 foot diving σ2=0.026, θ=2.98, a=0.042 wing diving σ2=0.026, θ=3.42, a=0.042
13	OU1	6.67E-08	33.100	471.1	1	a=0.039,σ^2= 0.026, θ=2.71
14	Trend	8.78E-22	97.000	535.0	1	σ2=0.000003, z_0=2.80, slope=100.0
15	BMS	2.05E-26	118.300	556.3	4 (non-diving, plunge, foot, wing)	non-diving σ2=0.021, θ=2.87 plunge diving σ2=0.029, θ=2.87 foot diving σ2=0.012, θ=2.87 wing diving σ2=0.011, θ=2.87
16	BM1	1.08E-29	133.400	571.4	1	σ^2= 0.021, θ=2.83
17	BMS	3.96E-30	135.400	573.4	2 (non-diving, diving)	non-diving σ2=0.0212, θ=2.83 diving σ2=0.0213, θ=2.83
18	EB	3.88E-30	135.450	573.5	1	σ2=0.021, z_0=2.83, a=0.00
19	BMS	1.95E-30	136.800	574.8	3 (non-diving, diving, flightless)	non-diving σ2=0.021, θ=2.83 diving σ2=0.022, θ=2.83 flightless σ2=0.016, θ=2.83